

AUTONOMOUS HERDING OF UNCONTROLLED UNCERTAIN AGENTS: A
SWITCHED SYSTEMS APPROACH

By

RYAN ANDREW LICITRA

A DISSERTATION PRESENTED TO THE GRADUATE SCHOOL
OF THE UNIVERSITY OF FLORIDA IN PARTIAL FULFILLMENT
OF THE REQUIREMENTS FOR THE DEGREE OF
DOCTOR OF PHILOSOPHY

UNIVERSITY OF FLORIDA

2017

© 2017 Ryan Andrew Licitra

To my wife Brittani, my daughter Zoe, and my parents, John and Julie, for the boundless
inspiration and encouragement

ACKNOWLEDGMENTS

I would like to express gratitude towards Dr. Warren E. Dixon, whose support and encouragement was indispensable to my academic success. As my academic advisor, he provided me with guidance and knowledge that helped to shape my research and therefore this dissertation. As a mentor, he provided me with the inspiration to develop professionally and prepared me for a future as a researcher. I would also like to extend gratitude to my committee members Dr. Prabir Barooah, Dr. Carl Crane, and Dr. John Shea for their time and valuable insights. I would also like to thank my colleagues at the University of Florida Nonlinear Controls and Robotics laboratory for the countless fruitful discussions that have helped shape the ideas in this dissertation, as well as for helping make my time in graduate school as enjoyable as possible. I am also thankful for my family and friends, whose support and encouragement were invaluable in the completion of this dissertation.

TABLE OF CONTENTS

	<u>page</u>
ACKNOWLEDGMENTS	4
LIST OF TABLES	7
LIST OF FIGURES	8
LIST OF ABBREVIATIONS	10
ABSTRACT	11
CHAPTER	
1 INTRODUCTION	13
1.1 Motivation and Literature Review	13
1.2 Contributions	14
2 SINGLE AGENT HERDING OF N-AGENTS: A SWITCHED SYSTEMS AP- PROACH	16
2.1 Problem Formulation	16
2.2 Control Objective	19
2.3 Control Development	19
2.4 Stability Analysis	20
2.4.1 Convergence of Currently <i>Chased</i> Target	21
2.4.2 Divergence of <i>Unchased</i> Target	22
2.4.3 Target Switched Systems Analysis	24
2.5 Simulation Results	25
2.6 Concluding Remarks	27
3 SWITCHED ADAPTIVE HERDING OF N-AGENTS WITH INTEGRAL CON- CURRENT LEARNING	30
3.1 Problem Formulation	30
3.2 Control Development	33
3.3 Stability Analysis	36
3.3.1 Target Operating in the <i>Chased</i> Mode	37
3.3.2 Target Operating in the <i>Unchased</i> Mode	39
3.3.3 Combined Analysis	40
3.4 Simulations	42
3.5 Experiments	44
3.6 Concluding Remarks	45
4 HERDING OF MULTIPLE AGENTS WITH UNSTRUCTURED UNCERTAIN DYNAMICS USING NEURAL NETWORKS	50

4.1	Problem Formulation	50
4.2	Control Objective	52
4.3	Control Development	54
4.3.1	Herding Controller	54
4.3.2	Function Approximation	56
4.4	Stability Analysis	58
4.4.1	Target Operating in the <i>Chased Mode</i>	59
4.4.2	Target Operating in the <i>Unchased Mode</i>	61
4.4.3	Combined Analysis	62
4.5	Experiments	65
4.5.1	Switching Strategy	65
4.5.2	Grouping Objective	66
4.5.3	Partitioning Objective	66
4.6	Concluding Remarks	69
5	COOPERATIVE TWO-PHASE (GROUP AND RELOCATE) HERDING OF MULTIPLE AGENTS WITH UNCERTAIN DYNAMICS	73
5.1	Problem Formulation	73
5.2	Grouping Phase	75
5.2.1	Grouping Objective	76
5.2.2	Grouping Controller	76
5.2.3	Grouping Stability Analysis	79
5.2.3.1	Target i is operating in the <i>chased mode</i>	80
5.2.3.2	Target i is operating in the <i>unchased mode</i>	83
5.2.3.3	Combined analysis	83
5.3	Relocating Phase	84
5.3.1	Relocating Objective	84
5.3.1.1	Multiple herders and a single target	87
5.3.1.2	Extension to an ensemble of targets	89
5.3.2	Relocation Controller	90
5.3.3	Relocation Stability Analysis	95
5.4	Simulations	96
5.5	Concluding Remarks	96
6	CONCLUSIONS	102
	REFERENCES	104
	BIOGRAPHICAL SKETCH	108

LIST OF TABLES

<u>Table</u>	<u>page</u>
2-1 Simulation gains	26
2-2 System parameters	26
2-3 Average dwell times	26
2-4 Monte Carlo simulations	27
3-1 Simulation gains	42
3-2 Simulation system parameters	43

LIST OF FIGURES

<u>Figure</u>	<u>page</u>
2-1 The states of the herder and targets using the robust controller in a two-dimensional workspace.	28
2-2 Two-dimensional plot of the paths of the herder and targets using the robust controller.	28
2-3 The states of the herder and targets using the robust controller in a three-dimensional workspace.	29
2-4 Three-dimensional plot of the paths of the herder and targets using the robust controller.	29
3-1 The states of the herder and targets using the adaptive controller in a two-dimensional workspace.	43
3-2 Two-dimensional plot of the paths of the herder and targets using the adaptive controller.	44
3-3 Adaptive estimate errors for the 2D simulation.	45
3-4 The states of the herder and targets using the adaptive controller in a three-dimensional workspace.	46
3-5 Three-dimensional plot of the paths of the herder and targets using the adaptive controller.	47
3-6 Adaptive estimate errors for the 3D simulation.	47
3-7 Overall herder and target trajectories, with each agent's starting location marked by a circle, and ending locations marked by an X.	48
3-8 Starting and ending positions of all agents.	48
3-9 Norms of the target errors. Each agent is driven to within 0.5 m of their goal location (gray dotted line).	49
3-10 The actual vs. estimated parameters are shown.	49
4-1 The herder and target paths with the objective of regulating all targets to the center.	66
4-2 The starting and ending herder and target positions for the experiment with the objective of regulating all targets to the center.	67
4-3 The norm of the target positions for the first experiment.	67
4-4 The herder controller for the first experiment.	68

4-5	Adaptive weight estimates for an example target during the first experiment.	68
4-6	Adaptive weight estimates for an example target during the first experiment.	69
4-7	The herder and target paths with the objective of partitioning targets by color.	70
4-8	The starting and ending herder and target positions for the experiment with the objective of partitioning targets by color.	70
4-9	The norm of the target positions for the second experiment.	71
4-10	The herder controller for the second experiment.	71
4-11	Adaptive weight estimates for an example target during the second experiment.	72
4-12	Adaptive weight estimates for an example target during the second experiment.	72
5-1	The ideal unicycle model in [1] is used to model the ensemble of target agents.	85
5-2	To ensure that all target agents are regulated to the neighborhood $B_{r_g}(x_g)$, the maximum allowable radius of the <i>herd</i> is $r_{\max} = r_g - L$	86
5-3	The configuration with n_h herders and a single target is shown. The target, \bar{x} , represents a single sheep as an example, but will later represent the mean target location.	87
5-4	The grouping phase is initialized at $t = 0$ s.	97
5-5	The grouping phase is completed at $t = 35$ s.	97
5-6	The relocating phase is initialized at $t = 36$ s. The point p (black dot) is to be driven to the goal location (green cross).	98
5-7	The relocating phase continues at $t = 56$ s. Note that the radius of the frontal arc has increased to compensate for ensemble dispersion.	98
5-8	The relocating phase continues at $t = 75$ s.	99
5-9	The relocating phase is completed at $t = 98$ s. The point p (black dot) has been successfully driven to the goal location x_g . The final radius satisfies $r \leq r_{\max}$, where $r_{\max} = r_g - L$, and thus all targets are regulated to $B_{r_g}(x_g)$	99
5-10	The parameter estimation error is shown.	100
5-11	The point offset error is shown.	100

LIST OF ABBREVIATIONS

FE	Finite excitation
ICL	Integral concurrent learning
LP	Linear in the uncertain parameters
NN	Neural network
PE	Persistence of excitation

Abstract of Dissertation Presented to the Graduate School
of the University of Florida in Partial Fulfillment of the
Requirements for the Degree of Doctor of Philosophy

AUTONOMOUS HERDING OF UNCONTROLLED UNCERTAIN AGENTS: A
SWITCHED SYSTEMS APPROACH

By

Ryan Andrew Licitra

December 2017

Chair: Warren E. Dixon

Major: Mechanical Engineering

Some network systems include agents that are only indirectly controllable through the influence of other agents. Such indirectly controllable agents can include non-cooperative enemies, uncontrollable allies, or unactuated entities in general. In any of these cases, a unique challenge arises when specific objectives and behaviors are desired for these agents. Motivating examples for this type of problem include autonomous escort problems, pursuit and capture, search and rescue, corralling/collection of payloads, wildlife control, traffic pattern regulation, etc. By modeling the interaction between these uncontrollable agents and the agents in the system that are controllable, control design methods may be employed to accomplish certain tasks. In a general sense, a herding task can be defined as using controllable agents to influence the states of uncontrollable agents in a way that enables system-wide objectives to be accomplished. The interaction between the uncontrollable (target) agents and controllable (herder) agents can have various models, depending on the nature of the system and objectives.

This dissertation investigates modeling, control design, and stability analysis for systems with multiple uncontrollable agents which behave according to uncertain nonlinear dynamics. In Chapter 2, a robust controller and dwell time conditions are developed for a single herding agent tasked with regulating multiple target agents to a desired goal location. Chapter 3 provides a solution to the same problem using an adaptive controller and similar dwell time conditions, and additionally incorporates online

learning of target agent uncertainties using integral concurrent learning (ICL) methods. In Chapter 4, a more general model of the target agents (i.e. the herder is less informed) is learned by the herding agent online using neural networks (NN) and dwell time conditions are developed to assist in the design of a switching strategy for the herder. Finally, in Chapter 5, a two-phase cooperative herding controller is developed for a small team of herders to group and relocate a larger team of uncertain target agents. Each chapter includes simulation and/or experimental results to demonstrate the performance of developed methods.

CHAPTER 1 INTRODUCTION

1.1 Motivation and Literature Review

With increased availability and efficiency of robotic vehicles in recent years, the use of networks of autonomous agents has never been more prevalent. In many applications, networks of cooperative agents are controlled to accomplish various objectives, including consensus, formation control, containment control, etc. [2–7]. The terms herding and flocking are sometimes used to describe consensus problems for networks of controllable agents [8–10]. Since these results assume that all agents in the system are directly controllable, they are referred to as *direct* herding problems.

However, in some results, there may be agents in the network that aren't directly controllable, i.e., their dynamics don't explicitly contain a control input [1, 11–13]. In these scenarios, the uncontrolled agents must be influenced through potentially uncertain interactions with controllable agents. This class of problems is referred to as *indirect* herding problems, due to the fact that some agents must be indirectly controlled to accomplish the objective.

In the field of game theory, the pursuer-evader problem (see [14, 15]) is analogous to the *indirect* herding problem. In these results, uncontrollable evaders are essential to the system objective, but don't cooperate to achieve it. In contrast to this dissertation, the vast majority of these results aim to capture (intercept) the evaders. The objective in this dissertation entails both the capture and regulation of agents.

There are some results that examine the pursuer-evader problem with a herding-like objective. The results in [16–20] include the requirement that interception must occur at a specified location. Since only the pursuer agents are controllable, these herding pursuer-evader problems can also be labeled as *indirect* herding problems.

Motivated by observations from nature and heuristic experimental development (cf. [21–25]), several solution methods have been developed for *indirect* herding

problems. In [16], the *indirect* herding pursuer-evader problem is solved for a single pursuer and single evader with known dynamics by solving an on-line optimal control problem. Approaches such as [17–19] solve the indirect herding pursuer-evader problem by using off-line numerical solutions to a differential game where there are equal or more pursuers that chase evaders with known dynamics. In [26], the authors employ sliding-mode control strategies to achieve asymptotic regulation of the targets, but the results depend on the presence of more pursuers than evaders. The result in [20] extends the problem to allow for more evaders than pursuers but the extra evaders aren't necessarily guaranteed to be captured. A stability proof is provided for pursuit of a single evader in [27], but the result relies on multiple pursuers, only considers linear target dynamics without uncertainty, and the objective ends upon capture, regardless of location. The solution in [13] develops a forcing function, based on two or more herders forming an arc, that is used to direct a single target along a desired trajectory. The result in [1] uses a similar arc-based approach to regulate the mean location of a larger herd to a desired goal by considering the entire herd as a single unicycle.

1.2 Contributions

The work in this dissertation seeks to solve the *indirect* herding problem with more target agents than herders. The fact that the herders are outnumbered motivates the use of a switched systems analysis to develop dwell time conditions which dictate how long the herder can chase any given target before it must switch to another target, which is unnecessary when the herder team isn't outnumbered by the targets (cf., [13, 16–19]). While the development is agnostic to the specific design of the switching strategy, a key contribution in this dissertation is in the development of the sufficient dwell time conditions in each of the following chapters.

In this dissertation, the interaction between the herder and targets are modeled using artificial potential fields [28]. In Chapter 2, a robust controller and dwell time

conditions are developed to control one herder to guarantee convergence of multiple targets to unique goal locations. The uncertainties in the system are compensated for using sliding-mode control. The development in Chapter (2) is the first use of switched systems methods to address the herding problem in scenarios where the herder is outnumbered.

Chapter 3 presents a solution to the same problem, using adaptive rather than robust methods. An integral concurrent learning (ICL) scheme eliminates the need for the persistence of excitation (PE) condition usually associated with traditional adaptive control, and instead requires that a finite excitation (FE) condition, which can be verified online and satisfied in finite time, be satisfied. The ICL is used to improve the parameter estimation and facilitate the switched systems analysis, yielding dwell time conditions that must be satisfied to ensure uniformly ultimately bounded convergence.

The work in Chapter 4 extends the results in the previous chapters by further generalizing the dynamics. The uncertain functions that represent target/herder interaction and flocking or other behaviors are learned online using NN approximation methods and ICL. Dwell time conditions similar to those in Chapter 3 also yield ultimately bounded convergence.

In Chapter 5, a two-phase herding problem is examined for a team of n_h herders and n_t targets, for $n_h < n_t$. First, the herders are tasked with the goal of grouping the targets using methods from the previous chapters, and then relocating them as a single herd to a desired goal location. The second phase uses a similar approach as in [1, 13], albeit considering multiple agents with uncertain dynamics. The ultimately bounded convergence in the grouping phase, combined with asymptotic stability in the relocating phase, makes it possible to guarantee all targets are regulated to a neighborhood about the goal location.

CHAPTER 2 SINGLE AGENT HERDING OF N-AGENTS: A SWITCHED SYSTEMS APPROACH

In this chapter, the interaction between the herder and targets is modeled as a nonlinear function similar to a navigation function, and then a robust controller is developed based on a Lyapunov-based analysis. One herder and multiple targets are considered and exponential regulation of the targets is guaranteed through a switched-systems framework. Since the herder is outnumbered, a challenge arises from the fact that the continuous target dynamics will be affected by the discontinuities in the requisite switching signal. This challenge is overcome using switched systems analysis for subsystems with common Lyapunov functions. The main contribution of this chapter is in the development of sufficient dwell time conditions of the herder's switching signal, which must be met to ensure exponential regulation of every target. Moreover, the analysis is agnostic to the design of the herding strategy.

2.1 Problem Formulation

The overall strategy is to model the target agents motion based on their tendency to be repelled by the herder, as well as their tendency to escape; design a control law for the herder such that it leverages its position to drive a target to a desired location; and develop switching conditions for the herding agent to ensure the regulation of multiple agents to their respective goal locations. This chapter presents a solution using a robust sliding mode controller to compensate for uncertainties in the target motion model, as well as an average dwell time condition that must be met to ensure overall exponential convergence of each target agent.

A single herding agent is tasked with regulating $n_t > 1$ fleeing targets to a specified goal location. Each target's state is denoted by $x_i \in \mathbb{R}^n$, with specified goal location $x_i^g \in \mathbb{R}^n$, $i \in \{1, 2, \dots, n_t\}$, and the herder state is $y \in \mathbb{R}^n$. To quantify the herding objective, the error between the i^{th} target agent and its specified goal location is defined

as

$$\bar{x}_i = x_i - x_i^g. \quad (2-1)$$

The herder is to be controlled such that each target agent is individually regulated toward its specified goal location, but is only able to pursue one target at a time, meaning that $n_t - 1$ targets flee without pursuit at a given time.

The herder selects a single target to chase at any given time. The herder will switch to another target based on a switching signal that meets the developed dwell time conditions. The currently *chased* target's interaction with the herder is modeled by a nonlinear function of the distance between the target and herder, while an additional term in the dynamics represents the target's desire to flee the goal location. While many models for the target motion could be considered, the model in this chapter is based on the following properties.

Property 1. The targets are content to stay at rest when the herder is not nearby.

Property 2. The targets are inclined to escape the goal location.

Property 3. The targets seek to avoid the herder.

Assumption 2.1. The herder has approximate knowledge of each target's dynamics (i.e. the dynamics contain parametric uncertainty).

Based on Properties 1-3, and using (2-1), the motion of the i^{th} target when it is the currently *chased* target can be modeled as

$$\dot{x}_i = -\alpha_{i0} \nabla_{x_i} \phi(x_i, y) + \beta_i \bar{x}_i \phi(x_i, y), \quad (2-2)$$

where $\phi : \mathbb{R}^n \times \mathbb{R}^n \rightarrow \mathbb{R}$ is a nonlinear kernel function, $\nabla_{x_i}(\bullet)$ is the column vector representation of the spatial gradient operator with respect to x_i , and $\alpha_{i0} \in \mathbb{R}^+$ and $\beta_i \in \mathbb{R}^+$, $i \in \{1, 2, \dots, n_t\}$ are unknown positive constant parameters with known bounds. The first term in (2-2) models the repulsion interaction between the herder and the chased target, while the second term represents the target's tendency to escape from the origin. The currently *chased* target's tendency to repel the herder is captured by a

Gaussian kernel, defined as

$$\phi(x_i, y) \triangleq \exp(-\chi_i), \quad (2-3)$$

where

$$\chi_i \triangleq \frac{1}{2\sigma^2} (x_i - y)^T (x_i - y), \quad (2-4)$$

and $\sigma^2 \in \mathbb{R}^+$ is a known parameter of the Gaussian kernel. The model in (2-2) satisfies the abstract qualities in Properties 1-3. While the subsequent development is based on the model, the strategy used in this chapter can also be applied to more generalized models.

Taking the gradient of the first term in (2-2), using (2-3), and simplifying yields

$$\dot{x}_i = \alpha_i (x_i - y) e^{-\chi_i} + \beta_i \bar{x}_i e^{-\chi_i}, \quad (2-5)$$

where $\alpha_i = \frac{\alpha_{i0}}{\sigma^2}$. The parameters $\alpha_i, \beta_i \forall i \in \{1, 2, \dots, n_t\}$ for each agent share common upper and lower bounds (denoted by $(\bar{\bullet})$ and $(\underline{\bullet})$, respectively) $\bar{\alpha} \in \mathbb{R}^+, \underline{\alpha} \in \mathbb{R}^+, \bar{\beta} \in \mathbb{R}^+$, and $\underline{\beta} \in \mathbb{R}^+, .$ Due to the nature of the Gaussian kernel, the escape term in (2-5) is mitigated as $\|x_i - y\|$ tends to infinity, which causes the agent to escape less quickly, and is maximized as $\|x_i - y\|$ tends to zero, representing the target's desire to escape as the herder closes in.

Similarly, the other $n_t - 1$ targets also have a desire to flee the goal location, but since they aren't actively being chased by the herder, they will not be repelled from the herder as strongly as the currently *chased* target. These other targets, called the *unchased* targets, will behave according to the motion model

$$\dot{x}_i = \gamma \alpha_i (x_i - y) e^{-\chi_i} + \beta_i \bar{x}_i e^{-\chi_i}, \quad (2-6)$$

where $\gamma \in (0, 1)$ is a known parameter that scales the effect of the herder on an *unchased* target. Similar to (2-2), it is clear that the model in (2-6) also satisfies Properties 1-3.

The motion of the herder is governed by the following single integrator dynamics

$$\dot{y} = u_y, \quad (2-7)$$

where $u_y \in \mathbb{R}^n$ is the control input for the herder.

2.2 Control Objective

To complete the herding task as defined, the control objective is to design a controller for the herding agent which ensures that all of the target agents are exponentially regulated to a specified goal location, using the position of each agent as feedback. This will be accomplished by first analyzing the convergence of each target individually, and use switched-systems analysis tools to develop dwell time conditions that the herder uses to develop a switching strategy between target agents such that all targets are regulated to their goal. Since the *chased* target agent dynamics in (2-2) do not directly contain a control input, a backstepping strategy is used to inject the desired herder state as a virtual controller, $y_d \in \mathbb{R}^n$, into (2-5) in an effort to regulate the *chased* target to its goal location. The mismatch between the actual and desired herder state is quantified by the backstepping error

$$e_y(t) \triangleq y_d(t) - y(t), \quad (2-8)$$

which will be driven to zero exponentially fast using an adaptive controller with integral concurrent learning to compensate for uncertainties in the target's motion model.

2.3 Control Development

Since each target's goal location is static, it is trivial to see that the time derivative of (2-1) is equivalent to the currently *chased* target's dynamics in (2-5). Thus, using (2-8), the time derivative of (2-1) can be rewritten for the *chased* target with the injected virtual control term as

$$\dot{\bar{x}}_i = \alpha_i \left(x_i + e_y - y_d + \frac{\beta_i}{\alpha_i} \bar{x}_i \right) e^{-\lambda_i}. \quad (2-9)$$

When the i^{th} target is the currently *chased* target, it behaves according to (2-9). To influence this target, the herder's desired state is designed as

$$y_d = K_1 \bar{x}_i + x_i^g, \quad (2-10)$$

where $K_1 = k_1 + k_2$, $k_1, k_2 \in \mathbb{R}^+$ are constant positive control gains. Using (2-10), (2-9) can be rewritten as

$$\dot{\bar{x}}_i = \alpha_i \left(-k_1 \bar{x}_i - \left(k_2 - \left(\frac{\beta_i}{\alpha_i} + 1 \right) \right) \bar{x}_i + e_y \right) e^{-\alpha_i t}. \quad (2-11)$$

To ensure that the herder trajectory follows the desired state, the backstepping dynamics must also be considered. Taking the time derivative of (2-8), and using (2-5) and (2-7), yields

$$\begin{aligned} \dot{e}_y &= \dot{y}_d - \dot{y} \\ &= K_1 (\alpha_i (x_i - y) + \beta_i \bar{x}_i) e^{-\alpha_i t} - u_y. \end{aligned} \quad (2-12)$$

The herder's control law is then designed as

$$u_y = k_y e_y + \bar{x}_i e^{-\alpha_i t} + \text{sgn}(e_y) e^{-\alpha_i t} (k_3 \|x_i - y\| + k_4 \|\bar{x}_i\|), \quad (2-13)$$

where $k_y, k_3, k_4 \in \mathbb{R}^+$ are constant positive control gains. Substituting (2-13) into (2-12) yields the closed-loop backstepping dynamics

$$\dot{e}_y = K_1 (\alpha_i (x_i - y) + \beta_i \bar{x}_i) e^{-\alpha_i t} - k_y e_y - \bar{x}_i e^{-\alpha_i t} - \text{sgn}(e_y) e^{-\alpha_i t} (k_3 \|x_i - y\| + k_4 \|\bar{x}_i\|). \quad (2-14)$$

2.4 Stability Analysis

In the following stability analysis, convergence of the subsystems will be examined before switched systems analysis tools are used to show overall stability. In Section 2.4.1, Theorem 2.1 proves that the i^{th} target is exponentially regulated to the origin when it is the currently *chased* target. Theorem 2.2 in Section 2.4.2 shows that when

the i^{th} target is an *unchased* target, it's trajectory is exponentially unstable. Finally, in Section 2.4.3, Theorem 2.3 provides an overall exponential bound for the i^{th} target, provided that dwell time conditions are met.

2.4.1 Convergence of Currently *Chased* Target

In this section, an exponential bound is developed for the *chased* target, using a sliding mode controller to compensate for the uncertainties in the system.

Theorem 2.1. *The controller given in (2–10) and (2–13) ensures that all system signals are bounded under closed-loop operation and that the currently chased target is globally exponentially regulated in the sense that*

$$\|\bar{x}_i(t)\| \leq \sqrt{\frac{\lambda_2}{\lambda_1}} \|z_i(0)\| \exp\left(-\frac{\lambda_s}{2}t\right), \quad (2-15)$$

where λ_s is a positive constant decay rate, and

$$z_i \triangleq \begin{bmatrix} \bar{x}_i^T & e_y^T \end{bmatrix}^T,$$

provided that the gains are selected according to the sufficient conditions

$$k_2 \geq \frac{\bar{\beta}}{\underline{\alpha}} + 1, \quad k_3 \geq K_1 \bar{\alpha}, \quad k_4 \geq K_1 \bar{\beta}. \quad (2-16)$$

Proof. Let $V_i^s : \mathbb{R}^n \times \mathbb{R}^n \rightarrow \mathbb{R}$ be a positive definite, continuously differentiable candidate Lyapunov function, defined as

$$V_i^s(z_i(t)) \triangleq \frac{1}{2\alpha_i} \bar{x}_i^T \bar{x}_i + \frac{1}{2} e_y^T e_y, \quad (2-17)$$

which can be bounded as

$$\lambda_1 \|z_i(t)\|^2 \leq V_i^s(z_i(t)) \leq \lambda_2 \|z_i(t)\|^2, \quad (2-18)$$

where $\lambda_1 = \min \left\{ \frac{1}{2\bar{\alpha}}, \frac{1}{2} \right\}$ and $\lambda_2 = \max \left\{ \frac{1}{2\bar{\alpha}}, \frac{1}{2} \right\}$. Using (2-11) and (2-14), the time derivative of (2-17) can be written as

$$\begin{aligned} \dot{V}_i^s = & -k_1 \bar{x}_i^T \bar{x}_i e^{-\chi_i} - \left(k_2 - \left(\frac{\beta_i}{\alpha_i} + 1 \right) \right) \bar{x}_i^T \bar{x}_i e^{-\chi_i} + \bar{x}_i^T e_y e^{-\chi_i} \\ & - k_y e_y^T e_y - e_y^T \bar{x}_i e^{-\chi_i} + K_1 \alpha_i e_y^T (x_i - y) e^{-\chi_i} + K_1 \beta_i e_y^T \bar{x}_i e^{-\chi_i} \\ & - \text{sgn}(e_y) (k_3 \|x_i - y\| + k_4 \|\bar{x}_i\|) e^{-\chi_i}. \end{aligned} \quad (2-19)$$

Provided that the gain conditions (2-16) are satisfied, and using the fact that $e^{-\chi_i} \leq 1$, $\forall i \in \{1, 2, \dots, n_t\}$, (2-19) can be upper bounded as

$$\dot{V}_i^s \leq -k_1 \|\bar{x}_i\|^2 e^{-\chi_i} - k_y \|e_y\|^2. \quad (2-20)$$

Since $V_i^s \geq 0$ and $\dot{V}_i^s \leq 0$, $V_i^s \in \mathcal{L}_\infty$; therefore, $\bar{x}_i, e_y \in \mathcal{L}_\infty$. Since $\bar{x}_i \in \mathcal{L}_\infty$, $y_d \in \mathcal{L}_\infty$ from (2-10), and since $e_y, y_d \in \mathcal{L}_\infty$, $y \in \mathcal{L}_\infty$ from (2-8); hence, using (2-4), $\chi_i \in \mathcal{L}_\infty$. Based on these facts, the controller in (2-13) is bounded. Since $\chi_i \in \mathcal{L}_\infty$,

$$\exists \bar{\chi}_i > 0 : \chi_i(t) \leq \bar{\chi}_i \quad \forall t. \quad (2-21)$$

Using (2-21), (2-20) can be upper bounded as

$$\dot{V}_i^s \leq -\lambda_3 \|z_i\|^2, \quad (2-22)$$

where $\lambda_3 = \min \{k_1 c, k_y\}$, and $c = \min_i e^{-\bar{\chi}_i}$. From (2-18), (2-22) can be upper bounded as

$$\dot{V}_i^s \leq -\lambda_s V_i^s, \quad (2-23)$$

where $\lambda_s = \frac{\lambda_3}{\lambda_2}$. Using the Comparison Lemma [29, Lemma 3.4] on (2-23), and upper bounding yields (2-15). \square

2.4.2 Divergence of *Unchased* Target

The analysis in the following section provides an exponentially unstable bound for *unchased* targets.

Theorem 2.2. *Based on the motion model in (2–6), the trajectory of each unchased target will behave according to the exponential bound*

$$\|\bar{x}_i(t)\| \leq \sqrt{\frac{\lambda_5}{\lambda_4}} \|z_i(0)\| \exp\left(\frac{\lambda_u}{2}t\right), \quad (2-24)$$

where λ_u is a positive constant growth rate.

Proof. Let $V_i^u : \mathbb{R}^n \times \mathbb{R}^n \rightarrow \mathbb{R}$ be a positive definite, continuously differentiable candidate Lyapunov function defined as

$$V_i^u(z_i(t)) \triangleq \frac{1}{2\beta_i} \bar{x}_i^T \bar{x}_i + \frac{1}{2} e_y^T e_y, \quad (2-25)$$

which can be bounded as

$$\lambda_4 \|z_i(t)\|^2 \leq V_i^u(z_i(t)) \leq \lambda_5 \|z_i(t)\|^2,$$

where $\lambda_4 = \min\left\{\frac{1}{2\beta}, \frac{1}{2}\right\}$ and $\lambda_5 = \max\left\{\frac{1}{2\beta}, \frac{1}{2}\right\}$. Using (2–6) and (2–14), and provided that the second and third gain conditions in (2–16) are satisfied, the time derivative of (2–25) can be upper bounded by

$$\dot{V}_i^u \leq \left(\frac{(3+K_1)\gamma\bar{\alpha}}{2\beta} + 1\right) \|\bar{x}_i\|^2 + \left(\frac{\gamma\bar{\alpha} + \bar{\beta}}{2\beta} - k_y\right) \|e_y\|^2 + \left(\frac{K_1\gamma\bar{\alpha} + \bar{\beta}}{2\beta}\right) \|\bar{x}_c\|^2, \quad (2-26)$$

where the terms with the subscript c refer to the currently *chased* target (since the i^{th} target is an *unchased* target for the analysis in this section). Since the currently *chased* target trajectory is bounded by (2–15) in Section 2.4.1, (2–26) can be further upper bounded by

$$\dot{V}_i^u \leq \lambda_6 \|z_i\|^2 + \frac{\lambda_2}{\lambda_1} \left(\frac{K_1\gamma\bar{\alpha} + \bar{\beta}}{2\beta}\right) \|z_i(0)\|^2 \exp(-\lambda_s t), \quad (2-27)$$

where $\lambda_6 = \max\left\{\frac{(3+K_1)\gamma\bar{\alpha}}{2\beta} + 1, \frac{\gamma\bar{\alpha} + \bar{\beta}}{2\beta} - k_y\right\}$. Then, (2–27) can be further simplified and upper bounded to yield (2–24). □

2.4.3 Target Switched Systems Analysis

Consider the convergence and divergence analysis of the i^{th} target in Sections 2.4.1 and 2.4.2, respectively. To facilitate the following stability analysis, let $T_i^u(t, \tau)$ denote the maximum total time that the i^{th} target is permitted to be unstable (i.e. to be *unchased*) during the time interval $[\tau, t)$, where $0 \leq \tau \leq t$. Additionally, let $N_{\sigma_i}(t, \tau) \in \mathbb{N}$ denote the number of times that the i^{th} target can switch between being *chased* or *unchased* in the interval $[\tau, t)$. The i^{th} target's switching signal

$$\sigma_i : [0, \infty) \rightarrow \{s, u\}, \quad (2-28)$$

where s denotes the stable dynamics, and u denotes the unstable dynamics, has an average dwell time τ_{ai} if there exist constants $N_{0i}, \tau_{ai} \in \mathbb{R}_{>0}$ such that

$$N_{\sigma_i}(t, \tau) \leq N_{0i} + \frac{t - \tau}{\tau_{ai}}, \quad \forall t \geq \tau \geq 0$$

(see [30]). The following switched systems analysis will provide an exponentially stable bound for the overall trajectory of the i^{th} target.

Theorem 2.3. *The i^{th} target's switched system, $\dot{x}_i = f_{\sigma_i}(x_i, y)$, given by (2-5) and (2-6), for the stable and unstable systems, respectively, and the piece-wise constant, right continuous switching signal (2-28) is globally exponentially stable as long as the total time spent in the unstable subsystem satisfies*

$$T_i^u(t, \tau) \leq T_{0i} + \rho(t - \tau), \quad \forall t \geq \tau \geq 0, \quad (2-29)$$

and the average dwell time satisfies

$$\tau_a > \frac{\ln \mu}{\lambda_s(1 - \rho) - \lambda_u \rho},$$

where $T_{0i} \in \mathbb{R}^+$ is an arbitrary positive constant, and $\rho, \lambda_s, \lambda_u, \mu \in \mathbb{R}^+$ are known positive constants that satisfy $\mu \geq 1$ and $\rho < \frac{\lambda_s}{\lambda_s + \lambda_u}$. Then, the overall trajectory of the i^{th} target

can be bounded by

$$\|\bar{x}_i(t)\| \leq \Lambda_i \|z_i(0)\| \exp(-\lambda t), \quad (2-30)$$

where $\Lambda_i \triangleq \left[\frac{\lambda_2}{\lambda_1} \mu^{N_{0i}} \exp((\lambda_s + \lambda_u) T_{0i}) \right]^{\frac{1}{2}} \in \mathbb{R}_{>0}$ and $\lambda \triangleq \frac{1}{2} \left(\lambda_s - (\lambda_s + \lambda_u) \rho - \frac{\ln \mu}{\tau_a} \right) \in (0, (1 - \rho) \lambda_s + \rho \lambda_u) \subset \mathbb{R}_{>0}$.

Proof. Exponential bounds have been established for *chased* and *unchased* agents.

From (2-17) and (2-25), it can be shown that $V_i^p \leq \mu V_i^q, \forall p, q \in \{s, u\}, \forall i \in \{1, 2, \dots, n_t\}$, where $\mu \triangleq \frac{\lambda_5}{\lambda_1}$. The remainder of the proof is omitted, as it is almost identical to [31, Lemma 1], with the exception that the class \mathcal{K}_∞ functions, α_1 and α_2 , are quadratic (see [32]), thus (2-30) is achieved. \square

Remark 2.1. The time constraint for the unstable subsystem (2-29) can trivially be satisfied in any practical application of this development. As T^u increases by necessity, T_0 can be increased arbitrarily to compensate. However, it is important to note that as $t \rightarrow \infty$, this constraint invokes the condition that each target must spend more time (after adjusting based on growth and decay rates of the subsystems), on average, in the stable subsystem than in the unstable system.

2.5 Simulation Results

Numerical simulation results are presented for the case of one herder pursuing $n_t = 3$ targets in a three-dimensional workspace. According to the selected gains shown in Table 2-1, and the parameters of the system shown in Table 2-2, the minimum average dwell time that meets the sufficient condition for each target agent is $\tau_{a,req} > 2.56$ s. Compare this to the values in Table 2-3 showing that each target's average dwell time satisfied these conditions in the following simulation. The switching law for the herder in this example is based on the distance of each target from the origin. Specifically, the herder selects the target furthest from the origin initially, regulates that target to a ball that is 10% (a design parameter) of the target's previous distance from the origin, switches to the furthest target at that time, and repeats. The initial

conditions for the 2D simulation were $x_1(0) = \begin{bmatrix} 0.2 & 1.9 \end{bmatrix}^T$, $x_2(0) = \begin{bmatrix} 0.5 & -1.8 \end{bmatrix}^T$,
 $x_3(0) = \begin{bmatrix} -1.5 & -0.6 \end{bmatrix}^T$, $y(0) = \begin{bmatrix} 1.1 & 1.7 \end{bmatrix}^T$, while the initial conditions for the
3D simulation were $x_1(0) = \begin{bmatrix} -1.7 & 0.2 & 0.5 \end{bmatrix}^T$, $x_2(0) = \begin{bmatrix} 2.1 & 1.1 & -0.5 \end{bmatrix}^T$,
 $x_3(0) = \begin{bmatrix} 0.2 & 1.8 & 2.3 \end{bmatrix}^T$, $y(0) = \begin{bmatrix} 0.8 & 0.9 & 3.1 \end{bmatrix}^T$.

Table 2-1. Simulation gains

k_1	k_2	k_3	k_4	k_y
2	1.125	0.25	2.2	0.5

Table 2-2. System parameters

Parameter	σ^2	α	β	γ
Value	2	1	0.2	0.2
Bounds	N/A	$\underline{\alpha} = 0.75, \bar{\alpha} = 1.25$	$\bar{\beta} = 0.35$	N/A

Table 2-3. Average dwell times

Simulation	$\tau_{a,req}$	$\tau_{a1,act}$	$\tau_{a2,act}$	$\tau_{a3,act}$
2-D	2.56	2.76	2.84	2.73
3-D	2.56	2.79	2.81	2.83

The following figures show the results for the designed controller. Figures 2-1 and 2-2 show the norm of the states and the overall path of the agents when using the robust controller with three target agents in two-dimensional space. Figures 2-3 and 2-4 show the norm of the states and the overall path of the agents when using the robust controller with three target agents in three-dimensional space.

Additionally, Monte Carlo simulations were performed to finely tune the controller for various scenarios. Each simulation was run with one herder and eight targets, driven to

an 'X' formation. Random gain selection was performed over 5,000 iterations for each simulation and the cost function $J = \int_0^{t_f} (\bar{x}^T \bar{x} + u_y^T u_y) dt$ was compared. Table 2-4 shows the quantitative results.

Table 2-4. Monte Carlo simulations

Simulation	α	β	γ	γ_r	J_{ave}
1	1.0	0.1	0.1	0.25	40.3
2	1.0	0.1	0.1	0.25	35.8
3	1.0	0.1	0.1	0.25	32.5
4	1.0	0.1	0.3	0.50	63.1
5	1.0	0.1	0.3	0.50	58.3
6	1.0	0.1	0.3	0.50	51.2
7	1.0	0.5	0.5	0.75	96.8
8	1.0	0.5	0.5	0.75	94.6
9	1.0	0.5	0.5	0.75	92.2

2.6 Concluding Remarks

A robust controller and switching conditions were synthesized using Lyapunov-based stability analysis for a single herding agent to ensure global exponential regulation of n_t uncertain target agents to the origin, despite their tendency to flee and lack of explicit control input. Simulation results demonstrate the validity of the results given for an example herder strategy.

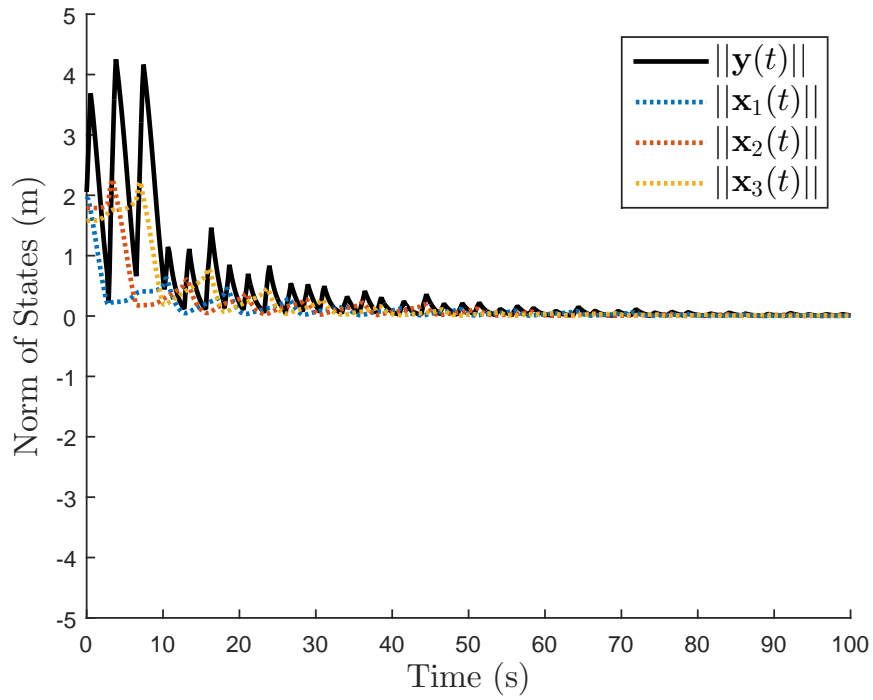


Figure 2-1. The states of the herder and targets using the robust controller in a two-dimensional workspace.

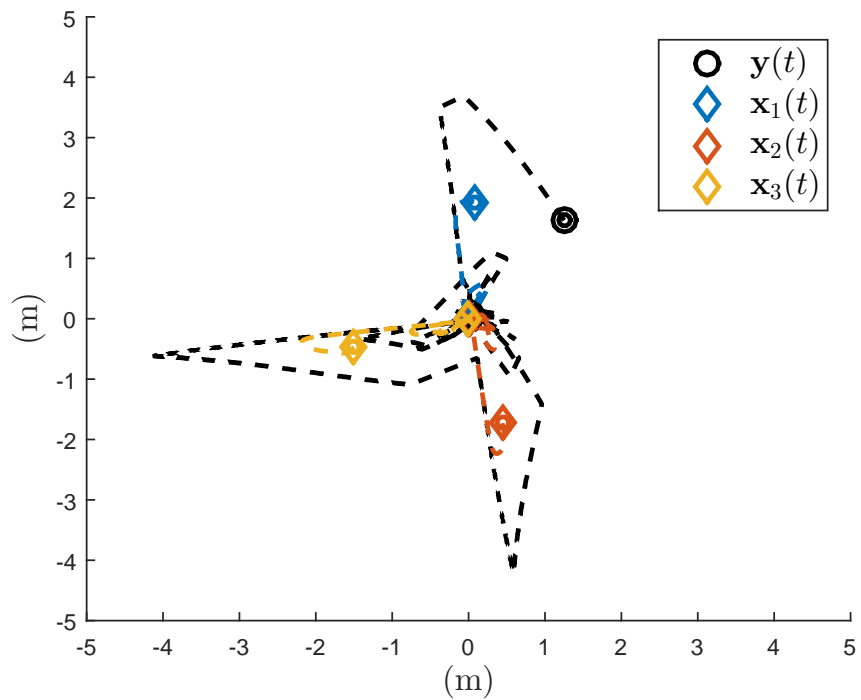


Figure 2-2. Two-dimensional plot of the paths of the herder and targets using the robust controller.

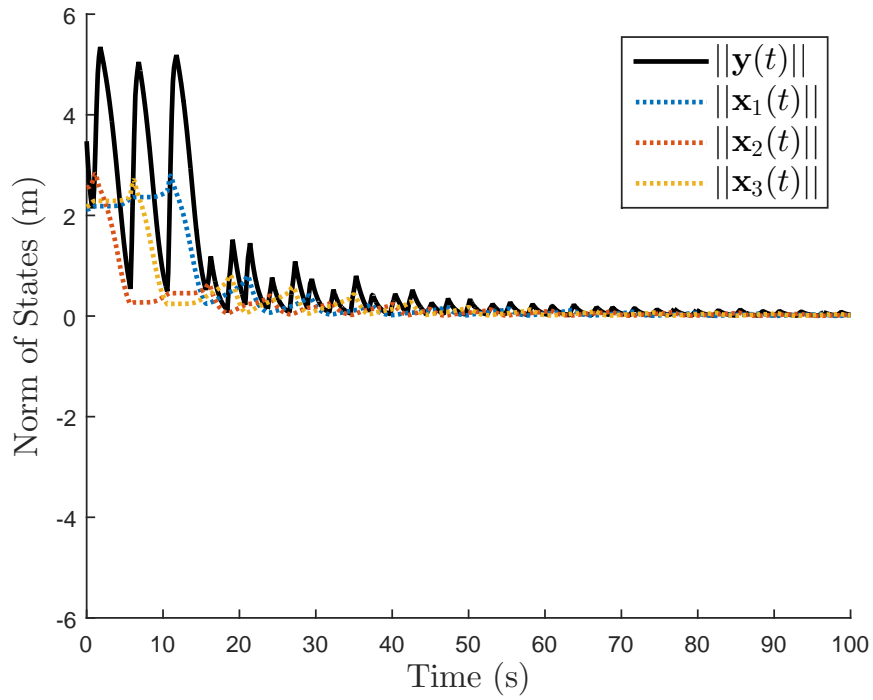


Figure 2-3. The states of the herder and targets using the robust controller in a three-dimensional workspace.

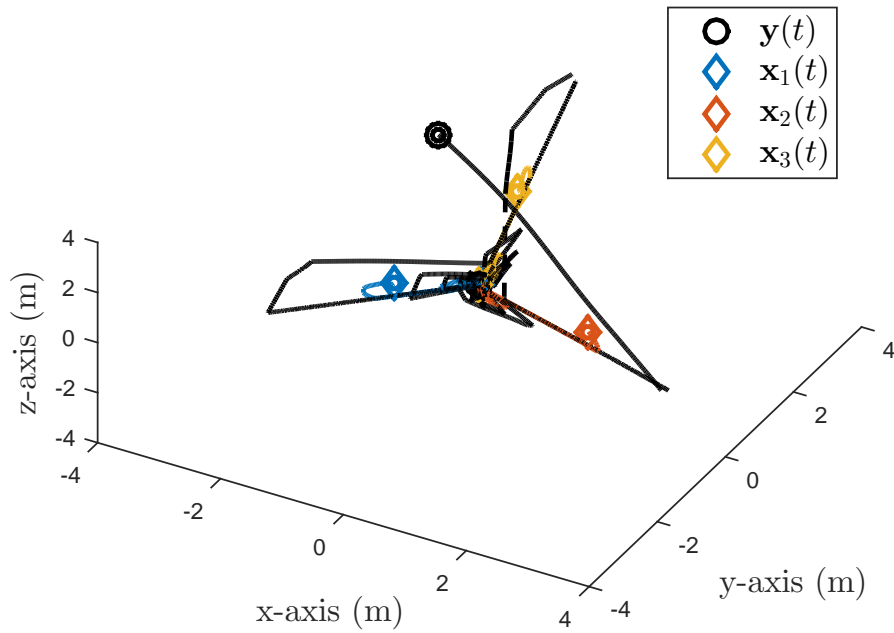


Figure 2-4. Three-dimensional plot of the paths of the herder and targets using the robust controller.

CHAPTER 3 SWITCHED ADAPTIVE HERDING OF N-AGENTS WITH INTEGRAL CONCURRENT LEARNING

In this chapter, an adaptive controller with ICL is developed for the same system as in Chapter 2, yielding uniformly ultimately bounded regulation of the target states to their unique goal location. The use of the ICL scheme eliminates the traditional (and unverifiable) PE condition that is usually necessary in adaptive control, and replaces it with an FE condition that can be verified online. The ICL improves the parameter estimation and facilitates the switched systems analysis.

3.1 Problem Formulation

The herder agent is tasked with regulating $n_t > 1$ targets to a goal location. Each target state is denoted by $x_i \in \mathbb{R}^n$, with a respective constant goal location $x_i^g \in \mathbb{R}^n$, $i \in \{1, 2, \dots, n_t\}$, and the herder state is $y \in \mathbb{R}^n$, where n is the dimensionality of the system. The target, goal, and herder states are assumed to be measurable (available for feedback control). To quantify the control objective, the herding error for each target, denoted by $\bar{x}_i \in \mathbb{R}^n$, is defined as

$$\bar{x}_i \triangleq x_i - x_i^g. \quad (3-1)$$

Unlike leader-follower networks where each agent's interaction is controlled, in the *indirect* herding problem, only the herder's action is controlled and each target's interaction with the herder is inherent to the dynamics of the target. For simplicity¹, the herder dynamics are given by $\dot{y} = u_y$, where $u_y \in \mathbb{R}^n$ is the subsequently developed herder control input. Each target's dynamic model is assumed to have several qualitative behaviors: targets are repelled by the herder, targets are repelled by the goal location, and

¹ The control development can be generalized to include herder dynamics (e.g., Euler-Lagrange dynamics) through modifications of the controller and stability results using known methods. Single integrator dynamics are used for simplicity and to focus on the technical challenges uniquely associated with the herding problem without involving additional (more common) challenges associated with herder dynamics.

otherwise the target remains at rest (i.e., as the norm of the herder distance to a target agent approaches infinity, the target dynamics approach zero).

Remark 3.1. The qualitative behaviors of the target agents are inspired by practical considerations and behaviors often seen in nature. The assumption that the targets are repelled by the herder is inherent to any herding problem (e.g., prey flee predators, sheep run from a herding dog) and additionally the targets will want to avoid the goal location (e.g., fish do not want to be herded to shallow water by dolphins). Target agents are considered to be content with their current position (e.g., an animal grazing) when the herder is not nearby, and therefore will remain in their current location. The Gaussian potential functions and exponentials used in (3–2) are commonly used functions (e.g., in path planning literature) to quantify such behaviors. However, other more generalized models are examined in subsequent chapters.

Given the objective to have one herder regulate the position of n_t targets, a unique challenge is that the herder is required to switch between target agents. The subsequent development assumes that the targets know when they are being chased, and in general, may respond differently when chased. That is, another qualitative behavior is a target may exhibit a more aggressive repulsion from the herder when chased.

To quantify this distinct behavior, let $t_{i,k}^c \in \mathbb{R}$ and $t_{i,k}^u \in \mathbb{R}$ denote the k^{th} instance when the i^{th} target is switched to the *chased* or *unchased* mode, respectively, where $k \in \mathbb{N}$. The contiguous dwell time in the k^{th} activation of the i^{th} target operating in the *chased* or *unchased* mode is denoted by $\Delta t_{i,k}^c \in \mathbb{R}$ and $\Delta t_{i,k}^u \in \mathbb{R}$, and defined as $\Delta t_{i,k}^c \triangleq t_{i,k}^u - t_{i,k}^c$ and $\Delta t_{i,k}^u \triangleq t_{i,k+1}^c - t_{i,k}^u$, respectively. The total amount of time each of these modes is active between switching instances a and b are denoted $T_i^c(a, b) \triangleq \sum_{l=a}^b \Delta t_{i,l}^c$ and $T_i^u(a, b) \triangleq \sum_{l=a}^b \Delta t_{i,l}^u$, respectively. To quantify the aforementioned

qualitative characteristics, the i^{th} target dynamics are modeled as

$$\dot{x}_i = \begin{cases} (\alpha_i (x_i - y) + \beta_i \bar{x}_i) e^{-\chi_i} & t \in [t_{i,k}^c, t_{i,k}^u) \\ (\gamma \alpha_i (x_i - y) + \beta_i \bar{x}_i) e^{-\chi_i} & t \in [t_{i,k}^u, t_{i,k+1}^c) \end{cases}, \quad (3-2)$$

$\forall k \in \mathbb{N}$, where $\gamma \in [0, 1]$ is a known parameter² that scales the repulsion effect of the herder on the targets operating in *unchased* mode, $\alpha_i \in \mathbb{R}$ and $\beta_i \in \mathbb{R}$, $i \in \{1, 2, \dots, n_t\}$ are unknown positive constant parameters with common (without loss of generality) upper and lower bounds denoted by $(\bar{\cdot})$ and $(\underline{\cdot})$, respectively, defined as $\bar{\alpha}$, $\underline{\alpha}$, $\bar{\beta}$, and $\underline{\beta}$, and the auxiliary function $\chi_i : \mathbb{R}^n \times \mathbb{R}^n \rightarrow \mathbb{R}$ is defined as $\chi_i \triangleq \frac{1}{2\sigma^2} (x_i - y)^T (x_i - y)$, where $\sigma^2 \in \mathbb{R}$ is a known positive constant that determines the radial size of the Gaussian potential function $e^{-\chi_i}$. The first term in each equation in (3-2) is a gradient of the Gaussian potential that models the repulsion interaction between the herder and the i^{th} target, while the second term represents the target's tendency to escape from the goal. To facilitate the subsequent control design and stability analysis, the uncertain parameters in (3-2) are grouped into the uncertain vector $\theta_i \in \mathbb{R}^2$ as $\theta_i \triangleq \begin{bmatrix} \alpha_i & \beta_i \end{bmatrix}^T$, while $\hat{\theta}_i \in \mathbb{R}^2$ denotes a subsequently designed adaptive estimate of θ_i , and $\tilde{\theta}_i \in \mathbb{R}^2$ denotes the estimation error, defined as $\tilde{\theta}_i \triangleq \theta_i - \hat{\theta}_i \forall i \in \{1, 2, \dots, n_t\}$.

Remark 3.2. The following design strategy can be applied to more generalized models, as long as certain properties that are standard in Lyapunov switching stability analysis (e.g., continuous dynamics between switches) or unique to this problem (e.g., error term $x_i - y$ present in the target dynamics to facilitate backstepping) are satisfied. The first term in (3-2) is derived from taking the negative gradient of a potential function of the square of the norm of the error term $x_i - y$. The gradient of various kernel functions

² The scaling parameter γ is required to be known since it is unclear how to learn parameters during the periods in which a target operates in the *unchased* mode.

(Gaussian, Epanechnikov, etc.) satisfy this property. Moreover, function approximation strategies could be employed to learn models without a known form.

Given the different dynamics for the *chased* and *unchased* modes in (3–2), the subsequent development entails the design of a herding controller and switching conditions to ensure the switched system is stable. Since the target agent dynamics in (3–2) do not explicitly contain a control input, a backstepping strategy is used to inject the desired herder state as a virtual controller, $y_d \in \mathbb{R}^n$, into the dynamics of the target currently operating in the *chased* mode. Therefore, in addition to regulating the target herding error, the subsequent development also entails minimizing the backstepping error $e_y \in \mathbb{R}^n$, defined as

$$e_y(t) \triangleq y_d(t) - y(t). \quad (3-3)$$

3.2 Control Development

The following development is based on the strategy that the herder switches between targets to achieve the overall herding objective. Since the herder only chases one target at a time, the herder's controller always uses the i^{th} target as the *chased* target (i.e., unless otherwise stated, the development in this section considers that the i^{th} target is the one currently operating in *chased* mode ($t \in [t_{i,k}^c, t_{i,k}^u)$, $\forall k \in \mathbb{N}$)). To develop the controller, the *chased* target dynamics in (3–2), as well as the backstepping error in (3–3), are used to express the open-loop target herding error dynamics as

$$\dot{\tilde{x}}_i = \alpha_i \left(x_i + e_y - y_d + \frac{\beta_i}{\alpha_i} \tilde{x}_i \right) e^{-x_i}. \quad (3-4)$$

Based on (3–4) and the subsequent stability analysis, the herder's desired state is designed as

$$y_d \triangleq K_1 \tilde{x}_i + x_i^g, \quad (3-5)$$

where $K_1 = k_1 + k_2$ and k_1, k_2 are positive constant control gains. Using (3-5), (3-4) can be rewritten as

$$\dot{\bar{x}}_i = \alpha_i \left(-k_1 \bar{x}_i - \left(k_2 - \left(\frac{\beta_i}{\alpha_i} + 1 \right) \right) \bar{x}_i + e_y \right) e^{-\lambda_i}. \quad (3-6)$$

Given the herder's desired state in (3-5), the backstepping error dynamics can be determined by taking the time derivative of (3-3), and using the *chased* dynamics in (3-2) and the herder dynamics to obtain

$$\begin{aligned} \dot{e}_y &= K_1 (\alpha_i (x_i - y) + \beta_i \bar{x}_i) e^{-\lambda_i} - u_y \\ &= Y_i \theta_i - u_y, \end{aligned} \quad (3-7)$$

where $Y_i : \mathbb{R}^n \times \mathbb{R}^n \rightarrow \mathbb{R}^{n \times 2}$ is the regression matrix for the currently *chased* target, defined as $Y_i \triangleq \begin{bmatrix} K_1 (x_i - y) e^{-\lambda_i} & K_1 \bar{x}_i e^{-\lambda_i} \end{bmatrix}$, and θ_i contains the unknown parameters associated with the target currently operating in *chased* mode. Based on (3-7) and the subsequent stability analysis, the herder control law is designed as

$$u_y \triangleq k_y e_y + \bar{x}_i e^{-\lambda_i} + Y_i \hat{\theta}_i, \quad (3-8)$$

where k_y is a positive constant control gain. Using (3-8), the closed-loop backstepping dynamics are

$$\dot{e}_y = -k_y e_y - \bar{x}_i e^{-\lambda_i} + Y_i \tilde{\theta}_i. \quad (3-9)$$

The parameter estimate for the *chased* target $\hat{\theta}_i$ in (3-8) is generated from the ICL-based adaptive update law

$$\dot{\hat{\theta}}_i \triangleq \text{proj} \{ \Gamma Y_i^T e_y + k_{cl} \Gamma S_{cl} \} \quad (3-10)$$

where $\text{proj} \{ \cdot \}$ is a smooth projection operator, $S_{cl} \triangleq \sum_{j=1}^{N_i} \left(\mathcal{Y}_{ij}^T \left(K_1 (\bar{x}_i(t_j) - \bar{x}_i(t_j - \Delta t)) - \mathcal{Y}_{ij} \hat{\theta}_i \right) \right)$, $\Gamma \in \mathbb{R}^{2 \times 2}$ and $k_{cl} \in \mathbb{R}$ are constant, positive definite control gains, $N_i \in \mathbb{Z}$ is a constant that represents the number of saved data points for the data stack of the i^{th} target, $t_j \in [0, t]$ are time points between the

initial time and the current time, $\Delta t \in \mathbb{R}$ is a positive constant denoting the size of the window of integration, $\mathcal{Y}_{ij} \triangleq \mathcal{Y}_i(t_j) \in \mathbb{R}^{n \times 2}$ is the integrated regression matrix at $t = t_j$,

$$\mathcal{Y}_i(t) \triangleq \begin{cases} 0_{n \times 2} & t \in [0, \Delta t] \\ \int_{t-\Delta t}^t Y_i(x_i(\varsigma), y(\varsigma)) d\varsigma & t > \Delta t \end{cases}, \quad (3-11)$$

and $0_{n \times 2}$ denotes an $n \times 2$ matrix of zeros.

Remark 3.3. The first term in (3-10) is a traditional gradient-based adaptive control term, which uses the system error signal as feedback to estimate the unknown parameter vector θ_i and is used to cancel coupled terms in the stability analysis. A smooth projection operator is used to bound the adaptive update law to facilitate the analysis prior to parameter identification. See Remark 3.6 or Section 4.4 in [33] for details of the projection operator. The summation of terms are unique to integral concurrent learning and involve the use of recorded (concurrent to the controller execution) input/output data for parameter identification with finite excitation. In particular, \mathcal{Y}_{ij} refers to a single data point of the integral of the regression matrix Y_i , relaxing the need for measurement of higher order derivative terms (in this case velocity). Since integral concurrent learning is based on collecting input/output data, it can be employed independently of the dynamics of the model provided the uncertainty satisfies the linear-in-the-uncertain-parameters (LP) assumption. Moreover, as long as the system dimension is 2 or greater, the 2 unknown parameters could be computed using a least squares formulation (which requires the FE condition in this chapter) or by simply measuring the velocity at any instance that the target, herder, and goal are non-collinear, however it is not assumed that velocity measurements are available in this chapter (and the use of an ICL-based update law eliminates this requirement).

The data points that are saved are selected to maximize the minimum eigenvalue of $\sum_{j=1}^{N_i} (\mathcal{Y}_{ij}^T \mathcal{Y}_{ij})$ (See [34] for methods of selecting data for concurrent learning).

Integrating the definition of $Y_i \theta_i$, applying the Fundamental Theorem of Calculus, and

substituting in (3–11) yields $K_1 (\bar{x}_i(t) - \bar{x}_i(t - \Delta t)) = \mathcal{Y}_i(t) \theta_i \quad \forall t > \Delta t$, which can be used to rewrite the adaptive update law (3–10) in the following equivalent but non-implementable³ form:

$$\dot{\hat{\theta}}_i = \text{proj} \left\{ \Gamma Y_i^T e_y + k_{cl} \Gamma \sum_{j=1}^{N_i} (\mathcal{Y}_{ij}^T \mathcal{Y}_{ij}) \tilde{\theta}_i \right\}. \quad (3-12)$$

Additionally, since it is infeasible to learn the parameters of targets operating in the *unchased* mode, the adaptive update law will be turned off during these periods, i.e., $\dot{\hat{\theta}}_i = 0, \quad \forall t \in [t_{i,k}^u, t_{i,k+1}^c), \quad \forall k \in \mathbb{N}$.

3.3 Stability Analysis

The subsequent stability analysis considers the behavior of the i^{th} target when it is in the *chased* and *unchased* modes. Two time phases must be also considered: an initial phase before sufficient data has been collected to satisfy the FE condition, and a second phase after sufficient excitation has occurred. Specifically, ICL assumes that the following FE⁴ condition is satisfied

$$\exists \underline{\lambda}, \tau_i > 0 : \forall t \geq \tau_i, \lambda_{\min} \left\{ \sum_{j=1}^{N_i} \mathcal{Y}_{ij}^T \mathcal{Y}_{ij} \right\} \geq \underline{\lambda}, \quad (3-13)$$

where $\lambda_{\min} \{ \cdot \}$ refers to the minimum eigenvalue of $\{ \cdot \}$. In Section 3.3.1, Lemma 3.1 shows that during periods when a target is *chased*, the system states associated with the i^{th} target are asymptotically stable prior to sufficient excitation ($t \in [0, \tau_i)$) and exponentially stable after sufficient excitation ($t \in [\tau_i, \infty)$). Lemma 3.2 in Section 3.3.2 shows that when the i^{th} target is *unchased*, the target states remain bounded for all bounded t . Once these convergence analyses have been completed, a combined

³ The expression in (3–12) contains $\tilde{\theta}_i$ which is unknown.

⁴ The condition in (3–13) requires that the system be sufficiently excited, which is a milder (can be satisfied in finite time τ_i) condition than the typical PE condition.

analysis will be carried out to discover how the overall system evolves when subject to a discrete switching signal. Specifically, in Section 3.3.3, Theorems 3.1 and 3.2 provide an ultimate bound for the system states associated with the i^{th} target during the two time phases, respectively, provided that the developed dwell time conditions are met. The ultimate bound in Theorem 3.2 is proven to be smaller than that in Theorem 3.1 based on the fact that the system states converge exponentially during periods that the target operates in chased mode once (3–13) is satisfied (up until the point that (3–13) is satisfied there are additional terms that prevent pure exponential convergence).

To facilitate the following analysis, let $V_i : \mathbb{R}^n \times \mathbb{R}^n \times \mathbb{R}^2 \rightarrow \mathbb{R}$ be a positive definite, continuously differentiable candidate Lyapunov function, defined as

$$V_i(z_i(t)) \triangleq \frac{1}{2\alpha_i} \bar{x}_i^T \bar{x}_i + \frac{1}{2} e_y^T e_y + \frac{1}{2} \tilde{\theta}_i^T \Gamma^{-1} \tilde{\theta}_i, \quad (3-14)$$

which can be bounded by

$$c_1 \|z_i(t)\|^2 \leq V_i(z_i(t)) \leq c_2 \|z_i(t)\|^2, \quad (3-15)$$

where $z_i \triangleq \begin{bmatrix} \bar{x}_i^T & e_y^T & \tilde{\theta}_i^T \end{bmatrix}^T$ and $c_1, c_2 \in \mathbb{R}$ are known positive bounding constants.

Moreover, since the use of the projection algorithm in (3–12) ensures that $\tilde{\theta}_i, \hat{\theta}_i \in \mathcal{L}_\infty$, then the Lyapunov function candidate can also be upper bounded as

$$V_i(z_i(t)) \leq c_3 \left\| \begin{bmatrix} \bar{x}_i^T & e_y^T \end{bmatrix} \right\|^2 + c_4, \quad (3-16)$$

where $c_3, c_4 \in \mathbb{R}$ are known positive bounding constants.

3.3.1 Target Operating in the *Chased* Mode

Lemma 3.1. *The controller given in (3–5), (3–8), and the adaptive update law in (3–10) ensure that all system signals associated with the i^{th} target are bounded under closed-loop operation and that $\forall t \in [t_{i,k}^c, t_{i,k}^u), \forall k \in \mathbb{N}$,*

$$\|z_i(t)\|^2 \leq \frac{c_2}{c_1} \|z_i(t_{i,k}^c)\|^2 e^{-\lambda_1(t-t_{i,k}^c)} + \frac{c_4}{c_1} \quad (3-17)$$

provided that the gains are selected according to the sufficient condition

$$k_2 \geq \frac{\bar{\beta}}{\alpha} + 1. \quad (3-18)$$

Moreover, provided the inequality in (3-13) is satisfied (i.e., the trajectories are sufficiently exciting), then $\forall t \in [t_{i,k}^c, t_{i,k}^u) \cap [\tau_i, \infty)$, $\forall k \in \mathbb{N}$,

$$\|z_i(t)\|^2 \leq \frac{c_2}{c_1} \|z_i(t_{i,k}^c)\|^2 e^{-\lambda_2(t-t_{i,k}^c)}. \quad (3-19)$$

Proof. Using (3-6), (3-9), and (3-12), and provided that the gain condition (3-18) is satisfied, the time derivative of (3-14) during $t \in [t_{i,k}^c, t_{i,k}^u)$, $\forall k \in \mathbb{N}$ can be upper bounded as

$$\dot{V}_i(z_i(t)) \leq -k_1 \|\bar{x}_i(t)\|^2 e^{-\chi_i} - k_y \|e_y(t)\|^2. \quad (3-20)$$

Since $V_i \geq 0$ and $\dot{V}_i \leq 0$, $V_i \in \mathcal{L}_\infty$; therefore, $\bar{x}_i, e_y, \bar{\theta}_i \in \mathcal{L}_\infty$. Since $\bar{x}_i \in \mathcal{L}_\infty$ and the goal position $x_i^g \in \mathcal{L}_\infty$ by assumption then (3-5) and the target herding error can be used to prove that $x_i, y_d \in \mathcal{L}_\infty$. Since $e_y, y_d \in \mathcal{L}_\infty$, (3-3) indicates that $y \in \mathcal{L}_\infty$. Since $x_i, y \in \mathcal{L}_\infty$, then $\chi_i \in \mathcal{L}_\infty$. Since $\chi_i \in \mathcal{L}_\infty$, then $e^{-\chi_i} > 0$: $\chi_i(t) \leq \bar{\chi}_i \quad \forall t \in [t_{i,k}^c, t_{i,k}^u)$, $\forall k \in \mathbb{N}$. The facts that $x_i, \bar{x}_i, y, \chi_i \in \mathcal{L}_\infty$ can be used to show that the regression matrix $Y_i \in \mathcal{L}_\infty$, and hence, $u_y \in \mathcal{L}_\infty$ from (3-8).

Based on (3-16), the inequality in (3-20) can be upper bounded as

$$\dot{V}_i(z_i(t)) \leq -\lambda_1 (V_i(z_i(t)) - c_4) \quad (3-21)$$

where $\lambda_1 \triangleq \frac{1}{c_3} \min \left\{ k_1 \min_i e^{-\bar{\chi}_i}, k_y \right\}$. Applying the Comparison Lemma [29, Lemma 3.4] to (3-21) yields

$$V_i(z_i(t)) \leq V_i(z_i(t_{i,k}^c)) e^{-\lambda_1(t-t_{i,k}^c)} + c_4, \quad (3-22)$$

$\forall t \in [t_{i,k}^c, t_{i,k}^u)$, $\forall k \in \mathbb{N}$, which can be used with (3-15) to yield (3-17). Once sufficient data has been collected (i.e., $t \in [t_{i,k}^c, t_{i,k}^u) \cap [\tau_i, \infty)$), it can be shown using (3-15) that

$$\dot{V}_i(z_i(t)) \leq -\lambda_2 V_i(z_i(t)), \quad (3-23)$$

$\forall t \in [t_{i,k}^c, t_{i,k}^u) \cap [\tau_i, \infty)$, $\forall k \in \mathbb{N}$, where $\lambda_2 \triangleq \frac{1}{c_2} \min \left\{ k_1 \min_i e^{-\bar{x}_i}, k_y, k_{cl} \lambda \right\}$. Applying the Comparison Lemma [29, Lemma 3.4] to (3–23) yields

$$V_i(z_i(t)) \leq V_i(z_i(t_{i,k}^c)) e^{-\lambda_2(t-t_{i,k}^c)} \quad (3-24)$$

$\forall t \in [t_{i,k}^c, t_{i,k}^u) \cap [\tau_i, \infty)$, $\forall k \in \mathbb{N}$, which can be used with (3–15) to yield (3–19). \square

3.3.2 Target Operating in the *Unchased* Mode

Lemma 3.2. *During $t \in [t_{i,k}^u, t_{i,k+1}^c)$, $\forall k \in \mathbb{N}$, the system states associated with the i^{th} target remain bounded for all bounded t .*

Proof. Using (3–2), (3–9), and $\dot{\hat{\theta}}_i = 0$, the time derivative of (3–14) during $t \in [t_{i,k}^u, t_{i,k+1}^c)$, $\forall k \in \mathbb{N}$ can be upper bounded by

$$\dot{V}_i(z_i(t)) \leq \kappa_1 \|z_i(t)\|^2 + \kappa_2 \|\bar{x}_c(t)\|^2 + \kappa_3, \quad (3-25)$$

where $\kappa_1, \kappa_2, \kappa_3 \in \mathbb{R}$ are positive constants and the term with the subscript c refers to the target currently operating in *chased* mode. Using the fact that the currently *chased* target error trajectory is bounded based on the analysis in Section 3.3.1, (3–25) can be upper bounded as

$$\dot{V}_i(z_i(t)) \leq \kappa_1 \|z_i(t)\|^2 + \kappa_4, \quad (3-26)$$

where $\kappa_4 \in \mathbb{R}$ is a known positive bounding constant. Using (3–15), (3–26) can be upper bounded as

$$\dot{V}_i(z_i(t)) \leq \frac{\kappa_1}{c_1} V_i(z_i(t)) + \kappa_4. \quad (3-27)$$

Applying the Comparison Lemma [29, Lemma 3.4] to (3–27), and upper bounding, yields

$$V_i(z_i(t)) \leq \left(V_i(z_i(t_{i,k}^u)) + \frac{\kappa_4 c_1}{\kappa_1} \right) e^{\frac{\kappa_1}{c_1}(t-t_{i,k}^u)} - \frac{\kappa_4 c_1}{\kappa_1}. \quad (3-28)$$

\square

3.3.3 Combined Analysis

Consider the analysis of the i^{th} target in Sections 3.3.1 and 3.3.2, and recall the definitions of T_i^c and T_i^u from Section 3.2. The following switched systems analysis shows that the i^{th} target's error trajectory converges to an ultimate bound. To facilitate the analysis, let ν_1, ν_2 denote positive constants, where $\nu_1 \triangleq e^{\frac{\kappa_1}{c_1} T_i^u(km, (k+1)m-1) - \lambda_1 T_i^c(km, (k+1)m-1)}$, where $m \in \mathbb{N}$, c_1 is introduced in (3-15), λ_1 is introduced in (3-21), and κ_1 is introduced in (3-25).

Theorem 3.1. *The controllers in (3-5) and (3-8), and the adaptive update law in (3-10) ensure that all signals associated with the i^{th} target remain bounded for all time $t \in [0, \tau_i)$ and*

$$\limsup_t \|z_i(t)\|^2 \leq \frac{\nu_2}{c_1(1-\nu_1)} e^{\frac{\kappa_1}{c_1} T_{i,\max}^u}, \quad (3-29)$$

where $T_{i,\max}^u \triangleq \sup_k T_i^u(km, (k+1)m-1)$, provided there exists an $m < \infty$ and sequences $\{\Delta t_{i,k}^c\}_{k=0}^\infty$ and $\{\Delta t_{i,k}^u\}_{k=0}^\infty$ such that $\forall k \in \mathbb{N}$

$$T_i^u(km, (k+1)m-1) < \frac{\lambda_1 c_1}{\kappa_1} T_i^c(km, (k+1)m-1). \quad (3-30)$$

Remark 3.4. The inequality in (3-29) states that the square of the norm of the system states are worst-case bounded by the expression on the right hand side, which contains constants over which the user has some influence (based on the selection of gains and parameters).

Proof. Consider a single cycle of the i^{th} target switching to *chased*, *unchased*, and back to *chased* mode, i.e., $t \in [t_{i,k}^c, t_{i,k+1}^c)$. Using (3-22) and (3-28), the evolution of V_i over m cycles can be written as $V_i\left(z_i\left(t_{i,(k+1)m}^c\right)\right) \leq \nu_1 V_i\left(z_i\left(t_{i,km}^c\right)\right) + \nu_2$, where $\nu_1 < 1$ provided (3-30) is satisfied. Let $\{s_{i,k}\}_{k=0}^\infty$ be a sequence defined by the recurrence relation $s_{i,k+1} = M_1(s_{i,k})$, with initial condition $s_{i,0} = V_i(z_i(t_{i,0}^c))$, where $M_1 : \mathbb{R} \rightarrow \mathbb{R}$ is defined as $M_1(s) \triangleq \nu_1 s + \nu_2$. Since $\nu_1 < 1$, M_1 is a contraction [35, Definition 9.22], and thus all initial conditions, $s_{i,0}$, approach the fixed point $s = \frac{\nu_2}{1-\nu_1}$ [35, Theorem 9.23]. Since the sequence $\{s_{i,k}\}$ upper bounds V_i , in the sense that $V_i(z_i(t_{i,km}^c)) \leq s_{i,k}$, V_i is

ultimately bounded. However, since the dwell time condition (3–30) is specified over m cycles rather than a single cycle, V_i may grow within $\left[t_{i,km}^c, t_{i,(k+1)m}^c \right]$. Thus, the ultimate bound of z_i is given by (3–29). \square

Theorem 3.1 indicates that during the initial phase (i.e., $t \in [0, \tau_i)$), the closed-loop system is ultimately bounded. The following theorem establishes that when sufficient excitation occurs (i.e., $t \in [\tau_i, \infty)$), then the resulting bound can be decreased further. To facilitate this further analysis, let ν_3, ν_4 denote positive constants, where $\nu_3 \triangleq e^{\frac{\kappa_1}{c_1} T_i^u(km, (k+1)m-1) - \lambda_2 T_i^c(km, (k+1)m-1)}$, where $m \in \mathbb{N}$, c_1 is introduced in (3–15), λ_2 is introduced in (3–23), and κ_1 is introduced in (3–25).

Theorem 3.2. *The controllers in (3–5) and (3–8), and the adaptive update law in (3–10) ensure that all signals associated with the i^{th} target remain bounded for all time $t \in [\tau_i, \infty)$ and*

$$\limsup_t \|z_i(t)\|^2 \leq \frac{\nu_4}{c_1(1-\nu_3)} e^{\frac{\kappa_1}{c_1} T_{i,\max}^u}, \quad (3-31)$$

provided there exists an $m < \infty$ and sequences $\{\Delta t_{i,k}^c\}_{k=0}^\infty$ and $\{\Delta t_{i,k}^u\}_{k=0}^\infty$ such that $\forall k \in \mathbb{N}$

$$T_i^u(km, (k+1)m-1) < \frac{\lambda_2 c_1}{\kappa_1} T_i^c(km, (k+1)m-1). \quad (3-32)$$

Remark 3.5. The ultimate bound in (3–31) is smaller than that in (3–29) based on the fact that the $+c_4$ term in (3–22), used in Theorem 1, does not appear in (3–24), used in Theorem 2.

Proof. This proof follows the same strategy as that of Theorem 3.1 for $t \in$

$\left[t_{i,k}^c, t_{i,k+1}^c \right) \cap [\tau_i, \infty)$. Provided (3–32) is satisfied $\nu_3 < 1$. By establishing $\{s_{i,k}\}_{k=0}^\infty$ as a sequence defined by the recurrence relation $s_{i,k+1} = M_2(s_{i,k})$ with initial condition $s_{i,0} = V_i(z_i(t_{i,q_i}^c))$, where $q_i \triangleq \underset{k}{\operatorname{argmin}} \{t_{i,k}^c > \tau_i\}$ and $M_2 : \mathbb{R} \rightarrow \mathbb{R}$ is defined as $M_2(s) \triangleq \nu_3 s + \nu_4$, then following the same arguments in Theorem 3.1, the result in (3–31) can be concluded. \square

Remark 3.6. Let $\bar{T}_{tot}^c \in \mathbb{R}$ and $\bar{T}_{tot}^u \in \mathbb{R}$ denote the average total time target agents spend operating in the *chased* and *unchased* modes, respectively. Using (3–30) and (3–32), an average dwell time condition for all target agents over all time can be written as $\bar{T}_{tot}^u < \frac{\lambda_c c_1}{\kappa_1} \bar{T}_{tot}^c$, where $\lambda_c = \min \{\lambda_1, \lambda_2\}$. Since only one target will operate in the *chased* mode at any given time, for n_t targets the average total time targets spend operating in the *chased* mode is $\bar{T}_{tot}^c = \frac{1}{n_t} (\bar{T}_{tot}^c + \bar{T}_{tot}^u)$. Thus, the maximum number of target agents that a single herding agent can successfully herd must satisfy $n_t < \frac{\lambda_c c_1}{\kappa_1} + 1$.

3.4 Simulations

Numerical simulation results are presented for the case of one herder pursuing $n_t = 3$ targets in a three-dimensional workspace. The switching law for the herder in this example is based on the distance of each target from the origin. Specifically, the herder selects the target furthest from the origin initially, regulates that target to a ball that is 10% (a design parameter) of the target’s previous distance from the origin, switches to the furthest target at that time, and repeats. The initial conditions for the 2D simulation were $x_1(0) = \begin{bmatrix} 1.8 & -0.2 \end{bmatrix}^T$, $x_2(0) = \begin{bmatrix} 1.7 & -1.3 \end{bmatrix}^T$, $x_3(0) = \begin{bmatrix} 0.4 & 0.8 \end{bmatrix}^T$, $y(0) = \begin{bmatrix} -2.3 & 0.6 \end{bmatrix}^T$, while the initial conditions for the 3D simulation were $x_1(0) = \begin{bmatrix} -1.8 & 0.8 & 0.5 \end{bmatrix}^T$, $x_2(0) = \begin{bmatrix} -1.1 & 1.3 & 2.1 \end{bmatrix}^T$, $x_3(0) = \begin{bmatrix} 2.1 & 0.6 & 1.3 \end{bmatrix}^T$, $y(0) = \begin{bmatrix} -0.2 & 0.4 & -1.3 \end{bmatrix}^T$. For both simulations, the initial adaptive estimates were $\hat{\theta}(0) = \begin{bmatrix} 1.5 & 1 \end{bmatrix}^T$ and the integration window was $\Delta t = 0.5$ s.

Table 3-1. Simulation gains

k_1	k_2	Γ	k_{CL}	k_y
1.5	1.125	diag $\{0.41_n\}$	1	0.5

Table 3-2. Simulation system parameters

Parameter	σ^2	α	β	γ
Value	2	1	0.2	0.2
Bounds	N/A	$\underline{\alpha} = 0.75, \bar{\alpha} = 1.25$	$\bar{\beta} = 0.35$	N/A

The following figures show the results for the designed controller in real space. Figures 3-1 and 3-2 show the norm of the states and the overall path of the agents when using the robust controller with three target agents in two-dimensional space. Figures 3-4 and 3-5 show the norm of the states and the overall path of the agents when using the robust controller with three target agents in three-dimensional space. Figures 3-3 and 3-6 show the adaptive estimate error for the 2D and 3D case, respectively.

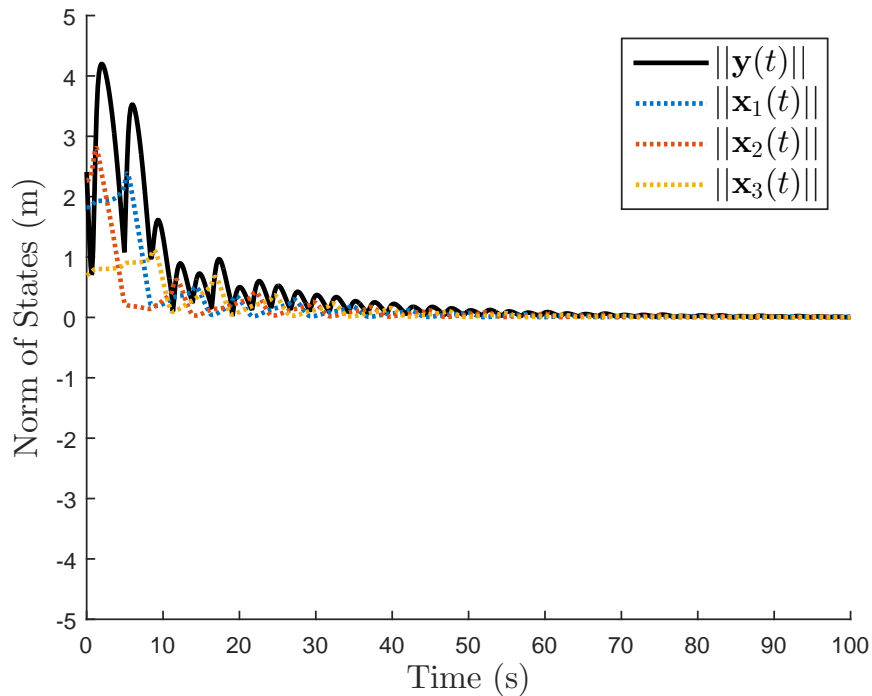


Figure 3-1. The states of the herder and targets using the adaptive controller in a two-dimensional workspace.

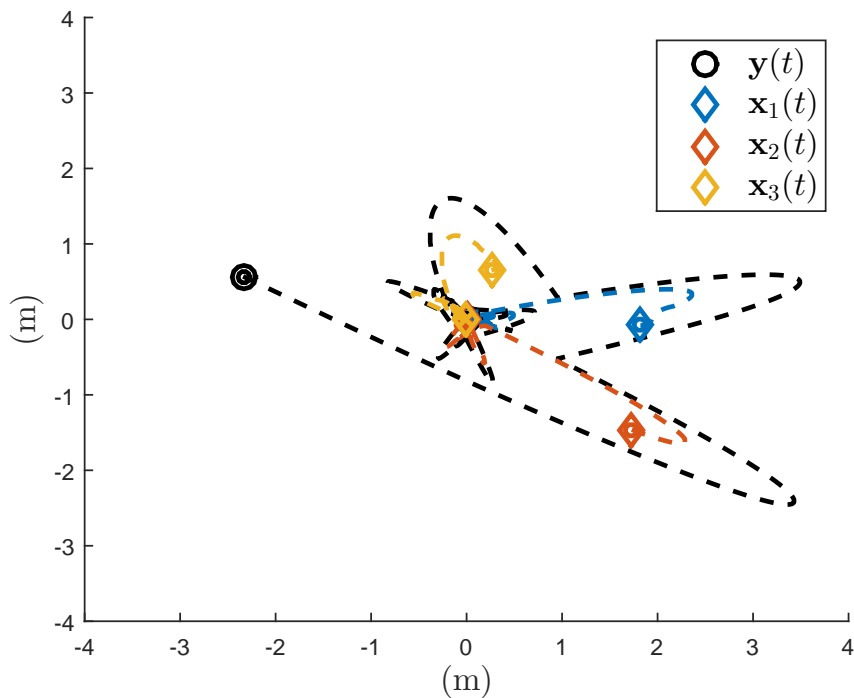


Figure 3-2. Two-dimensional plot of the paths of the herder and targets using the adaptive controller.

3.5 Experiments

Experimental results⁵ were obtained using Parrot Bebop 2 quadcopter platforms that served as a herding agent and three (i.e., $n_t = 3$) homogeneous target agents. A NaturalPoint, Inc. OptiTrack motion capture system was used to record the position of each agent at all times for feedback control. The switching strategy employed was as follows: the herder selects the target furthest from its goal initially, regulates that target to a ball that is 50% (a design parameter) of the target's previous distance, then switches to the next furthest target, and repeats until the target error is within some tolerance (0.5m was set as a reasonable stopping condition for the experiments). Since the agents were homogeneous, a single parameter estimate vector (and thus data

⁵ A video of a typical run of this experiment is available at [36]

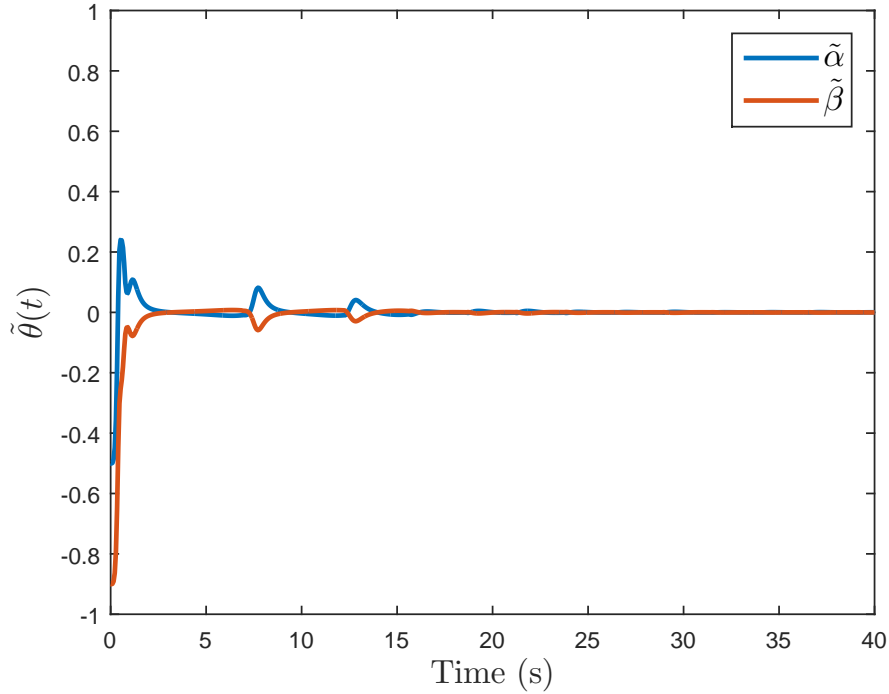


Figure 3-3. Adaptive estimate errors for the 2D simulation.

history stack) was shared between all agents. The goal locations for each target were $x_1^g = \begin{bmatrix} 0.0 & -0.5 \end{bmatrix}^T$, $x_2^g = \begin{bmatrix} 2.0 & 0.5 \end{bmatrix}^T$, $x_3^g = \begin{bmatrix} -2.0 & 0.5 \end{bmatrix}^T$. The constant parameters for the target dynamics are $\sigma^2 = 1$, $\alpha = 0.5$, $\beta = 0.05$, $\gamma = 0.1$, $\underline{\alpha} = 0.25$, $\bar{\alpha} = 0.75$, $\bar{\beta} = 0.075$, $\hat{\theta}(0) = \begin{bmatrix} 0.25 & 0.025 \end{bmatrix}^T$, and the integration window was $\Delta t = 0.1$ s. Figures 3-7 and 3-8 show the overall paths of the agents and their starting and ending positions, respectively, demonstrating that the herding agent successfully regulated the target agents within the 0.5m radius of the goal locations. Figure 3-9 gives the norms of the target errors versus time while 3-10 shows the ultimately bounded convergence of the adaptive estimate errors.

3.6 Concluding Remarks

An adaptive controller and switching conditions are developed using Lyapunov-based stability analysis for a single herding agent to ensure global exponential regulation of n_t uncertain target agents to the origin, despite their tendency to flee and lack of explicit control input. The unknown parameters are guaranteed to be learned online

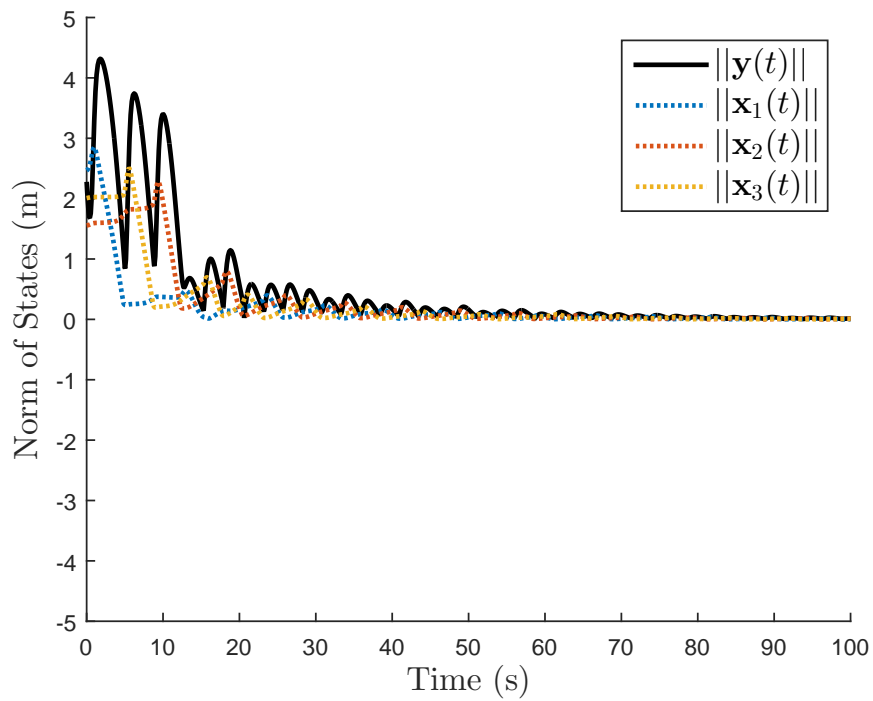


Figure 3-4. The states of the herder and targets using the adaptive controller in a three-dimensional workspace.

without the use of state derivatives or the need for persistence of excitation. Simulation and experimental results also demonstrate the validity of the results given for an example herder strategy.

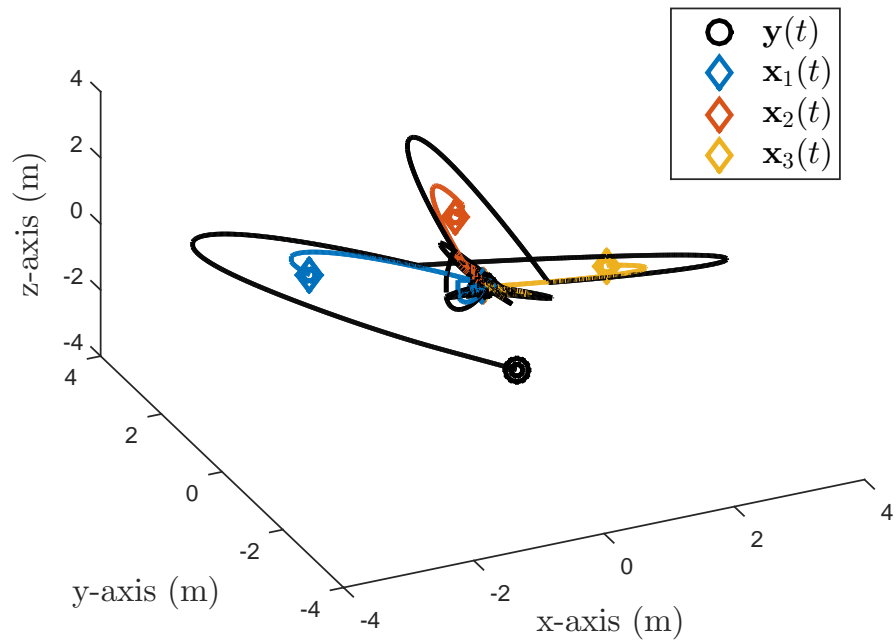


Figure 3-5. Three-dimensional plot of the paths of the herder and targets using the adaptive controller.

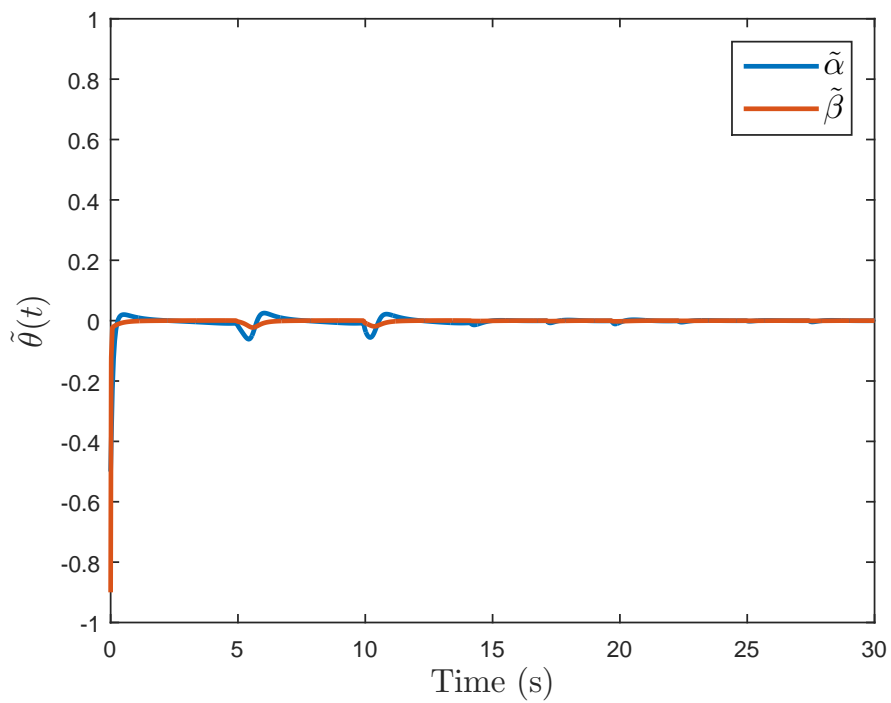


Figure 3-6. Adaptive estimate errors for the 3D simulation.

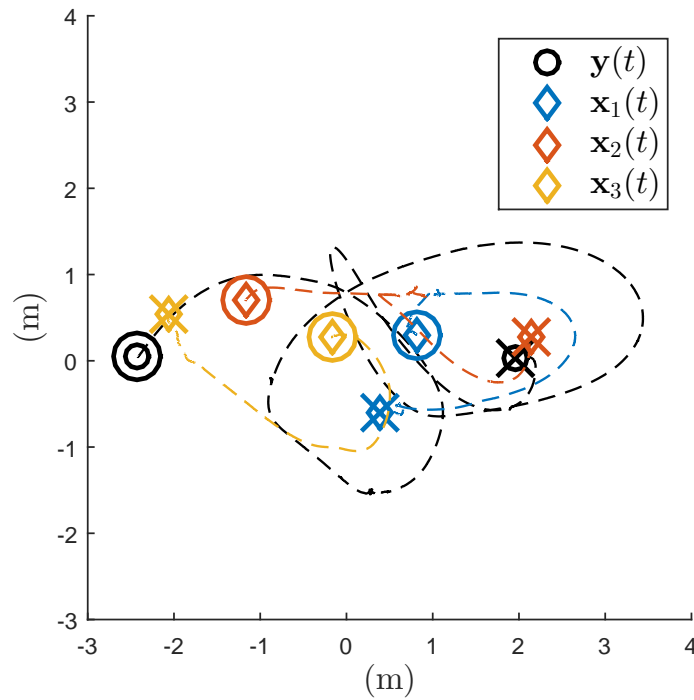


Figure 3-7. Overall herder and target trajectories, with each agent's starting location marked by a circle, and ending locations marked by an X.

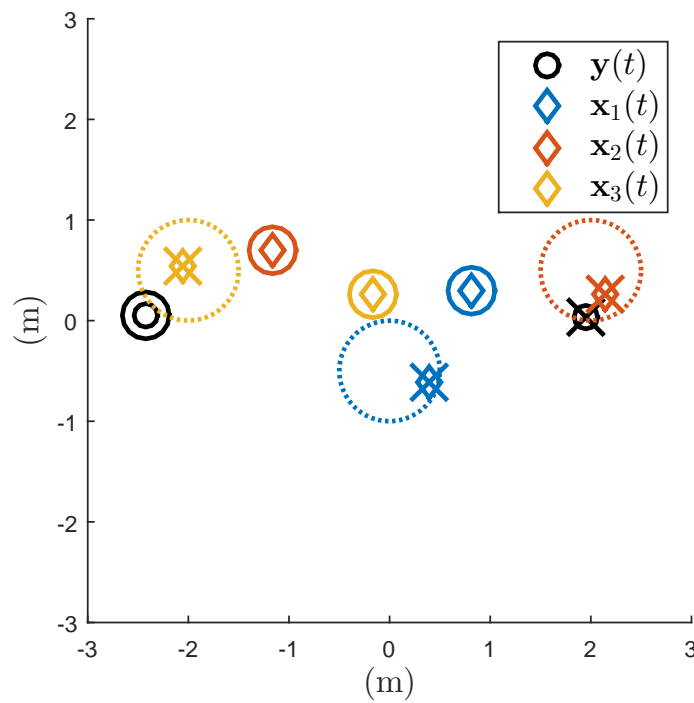


Figure 3-8. Starting and ending positions of all agents.

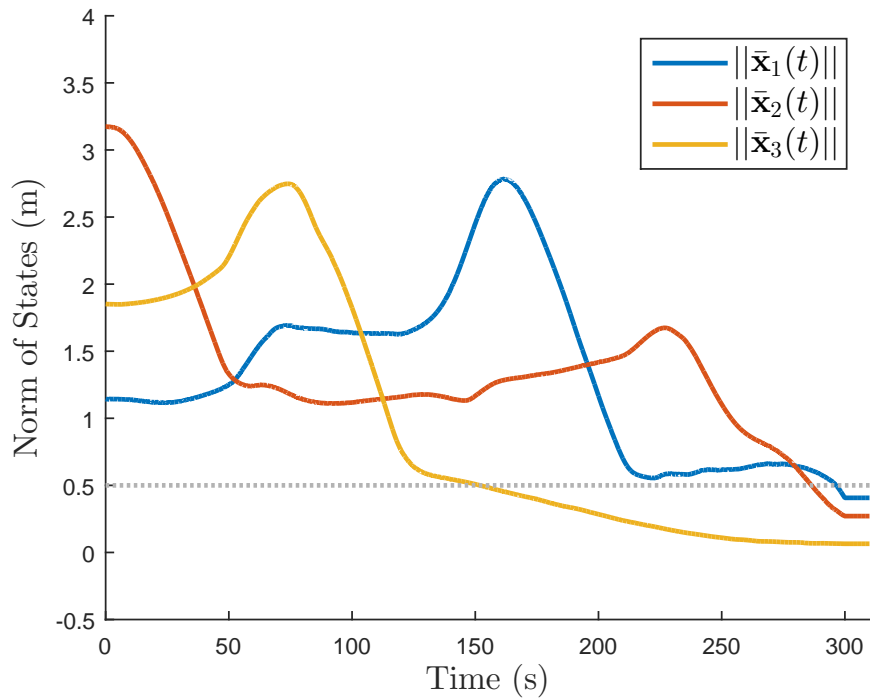


Figure 3-9. Norms of the target errors. Each agent is driven to within 0.5 m of their goal location (gray dotted line).

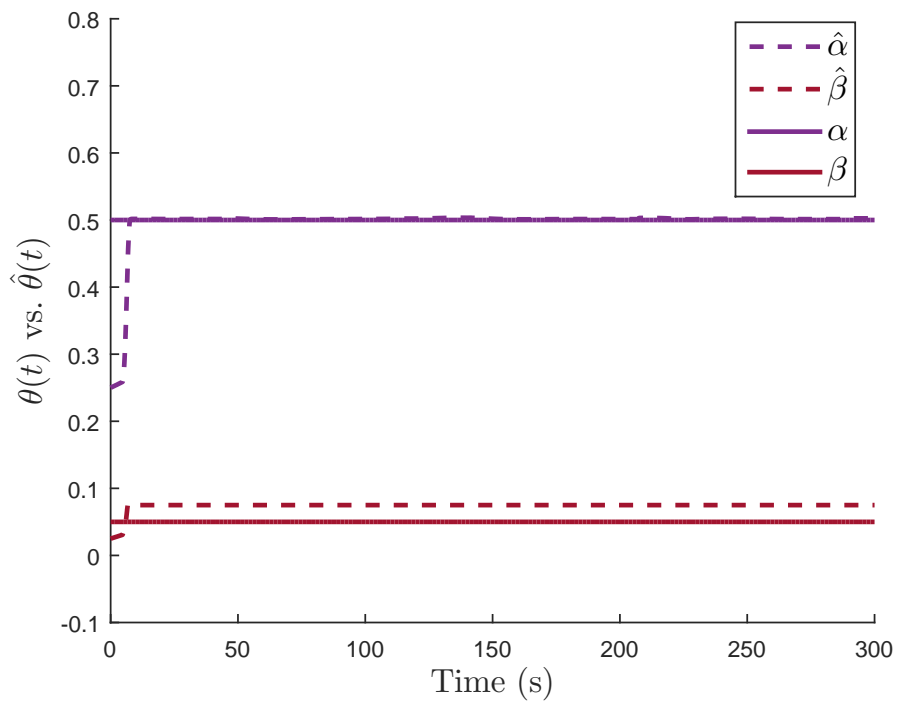


Figure 3-10. The actual vs. estimated parameters are shown.

CHAPTER 4
HERDING OF MULTIPLE AGENTS WITH UNSTRUCTURED UNCERTAIN DYNAMICS
USING NEURAL NETWORKS

In this chapter, NN are used to approximate unknown functions to compensate for the uncertainty and accomplish the herding task. The fact that the target dynamics contain unknown functions of unknown form motivates the use of function approximation techniques. With this, additional challenges arise in the use of a concurrent learning strategy, as well as in the switched systems analysis. Simulation and experimental results are provided to demonstrate the validity of the theory.

4.1 Problem Formulation

In this chapter, consider a network consisting of one herding agent and $n_t \in \mathbb{Z}_{>0}$ target agents. Let $\mathcal{T} \triangleq \{1, 2, \dots, n_t\}$ be the set of target agents. The herding agent is tasked with regulating the $n_t > 1$ targets to their respective constant goal locations, $x_i^g \in \mathbb{R}^n, \forall i \in \mathcal{T}$. The target, goal, and herder states are assumed to be available to the herder for feedback control at all times. In contrast to traditional leader-follower network problems where each agent's interaction is controlled to accomplish a common goal, in the *indirect* herding problem, only the herder's dynamics are directly controllable while the target states can only be influenced through interaction with the herder. The herder dynamics are given by

$$\dot{y} = h(x, y) + u_y, \quad (4-1)$$

where $x = \begin{bmatrix} x_1^T & x_2^T & \dots & x_{n_t}^T \end{bmatrix}^T$ is a stacked vector of all the target states, $h : \mathbb{R}^n \times \mathbb{R}^{nn_t} \rightarrow \mathbb{R}^n$ is an unknown function that represents the herder dynamics, and $u_y \in \mathbb{R}^n$ is the herder control law to be designed such that all targets are regulated to their goal locations (i.e., herding is accomplished). The target agents will be influenced through an unknown repulsion between the target and herder when it is nearby, and will additionally behave according to some unknown drift dynamics. Specifically, the i^{th} target's motion model is given by

$$\dot{x}_i = \alpha_i (\|x_i - y\|) (x_i - y) + f_i(x), \quad (4-2)$$

where $\alpha_i : \mathbb{R} \rightarrow \mathbb{R}$ is an unknown smooth transition function¹ that is bounded by

$$\underline{\alpha}_i \leq \alpha_i (\|x_i - y\|) \leq \bar{\alpha}_i,$$

$\underline{\alpha}_i, \bar{\alpha}_i, i \in \mathcal{T}$ are known positive constants, and $f_i : \mathbb{R}^n \rightarrow \mathbb{R}^n$ is an unknown function that represents the i^{th} target's drift dynamics, which is upper bounded as

$$\|f_i(x)\| \leq \bar{f}_i,$$

where $\bar{f}_i, i \in \mathcal{T}$, are known positive constants. The first term in (4-2) models the repulsion interaction between the herder and the i^{th} target. The targets all behave according to the similar motion model in (4-2), but will be heterogeneous in the fact that each target's model may differ in α_i and f_i .

Since a single herder is outnumbered by multiple targets, a switching strategy will be employed to ensure that the herding task is accomplished (i.e., all targets are regulated to their goal location). The herding agent will switch between chasing each target towards its goal location, one at a time, according to a switching strategy that must satisfy dwell time conditions to be designed in this chapter. Although the targets needn't know² whether they are being chased or not, this behavior will be captured by considering each target to be operating in either *chased* or *unchased* mode at any given time³. Thus, it will be advantageous to keep track of the various switching times and express trajectories in terms of them. Let $t_{i,k}^c \in \mathbb{R}$ and $t_{i,k}^u \in \mathbb{R}$ denote the k^{th} instance when the i^{th} target is switched to the *chased* or *unchased* mode,

¹ The function $\alpha_i (\|x_i - y\|)$ should smoothly transition between some positive constants $\bar{\alpha}_i$ and $\underline{\alpha}_i$, where $\bar{\alpha}_i > \underline{\alpha}_i \forall i \in \{1, 2, \dots, n_t\}$.

² This fact is used to facilitate the stability analysis. The targets all behave according to (4-2) at all times.

³ Exactly one target will be in *chased* mode, while all others operate in *unchased* mode, at any given time

respectively, where $k \in \mathbb{N}$. The contiguous dwell time in the k^{th} activation of the i^{th} target operating in the *chased* or *unchased* mode is denoted by $\Delta t_{i,k}^c \in \mathbb{R}$ and $\Delta t_{i,k}^u \in \mathbb{R}$, and defined as $\Delta t_{i,k}^c \triangleq t_{i,k}^u - t_{i,k}^c$ and $\Delta t_{i,k}^u \triangleq t_{i,k+1}^c - t_{i,k}^u$, respectively. The total amount of time each of these modes is active between switching instances a and b are denoted $T_i^c(a, b) \triangleq \sum_{l=a}^b \Delta t_{i,l}^c$ and $T_i^u(a, b) \triangleq \sum_{l=a}^b \Delta t_{i,l}^u$, respectively. The target operating in *chased* mode is denoted by the subscript $i = c$ (i.e., $x_i(t) = x_c(t)$, $\forall t \in [t_{i,k}^c, t_{i,k}^u)$, $\forall k \in \mathbb{N}$).

4.2 Control Objective

The goal of this work is to control the herder such that it regulates all target agents to their goal locations, despite the uncertainties in the system and the target's non-cooperative behavior. The following assumptions about the targets are utilized.

Assumption 4.1. The unknown functions in (4-1) and (4-2) are time-invariant, locally Lipschitz, autonomous functions (i.e., the functions $\alpha_i(\|x_i - y\|)$, $f_i(x)$, and $h(x, y)$ are not explicit functions of time, $\forall i \in \mathcal{T}$).

The herding error for each target, \bar{x}_i , is defined in (3-1). Since both (4-1) and (4-2) contain unknown dynamics, function approximation methods will be employed to estimate these uncertainties. The i^{th} target dynamics in (4-2) and the unknown dynamics in (4-1) can be written as

$$\dot{x}_i = F_i(\eta(t)) = \alpha_i(\|x_i - y\|)(x_i(t) - y(t)) + f_i(x(t)) \quad (4-3)$$

and

$$F_y(\eta(t)) = -h(x, y), \quad (4-4)$$

respectively, where $F_i : \mathbb{R}^{n(n_t+1)} \rightarrow \mathbb{R}^n$ and $F_y : \mathbb{R}^{n(n_t+1)} \rightarrow \mathbb{R}^n$ are unknown functions, and $\eta \in \mathbb{R}^{n(n_t+1)}$ is defined as $\eta \triangleq \begin{bmatrix} x^T & y^T \end{bmatrix}^T$. To facilitate the subsequent development, (4-3) and (4-4) are each approximated using a NN.

Let χ be a compact simply connected set such that $\chi \subset \mathbb{R}^{n(n_t+1)}$, and let $\Upsilon(\chi)$ be defined as the space where $F_i : \chi \rightarrow \mathbb{R}^n$ and $F_y : \chi \rightarrow \mathbb{R}^n$ are continuous $\forall i \in \mathcal{T}$. The

universal approximation property states that there exist weights and thresholds such that $F_i(\eta), F_y(\eta) \in \Upsilon(\chi), \forall i \in \mathcal{T}$, can be approximated by a NN as [37],

$$F_i(\eta(t)) = W_i^T \sigma_i(\eta(t)) + \varepsilon_i(\eta(t)), \quad (4-5)$$

and

$$F_y(\eta(t)) = W_y^T \sigma_y(\eta(t)) + \varepsilon_y(\eta(t)), \quad (4-6)$$

respectively, where $\sigma_i : \mathbb{R}^{n(n_t+1)} \rightarrow \mathbb{R}^{L_1}$ and $\sigma_y : \mathbb{R}^{n(n_t+1)} \rightarrow \mathbb{R}^{L_2}$ are known, bounded, locally Lipschitz, vector of basis functions, $W_i \in \mathbb{R}^{L_1 \times n}$ and $W_y \in \mathbb{R}^{L_2 \times n}$ are matrices of the unknown ideal weights, $L_1 \in \mathbb{N}$ is the number of neurons used in the NN in (4-7), $L_2 \in \mathbb{N}$ is the number of neurons used in the NN in (4-8), and $\varepsilon_i : \mathbb{R}^{n(n_t+1)} \rightarrow \mathbb{R}^n$ and $\varepsilon_y : \mathbb{R}^{n(n_t+1)} \rightarrow \mathbb{R}^n$ are the function approximation residuals.

Remark 4.1. The function approximation residual errors can be upper bounded by positive constants that can be made arbitrarily small based on the Stone-Weierstrass theorem [38], i.e., $\bar{\varepsilon}_i \triangleq \sup_{\eta \in \chi, t \in [0, \infty)} \|\varepsilon_i(\eta(t))\|, \forall i \in \mathcal{T}$, and $\bar{\varepsilon}_y \triangleq \sup_{\eta \in \chi, t \in [0, \infty)} \|\varepsilon_y(\eta(t))\|$. The Stone-Weierstrass requires that the states remain in a compact set (i.e., $\eta(t) \in \chi$). The subsequent stability proof shows that if $\eta(0)$ is bounded, then $\eta(t) \in \chi$.

Let

$$\tilde{W}_i(t) \triangleq W_i - \hat{W}_i(t)$$

and

$$\tilde{W}_y(t) \triangleq W_y - \hat{W}_y(t)$$

denote the parameter estimation error for the weights associated with the i^{th} target and the herder, respectively, where $\hat{W}_i \in \mathbb{R}^{L_1 \times n}$ is the estimate of the ideal function approximation weights associated with the i^{th} target, and $\hat{W}_y \in \mathbb{R}^{L_2 \times n}$ is the estimate of the ideal function approximation weights associated with the herder.

Based on (4-5), the dynamics in (4-2) can be rewritten as⁴

$$\dot{x}_i = W_i^T \sigma_i + \varepsilon_i, \quad (4-7)$$

while (4-1) can be rewritten using (4-6) as

$$\dot{y} = - (W_y^T \sigma_y + \varepsilon_y) + u_y. \quad (4-8)$$

Given that the target agent dynamics in (4-2) do not explicitly contain a control input, a backstepping strategy is used to inject the desired herder state as a virtual controller, $y_d \in \mathbb{R}^n$, into the dynamics of the target currently operating in the *chased* mode. Therefore, in addition to regulating the herding error in (3-1), the subsequent development will also focus on minimizing the backstepping error $e_y \in \mathbb{R}^n$, defined as

$$e_y(t) \triangleq y_d(t) - y(t). \quad (4-9)$$

4.3 Control Development

4.3.1 Herding Controller

In the following development, the herder switches between chasing each target to achieve the overall herding objective, and thus the controller always uses the currently *chased* target. In this section, the target denoted by x_c is the one currently operating in *chased* mode (i.e., $x_i(t) = x_c(t)$, $\forall t \in [t_{i,k}^c, t_{i,k}^u)$, $\forall k \in \mathbb{N}$). To develop the controller, the target dynamics in (4-2), as well as the backstepping error in (4-9), are used to express the time derivative of (3-1) as

$$\dot{\tilde{x}}_c = \alpha_c (x_c + e_y - y_d) + f_c. \quad (4-10)$$

⁴ For notational brevity, dependence on states and time will be henceforth suppressed, except for where necessary.

Based on the desire to regulate the herding error, the herder's desired state is designed as

$$y_d \triangleq K_{1,c}\bar{x}_c + x_c^g, \quad (4-11)$$

where⁵ $K_{1,i} = k_{1,i} + k_{2,i} + k_{n,i}$ and $k_{1,i}, k_{2,i}, k_{n,i}$ are positive constant control gains, $\forall i \in \{1, 2, \dots, n_t\}$ and $i = c$ is used for the virtual controller. Using (4-11), (4-10) can be rewritten as

$$\dot{\bar{x}}_c = \alpha_c (1 - K_{1,c}) \bar{x}_c + \alpha_c e_y + f_c. \quad (4-12)$$

The backstepping error dynamics can be determined by taking the time derivative of (4-9), and using the target dynamics in (4-2) and the herder dynamics in (4-1) to obtain

$$\dot{e}_y = K_{1,c}F_c(\eta_c) - h(\xi) - u_y. \quad (4-13)$$

Using (4-7) and (4-8), (4-13) can be rewritten as

$$\dot{e}_y = K_{1,c}(W_c^T \sigma_c + \varepsilon_c) + W_y^T \sigma_y + \varepsilon_y - u_y. \quad (4-14)$$

Based on (4-14) and the subsequent stability analysis, the herder control law is designed as

$$u_y \triangleq K_{2,c}e_y + K_{1,c}\hat{W}_c^T \sigma_c + \hat{W}_y^T \sigma_y + k_s \text{sgn}(e_y), \quad (4-15)$$

where, $\forall i \in \{1, 2, \dots, n_t\}$, $K_{2,i} = k_y + k_{3,i}$, $k_y, k_{3,i}, k_{s,i}$ are positive constant control gains, and $\text{sgn}(\cdot)$ is the signum function. Using (4-15), the closed-loop backstepping dynamics in (4-14) can be rewritten as

$$\dot{e}_y = K_{1,c}\tilde{W}_c^T \sigma_c + \tilde{W}_y^T \sigma_y + K_{1,c}\varepsilon_c + \varepsilon_y - K_{2,c}e_y - k_{s,c}\text{sgn}(e_y). \quad (4-16)$$

⁵ The gain parameter K_1 is a sum of positive gains for notational convenience in the stability analysis. In practice, this is implemented as a single quantity.

4.3.2 Function Approximation

Taking the transpose of (4–8) and integrating yields

$$\int_{t-\Delta t}^t \dot{y}^T(\varsigma) d\varsigma = - \int_{t-\Delta t}^t \sigma_y^T(y(\varsigma)) W_y d\varsigma - \int_{t-\Delta t}^t \varepsilon_y^T(y(\varsigma)) d\varsigma + \int_{t-\Delta t}^t u_y^T(\varsigma) d\varsigma, \quad (4-17)$$

where $\Delta t \in \mathbb{R}$ is a positive constant denoting the size of the window of integration. Using the Fundamental Theorem of Calculus, (4–17) can be rewritten as

$$\mathcal{U}_y(t) - y^T(t) + y^T(t - \Delta t) = \mathcal{Y}_y(t) W_y + \mathcal{E}_y(t), \quad \forall t \in [\Delta t, \infty), \quad (4-18)$$

where, $\forall t \in [\Delta t, \infty)$, $\mathcal{Y}_y(t) \triangleq \int_{t-\Delta t}^t \sigma_y^T(\eta(\varsigma)) d\varsigma$, $\mathcal{E}_y(t) \triangleq \int_{t-\Delta t}^t \varepsilon_y^T(\eta(\varsigma)) d\varsigma$, and $\mathcal{U}_y(t) \triangleq \int_{t-\Delta t}^t u_y^T(\varsigma) d\varsigma$. Similarly, taking the transpose of (4–7) and integrating yields

$$\int_{t-\Delta t}^t \dot{x}_i^T(\varsigma) d\varsigma = \int_{t-\Delta t}^t \sigma_i^T(\eta_i(\varsigma)) W_i d\varsigma + \int_{t-\Delta t}^t \varepsilon_i^T(\eta_i(\varsigma)) d\varsigma. \quad (4-19)$$

Using the Fundamental Theorem of Calculus, (4–19) can be rewritten as

$$x_i^T(t) - x_i^T(t - \Delta t) = \mathcal{Y}_i(t) W_i + \mathcal{E}_i(t), \quad \forall t \in [\Delta t, \infty), \quad (4-20)$$

where, $\forall t \in [\Delta t, \infty)$, $\mathcal{Y}_i(t) \triangleq \int_{t-\Delta t}^t \sigma_i^T(\eta_i(\varsigma)) d\varsigma$ and $\mathcal{E}_i(t) \triangleq \int_{t-\Delta t}^t \varepsilon_i^T(\eta_i(\varsigma)) d\varsigma$.

The parameter estimate for the weights associated with the herder (i.e., \hat{W}_y in (4–15)) is generated from the ICL-based adaptive update law [39, 40]

$$\dot{\hat{W}}_y \triangleq \text{proj} \left\{ \Gamma_y \sigma_y e_y^T + k_{CL,y} \Gamma_y \sum_{j=1}^{N_y} \mathcal{Y}_{y,j}^T \left(\mathcal{U}_{y,j} - \Delta y_j - \mathcal{Y}_{y,j} \hat{W}_y \right) \right\}, \quad (4-21)$$

where $\text{proj} \{ \cdot \}$ is a smooth projection operator,⁶ $\Gamma_y \in \mathbb{R}^{L_2 \times L_2}$ and $k_{CL,y} \in \mathbb{R}$ are constant, positive definite control gains, $\Delta y_j \triangleq y^T(t_j) - y^T(t_j - \Delta t)$, $N_y \in \mathbb{Z}$ is a constant that represents the number of saved data points for the data stack of the herder, and $t_j \in [\Delta t, t]$ represents time points when measurements are available. Likewise, the

⁶ See Remark 3.6 or Section 4.4 in [33] for details of the projection operator.

parameter estimate for the weights associated with the i^{th} target (i.e., \hat{W}_i) is generated from the ICL-based adaptive update law

$$\dot{\hat{W}}_i \triangleq \text{proj} \left\{ \Gamma_i K_{1,i} \sigma_i e_y^T + k_{CL,i} \Gamma_i \sum_{j=1}^{N_i} \mathcal{Y}_{i,j}^T \left(\Delta x_{i,j} - \mathcal{Y}_{i,j} \hat{W}_i \right) \right\}, \quad (4-22)$$

where, $\forall i \in \{1, 2, \dots, n_t\}$, $\Gamma_i \in \mathbb{R}^{L_1 \times L_1}$ and $k_{CL,i} \in \mathbb{R}$ are constant, positive definite control gains, $\Delta x_{i,j} \triangleq x_i^T(t_j) - x_i^T(t_j - \Delta t)$, $N_i \in \mathbb{Z}$ is a constant that represents the number of saved data points for the data stack of the i^{th} target, and $t_j \in [\Delta t, t]$ represent time points when measurements are available.

The idea behind concurrent learning is to utilize recorded input and output data to identify the ideal weights. The data points that are saved are selected to maximize the minimum eigenvalues of $\sum_{j=1}^{N_y} (\mathcal{Y}_{y,j}^T \mathcal{Y}_{y,j})$ and $\sum_{j=1}^{N_i} (\mathcal{Y}_{i,j}^T \mathcal{Y}_{i,j})$ ⁷. Using (4-18) and (4-20), the adaptive update laws in (4-21) and (4-22) can be rewritten in the following equivalent, but non-implementable⁸, forms, respectively:

$$\dot{\hat{W}}_y = \text{proj} \left\{ \Gamma_y \sigma_y e_y^T + k_{CL,y} \Gamma_y \sum_{j=1}^{N_y} \mathcal{Y}_{y,j}^T \mathcal{Y}_{y,j} \tilde{W}_y + k_{CL,y} \Gamma_y \sum_{j=1}^{N_y} \mathcal{Y}_{y,j}^T \mathcal{E}_{y,j} \right\} \quad (4-23)$$

$$\dot{\hat{W}}_i = \text{proj} \left\{ \Gamma_i K_{1,i} \sigma_i e_y^T + k_{CL,i} \Gamma_i \sum_{j=1}^{N_i} \mathcal{Y}_{i,j}^T \mathcal{Y}_{i,j} \tilde{W}_i + k_{CL,i} \Gamma_i \sum_{j=1}^{N_i} \mathcal{Y}_{i,j}^T \mathcal{E}_{i,j} \right\}, \quad (4-24)$$

for all $t > \Delta t$, where $\mathcal{E}_{y,j} \triangleq \mathcal{E}_y(t_j)$ and $\mathcal{E}_{i,j} \triangleq \mathcal{E}_i(t_j)$. Additionally, during periods that the i^{th} target is operating in *unchased* mode, the gradient term in (4-22) is turned off, i.e.,

$\forall t \in [t_{i,k}^u, t_{i,k+1}^c)$, $\forall k \in \mathbb{N}$,

$$\dot{\hat{W}}_i \triangleq \text{proj} \left\{ k_{CL,i} \Gamma_i \sum_{j=1}^{N_i} \mathcal{Y}_{i,j}^T \left(\Delta x_{i,j} - \mathcal{Y}_{i,j} \hat{W}_i \right) \right\},$$

⁷ See [34] for details on methods of selecting data.

⁸ The update laws (4-23) and (4-24) contain \tilde{W}_y and \tilde{W}_i , respectively, which are unknown.

which can be rewritten as

$$\dot{W}_i = \text{proj} \left\{ k_{CL,i} \Gamma_i \sum_{j=1}^{N_i} \mathcal{Y}_{i,j}^T \mathcal{Y}_{i,j} \tilde{W}_i + k_{CL,i} \Gamma_i \sum_{j=1}^{N_i} \mathcal{Y}_{i,j}^T \mathcal{E}_{i,j} \right\}. \quad (4-25)$$

4.4 Stability Analysis

This stability analysis considers the behavior of the i^{th} target when it is in the *chased* and *unchased* modes, and then a combined switched systems analysis to gain understanding of the overall state trajectories. In addition, two time phases must also be considered: an initial phase before there is sufficient excitation to satisfy the FE condition, and a second time phase after sufficient data has been collected. The following analysis assumes that the following FE⁹ conditions are satisfied [39, 40]

$$\begin{aligned} \exists \underline{\lambda}_y > 0, \tau_y > \Delta t : \forall t \geq \tau_y, \lambda_{\min} \left\{ \sum_{j=1}^{N_y} \mathcal{Y}_{y,j}^T \mathcal{Y}_{y,j} \right\} &\geq \underline{\lambda}_y, \\ \exists \underline{\lambda}_i > 0, \tau_i > \Delta t : \forall t \geq \tau_i, \lambda_{\min} \left\{ \sum_{j=1}^{N_i} \mathcal{Y}_{i,j}^T \mathcal{Y}_{i,j} \right\} &\geq \underline{\lambda}_i, \end{aligned} \quad (4-26)$$

where $\lambda_{\min} \{ \cdot \}$ refers to the minimum eigenvalue of $\{ \cdot \}$.

The stability analysis is developed as follows. Lemma 4.1 in Section 4.4.1 proves that during periods when a target operates in *chased* mode, the system states associated with the i^{th} target decay asymptotically prior to sufficient excitation (i.e., $t \in [0, \tau_i)$) and are exponentially stable after sufficient excitation (i.e., $t \in [\tau_i, \infty)$). Then in Section 4.4.2, Lemma 4.2 shows that the target states remain bounded for all bounded t when the i^{th} target is operating in *unchased* mode. Considering these results, the overall trajectories are analyzed in Theorems 4.1 and 4.2 in Section 4.4.3, and ultimate bounds are provided for the system states associated with the i^{th} target during the two time

⁹ The condition in (4-26) requires that the system be sufficiently excited, which is a milder (can be satisfied in finite time τ_i) condition than the typical PE condition.

phases, respectively, provided that the developed gain and dwell time conditions are met.

To facilitate the following analysis, let $V_i : \mathbb{R}^{2n+nL_1+nL_2} \rightarrow \mathbb{R}$ be a positive definite, continuously differentiable candidate Lyapunov function, defined as

$$V_i(z_i(t)) \triangleq \frac{1}{2}\bar{x}_i^T\bar{x}_i + \frac{1}{2}e_y^T e_y + \frac{1}{2}\text{tr}\left(\tilde{W}_i^T\Gamma_i^{-1}\tilde{W}_i\right) + \frac{1}{2}\text{tr}\left(\tilde{W}_y^T\Gamma_y^{-1}\tilde{W}_y\right), \quad (4-27)$$

which can be bounded as

$$\beta_1 \|z_i(t)\|^2 \leq V_i(z_i(t)) \leq \beta_2 \|z_i(t)\|^2, \quad (4-28)$$

where $z_i(t) \in \mathbb{R}^{2n+nL_1+nL_2}$ is defined as

$$z_i(t) \triangleq \begin{bmatrix} \bar{x}_i^T(t) & e_y^T(t) & \text{vec}\left(\tilde{W}_i(t)\right)^T & \text{vec}\left(\tilde{W}_y(t)\right)^T \end{bmatrix}^T, \quad (4-29)$$

$\text{tr}(\cdot)$ denotes the matrix trace operator, $\text{vec}(\cdot)$ denotes a stack of the columns of (\cdot) , and $\beta_1, \beta_2 \in \mathbb{R}$ are known positive bounding constants. Moreover, since the use of the projection algorithm in (4-21) and (4-22) ensures that $\tilde{W}_y, \hat{W}_y, \tilde{W}_i, \hat{W}_i \in \mathcal{L}_\infty$, then the Lyapunov function candidate can also be upper bounded as

$$V_i(z_i(t)) \leq \beta_3 \left\| \begin{bmatrix} \bar{x}_i^T & e_y^T \end{bmatrix} \right\|^2 + \beta_4, \quad (4-30)$$

where $\beta_3, \beta_4 \in \mathbb{R}$ are known positive bounding constants.

4.4.1 Target Operating in the *Chased* Mode

In this section, the i^{th} target is the one currently operating in the *chased* mode; however for clarity in the analysis that follows, the subscript i will be used in lieu of the subscript c . This notation is used to avoid confusion in the combined analysis in Section 4.4.3, where the state trajectories associated with the i^{th} target are considered over all time, switching between *chased* and *unchased* mode. The following Lemma establishes the stability of the i^{th} target during periods in which it operates in the *chased* mode.

Lemma 4.1. *The controller given in (4–11), (4–15), and the adaptive update laws in (4–21) and (4–22) ensure that all system signals associated with the i^{th} target are bounded under closed-loop operation and that $\forall t \in [t_{i,k}^c, t_{i,k}^u), \forall k \in \mathbb{N}$,*

$$\|z_i(t)\|^2 \leq \frac{\beta_2}{\beta_1} \|z_i(t_{i,k}^c)\|^2 e^{-\lambda_{1,i}(t-t_{i,k}^c)} + \frac{\kappa_{1,i}}{\beta_1} \quad (4-31)$$

provided that the gains are selected according to the sufficient conditions

$$k_{2,i} \geq \frac{3\bar{\alpha}_i}{2\underline{\alpha}_i}, \quad k_{3,i} \geq \frac{\bar{\alpha}_i}{2}, \quad k_{s,i} \geq c_{NN,i}. \quad (4-32)$$

Moreover, provided the inequality in (4–26) is satisfied (i.e., the trajectories are sufficiently exciting), then $\forall t \in [t_{i,k}^c, t_{i,k}^u) \cap [\tau_i, \infty), \forall k \in \mathbb{N}$,

$$\|z_i(t)\|^2 \leq \frac{\beta_2}{\beta_1} \|z_i(t_{i,k}^c)\|^2 e^{-\lambda_{2,i}(t-t_{i,k}^c)} + \frac{\kappa_{2,i}}{\beta_1}. \quad (4-33)$$

Proof. Using (4–12), (4–16), (4–23), and (4–24), the time derivative of (4–27) during $t \in [t_{i,k}^c, t_{i,k}^u), \forall k \in \mathbb{N}$ can be upper bounded as

$$\begin{aligned} \dot{V}_i \leq & -k_{1,i}\underline{\alpha}_i \|\bar{x}_i\|^2 - k_y \|e_y\|^2 - \left(k_{2,i} - \frac{3\bar{\alpha}_i}{2\underline{\alpha}_i}\right) \|\bar{x}_i\|^2 - \left(k_{3,i} - \frac{\bar{\alpha}_i}{2}\right) \|e_y\|^2 \\ & + (c_{NN,i} - k_{s,i}) \|e_y\| + \frac{\bar{f}_i}{4k_{n,i}\underline{\alpha}_i} + c_{CL,i}. \end{aligned} \quad (4-34)$$

where $c_{NN,i}$ and $c_{CL,i}$ are positive constants that upper bound the residual from the function approximation error and the ICL, respectively. Note that in (4–34), the terms containing the NN weight estimation errors are both upper bounded by zero since they are only negative semi-definite during the learning phase (i.e., before enough data has been collected). Provided the gain conditions in (4–32) are satisfied, (4–34) can be upper bounded as

$$\dot{V}_i(z_i(t)) \leq -k_{1,i}\underline{\alpha}_i \|\bar{x}_i\|^2 - k_y \|e_y\|^2 + C_{1,i}, \quad (4-35)$$

where $C_{1,i} = \frac{\bar{f}_i}{4k_{n,i}\underline{\alpha}_i} + c_{CL,i}$. Using (4–30), (4–35) can be upper bounded as

$$\dot{V}_i(z_i(t)) \leq -\lambda_{1,i}V_i(z_i(t)) + \lambda_{1,i}\beta_4 + C_{1,i} \quad (4-36)$$

where $\lambda_{1,i} \triangleq \frac{1}{\beta_3} \min \{k_{1,i}\alpha_i, k_y\}$. Applying the Comparison Lemma [29, Lemma 3.4] to (4–36) yields

$$V_i(z_i(t)) \leq V_i(z_i(t_{i,k}^c)) e^{-\lambda_{1,i}(t-t_{i,k}^c)} + \kappa_{1,i}, \quad (4-37)$$

$\forall t \in [t_{i,k}^c, t_{i,k}^u], \forall k \in \mathbb{N}$, where $\kappa_{1,i} = \left(\beta_4 + \frac{C_{1,i}}{\lambda_{1,i}}\right)$. Using (4–28), (4–31) can be obtained.

Once sufficient data has been collected (i.e., $t \in [t_{i,k}^c, t_{i,k}^u] \cap [\tau_y, \infty) \cap [\tau_i, \infty)$), and provided that the gain conditions in (4–32) are satisfied, the time derivative of (4–27) can be upper bounded as

$$\dot{V}_i \leq -k_{1,i}\alpha_i \|\bar{x}_i\|^2 - k_y \|e_y\|^2 - k_{CL,y}\lambda_y \|\tilde{W}_y\|^2 - k_{CL,i}\lambda_i \|\tilde{W}_i\|^2 + C_{1,i}.$$

Furthermore, (4–28) can be used to show that

$$\dot{V}_i(z_i(t)) \leq -\lambda_{2,i}V_i(z_i(t)) + C_{1,i}, \quad (4-38)$$

$\forall t \in [t_{i,k}^c, t_{i,k}^u] \cap [\tau_y, \infty) \cap [\tau_i, \infty), \forall k \in \mathbb{N}$, where $\lambda_{2,i} \triangleq \frac{1}{\beta_2} \min \{k_{1,i}\alpha_i, k_y, k_{CL,y}\lambda_y, k_{CL,i}\lambda_i\}$.

Applying the Comparison Lemma [29, Lemma 3.4] to (4–38) yields

$$V_i(z_i(t)) \leq V_i(z_i(t_{i,k}^c)) e^{-\lambda_{2,i}(t-t_{i,k}^c)} + \kappa_{2,i}, \quad (4-39)$$

$\forall t \in [t_{i,k}^c, t_{i,k}^u] \cap [\tau_y, \infty) \cap [\tau_i, \infty), \forall k \in \mathbb{N}$, where $\kappa_{2,i} = \frac{C_{1,i}}{\lambda_{2,i}}$. Then, (4–39) can be used with (4–28) to yield (4–33). \square

4.4.2 Target Operating in the *Unchased* Mode

In this section, the states associated with i^{th} target are shown to be bounded during periods in which it is not the currently *chased* target. Here, the subscript $i = c$ refers to the target that is currently operating in *chased* mode. These terms appear due to the fact that the virtual (4–11) and actual (4–15) control laws are designed in terms of the currently *chased* target, and thus will appear in this analysis with the inclusion of the state e_y in (4–27).

Lemma 4.2. *During $t \in [t_{i,k}^u, t_{i,k+1}^c), \forall k \in \mathbb{N}$, the system states associated with the i^{th} target remain bounded.*

Proof. Provided that the gain conditions in (4–32) are satisfied, and substituting (4–2), (4–16), (4–23), and (4–25), the time derivative of (4–27) during $t \in [t_{i,k}^u, t_{i,k+1}^c)$, $\forall k \in \mathbb{N}$ can be upper bounded as

$$\begin{aligned} \dot{V}_i \leq & \bar{\alpha}_i \|\bar{x}_i\|^2 + \bar{\alpha}_i \|\bar{x}_i\| \|x_i^g\| + \bar{\alpha}_i \|\bar{x}_i\| \|e_y\| + K_{1,i} \bar{\alpha}_i \|\bar{x}_i\| \|\bar{x}_c\| + \bar{\alpha}_i \|\bar{x}_i\| \|x_c^g\| \\ & + \|\bar{x}_i\| \|f_i\| + K_{1,i} \|e_y\| \|W_i^T \sigma_i\| + K_{1,i} \|e_y\| \left\| \hat{W}_c^T \sigma_c \right\| - k_y \|e_y\|^2 \end{aligned} \quad (4-40)$$

Using Young’s inequality, (4–28), and upper bounding the term $\|\bar{x}_c\|$ using the right hand side of (4–31), (4–40) can be further upper bounded by

$$\dot{V}_i(z_i(t)) \leq \lambda_{3,i} V_i(z_i(t)) + C_{2,i}. \quad (4-41)$$

where $\lambda_{3,i}, C_{2,i} \in \mathbb{R}$ are positive constants and $\lambda_{3,i} = \frac{1}{\beta_1} \max \left\{ \frac{\bar{\alpha}_i}{2} (5 + K_{1,i}) + \frac{1}{2}, K_{1,i} - k_y \right\}$.

Applying the Comparison Lemma [29, Lemma 3.4] to (4–41), and upper bounding, yields

$$V_i(z_i(t)) \leq (V_i(z_i(t_{i,k}^u)) + \kappa_{3,i}) e^{\lambda_{3,i}(t-t_{i,k}^u)} - \kappa_{3,i}, \quad (4-42)$$

where $\kappa_{3,i} = \frac{C_{2,i}}{\lambda_{3,i}}$. Furthermore, $\forall t \in [t_{i,k}^c, t_{i,k}^u) \cap [\tau_y, \infty) \cap [\tau_i, \infty)$, $\forall k \in \mathbb{N}$ (i.e., once enough data has been collected), the term $C_{2,i}$ in (4–41) is replaced with a smaller constant $C_{3,i}$ ($C_{3,i} < C_{2,i}$ because (4–33) is used to upper bound the term $\|\bar{x}_c\|$ instead of (4–31), and $\kappa_{2,i} < \kappa_{1,i}$), and the resulting differential inequality yields the solution

$$V_i(z_i(t)) \leq (V_i(z_i(t_{i,k}^u)) + \kappa_{4,i}) e^{\lambda_{3,i}(t-t_{i,k}^u)} - \kappa_{4,i}, \quad (4-43)$$

where $\kappa_{4,i} = \frac{C_{3,i}}{\lambda_{3,i}}$. □

4.4.3 Combined Analysis

In this section, switched systems analysis is used to show that the states associated with the i^{th} target converge to an ultimate bound. First, (4–37) and (4–42) are used to develop an ultimate bound during the learning phase (i.e., before enough data has been collected), and then an ultimate bound on the states during the second

phase (i.e., after learning has occurred) is synthesized based on (4–39) and (4–43).

To facilitate the analysis, let $\nu_{1,i}, \nu_{2,i}$ denote positive constants $\forall i \in \{1, 2, \dots, n_t\}$, where $\nu_{1,i} \triangleq e^{\lambda_{3,i} T_i^u (km, (k+1)m-1) - \lambda_{1,i} T_i^c (km, (k+1)m-1)}$, $m \in \mathbb{N}$, $\lambda_{1,i}$ is introduced in (4–36), and $\lambda_{3,i}$ is introduced in (4–41).

Theorem 4.1. *The controllers in (4–11) and (4–15), and the adaptive update laws in (4–21) and (4–22) ensure that all signals associated with the i^{th} target remain bounded for all time $t \in [0, \bar{\tau}_i)$, where $\bar{\tau}_i = \max\{\tau_y, \tau_i\}$, and*

$$\limsup_t \|z_i(t)\|^2 \leq \frac{\nu_{2,i}}{\beta_1(1-\nu_{1,i})} e^{\lambda_{3,i} T_{i,\max}^u}, \quad (4-44)$$

where $T_{i,\max}^u \triangleq \sup_k T_i^u(km, (k+1)m-1)$ and z_i was defined in (4–29), provided there exists an $m < \infty$ and sequences $\{\Delta t_{i,k}^c\}_{k=0}^\infty$ and $\{\Delta t_{i,k}^u\}_{k=0}^\infty$ such that $\forall k \in \mathbb{N}$

$$T_i^u(km, (k+1)m-1) < \frac{\lambda_{1,i}}{\lambda_{3,i}} T_i^c(km, (k+1)m-1). \quad (4-45)$$

Proof. Consider a single cycle of the i^{th} target switching to *chased*, *unchased*, and back to *chased* mode, i.e., $t \in [t_{i,k}^c, t_{i,k+1}^c)$. Using (4–37) and (4–42), the evolution of V_i over m cycles can be written as

$$V_i(z_i(t_{i,(k+1)m}^c)) \leq \nu_{1,i} V_i(z_i(t_{i,km}^c)) + \nu_{2,i}$$

where $\nu_{1,i} < 1$ provided (4–45) is satisfied. Let $\{s_{i,k}\}_{k=0}^\infty$ be a sequence defined by the recurrence relation $s_{i,k+1} = M_{1,i}(s_{i,k})$, with initial condition $s_{i,0} = V_i(z_i(t_{i,0}^c))$, where $M_{1,i} : \mathbb{R} \rightarrow \mathbb{R}$ is defined as $M_{1,i}(s) \triangleq \nu_{1,i}s + \nu_{2,i}$. Since $\nu_{1,i} < 1$, $M_{1,i}$ is a contraction [35, Definition 9.22], and thus all initial conditions, $s_{i,0}$, approach the fixed point $s = \frac{\nu_{2,i}}{1-\nu_{1,i}}$ [35, Theorem 9.23]. Since the sequence $\{s_{i,k}\}$ upper bounds V_i , in the sense that $V_i(z_i(t_{i,km}^c)) \leq s_{i,k}$, V_i is ultimately bounded. However, since the dwell time condition (4–45) is specified over m cycles rather than a single cycle, V_i may grow within $[t_{i,km}^c, t_{i,(k+1)m}^c)$. Thus, the ultimate bound of z_i is given by (4–44). \square

The analysis in Theorem 4.1 shows that the closed-loop system is ultimately bounded during the initial phase (i.e., $t \in [0, \bar{\tau}_i)$). To further reduce the ultimate bound on the states associated with the i^{th} target, the following theorem uses (4–39) and (4–43) to establish a smaller bound once sufficient excitation occurs (i.e., $t \in [\bar{\tau}_i, \infty)$). To facilitate the following theorem, let $\nu_{3,i}, \nu_{4,i}$ denote positive constants, where $\nu_{3,i} \triangleq e^{\lambda_{3,i}T_i^u(km, (k+1)m-1) - \lambda_{2,i}T_i^c(km, (k+1)m-1)}$, $m \in \mathbb{N}$, $\lambda_{2,i}$ is introduced in (4–38), and $\lambda_{3,i}$ is introduced in (4–41).

Theorem 4.2. *The controllers in (4–11) and (4–15), and the adaptive update laws in (4–21) and (4–22) ensure that all signals associated with the i^{th} target remain bounded for all time $t \in [\bar{\tau}_i, \infty)$ and*

$$\limsup_t \|z_i(t)\|^2 \leq \frac{\nu_{4,i}}{\beta_1(1 - \nu_{3,i})} e^{\lambda_{3,i}T_{i,\max}^u}, \quad (4-46)$$

provided there exists an $m < \infty$ and sequences $\{\Delta t_{i,k}^c\}_{k=0}^\infty$ and $\{\Delta t_{i,k}^u\}_{k=0}^\infty$ such that $\forall k \in \mathbb{N}$

$$T_i^u(km, (k+1)m-1) < \frac{\lambda_{2,i}T_i^c(km, (k+1)m-1)}{\lambda_{3,i}}. \quad (4-47)$$

Proof. This proof follows the same strategy as that of Theorem 4.1 for $t \in [t_{i,k}^c, t_{i,k+1}^c) \cap [\bar{\tau}_i, \infty)$. Provided (4–47) is satisfied $\nu_{3,i} < 1$. By establishing $\{s_{i,k}\}_{k=0}^\infty$ as a sequence defined by the recurrence relation $s_{i,k+1} = M_{2,i}(s_{i,k})$ with initial condition $s_{i,0} = V_i(z_i(t_{i,q_i}^c))$, where $q_i \triangleq \underset{k}{\operatorname{argmin}} \{t_{i,k}^c > \bar{\tau}_i\}$ and $M_{2,i} : \mathbb{R} \rightarrow \mathbb{R}$ is defined as $M_{2,i}(s) \triangleq \nu_{3,i}s + \nu_{4,i}$, then following the same steps as in Theorem 4.1, the result in (4–46) can be concluded. □

Remark 4.2. As long as (4–45) and (4–47) are satisfied, the results from Lemmas 4.1 and 4.2 and Theorems 4.1 and 4.2 ensure that all system states remain bounded for all time $t \geq 0$ (i.e., $\eta(t)$ is contained for all time in χ , defined as $\chi = \{\eta(t) \mid \|\eta(t)\| \leq \kappa_\chi \|\eta(0)\|\}$, where κ_χ is a positive constant). Thus, the Weierstrass approximation theorem holds.

4.5 Experiments

Experiments were performed to validate the theoretical work in this chapter. Two experiments are presented, both with one herder and six target agents (three pink targets and three yellow targets). A Parrot Bebop 2 quadcopter platform served as the herding agent and a NaturalPoint, Inc. OptiTrack motion capture system was used to record the position of each agent at all times for feedback control. To represent truly unactuated target agents, each was represented by a mobile platform constructed from paper plates and poster board. The air disturbance caused by the herder quadcopter propellers cause nearby target agents to slide away from the herder.

The unknown interactions between the herder and targets were approximated using a NN for each target. The drift dynamics of the targets and herder were assumed to be zero (i.e., $f_i(x) = h(x, y) = 0$), and therefore were not approximated in these experiments. The NN for each target agent used $L_1 = 200$ basis functions, with centers randomly distributed throughout four $2m \times 2m$ quadrants around the herder, and standard deviations of $0.3m$.

4.5.1 Switching Strategy

The above stability analysis, while being agnostic to the specific design of the herder's switching strategy, does impose dwell time conditions which must be met to ensure stability. The herder switching strategy used in these experiments was defined as follows. The herder selects the agent furthest from its goal to chase first, and drives the target error to some percentage of its previous error, $\gamma_r \in (0, 1)$ (referred to as the "herding ratio"), such that $\bar{x}_i(t_{i,k}^u) \leq \gamma_r \bar{x}_i(t_{i,k}^c)$, $\forall k \in \mathbb{N}$, $\forall i \in \mathcal{T}$. The herder then switches to the target with the largest current error and repeats the process until all targets are regulated to the neighborhood of their goal location, $B_R(x_i^g) \triangleq \{q \in \mathbb{R}^n \mid \|q - x_i^g\| \leq R\}$, $\forall i \in \mathcal{T}$.

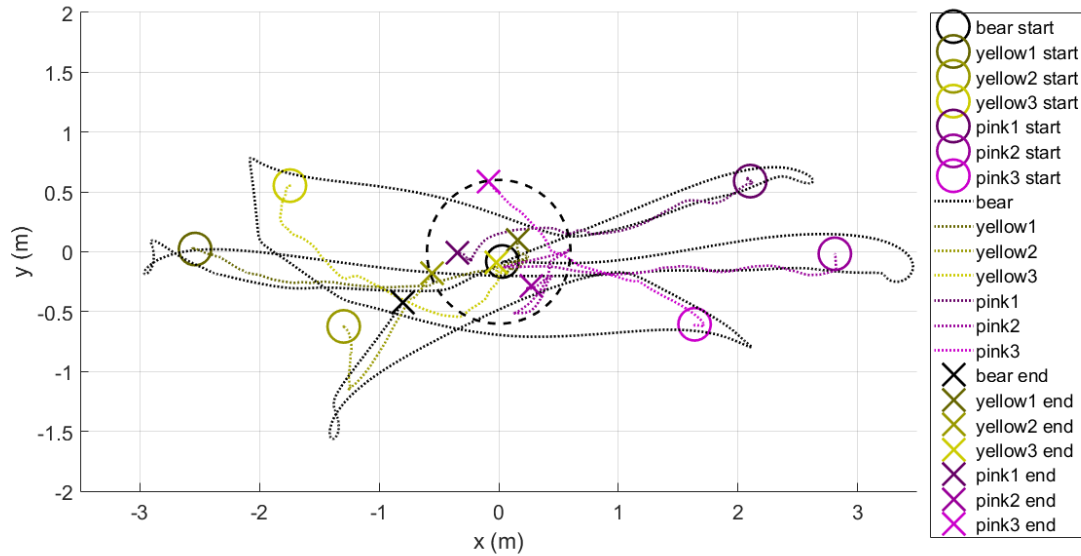


Figure 4-1. The herder and target paths with the objective of regulating all targets to the center.

4.5.2 Grouping Objective

In the first experiment, the herder was tasked with regulating all agents to a neighborhood of the origin, regardless of color. The herding ratio was selected to be $\gamma_r = 0.75$, and the goal neighborhood size was $R = 0.6 m$. Figures 4-1 and 4-2 show the overall paths and starting and ending positions, respectively, of all agents during the first experiment (regulate all agents to the center). The plot in Figure 4-3 shows the norms of each target error, while Figure 4-4 shows the herder control. Example NN weight estimates for the first experiment are shown for sample target agents in Figures 4-5 and 4-6.

4.5.3 Partitioning Objective

The objective for the second experiment was to regulate the target agents to different locations based on their color (the color of each agent is known). The herding ratio and goal neighborhood size were selected to be $\gamma_r = 0.4$, and $R = 0.5$, respectively.

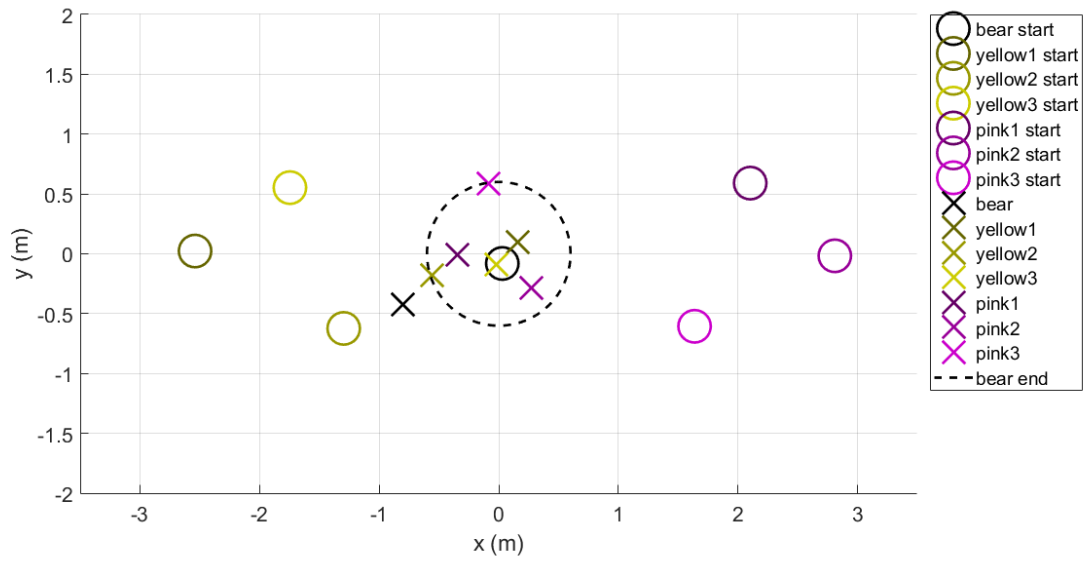


Figure 4-2. The starting and ending herder and target positions for the experiment with the objective of regulating all targets to the center.

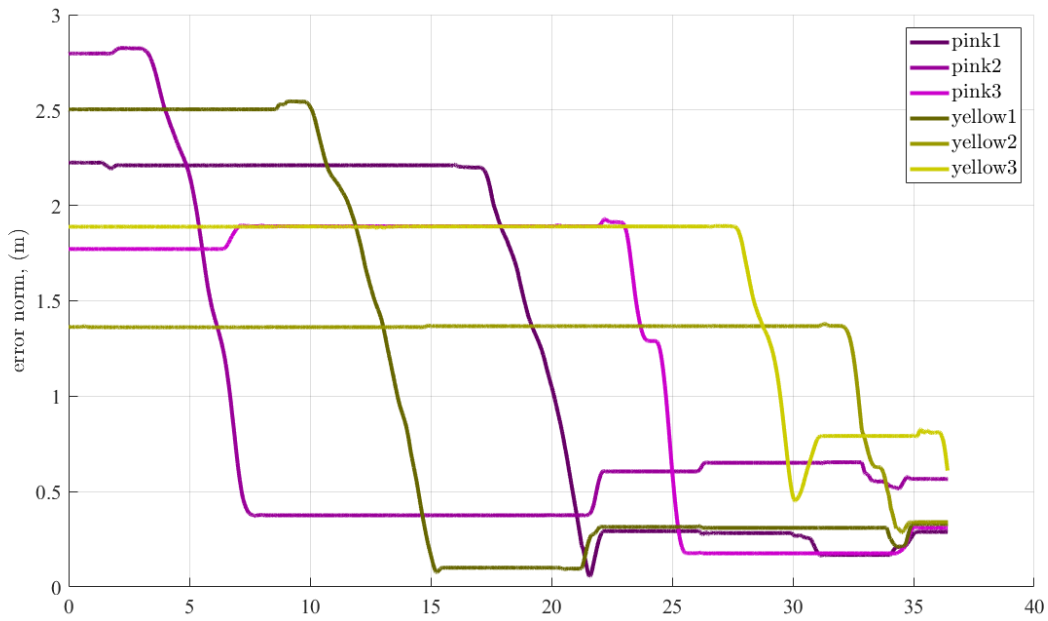


Figure 4-3. The norm of the target positions for the first experiment.

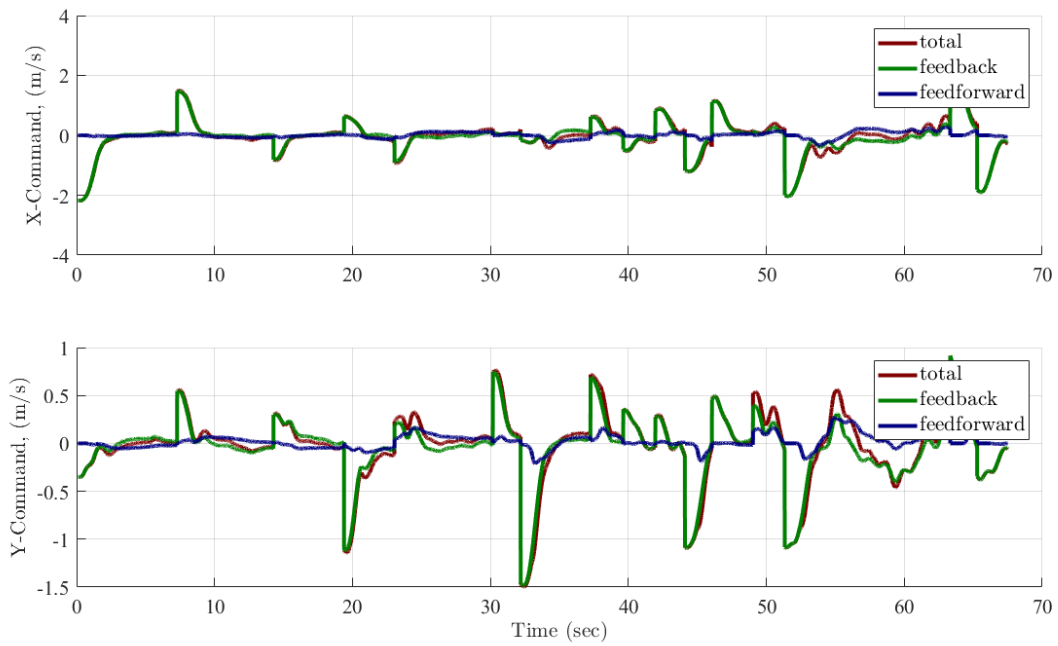


Figure 4-4. The herder controller for the first experiment.

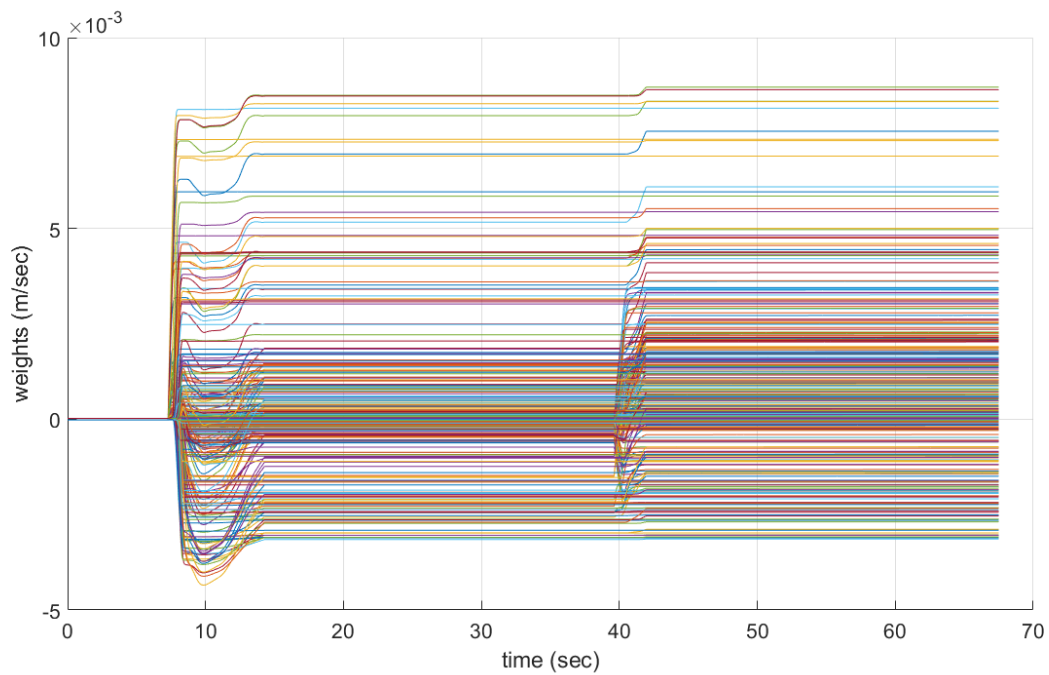


Figure 4-5. Adaptive weight estimates for an example target during the first experiment.

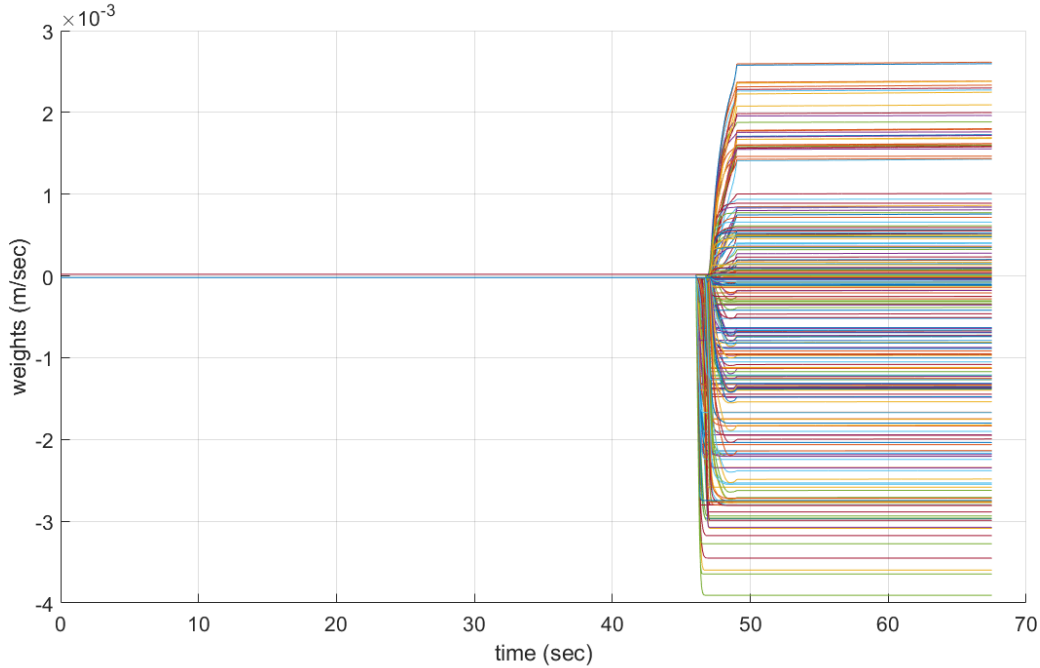


Figure 4-6. Adaptive weight estimates for an example target during the first experiment.

Figures 4-7 and 4-8 show the overall paths and starting and ending positions, respectively, of all agents for the second experiment (regulate agents to a certain location based on color). For the partitioning experiment, the plots of the target error norms and herder control are given in Figures 4-9 and 4-10, respectively. Each target's NN weight estimates are shown in Figures 4-11 and 4-12.

4.6 Concluding Remarks

In this chapter, NN function approximation techniques were employed to estimate unknown interaction and drift dynamics of multiple target agents. An adaptive controller and switching conditions were developed using Lyapunov-based stability analysis for a single herding agent to ensure uniformly ultimately bounded regulation of n_t uncertain target agents to the origin, despite their lack of explicit control input. An ICL scheme was used to guarantee ultimately bounded convergence of the ideal weight estimation error and enable the switched systems analysis. Experimental results are provided to validate the theoretical contribution in this chapter.

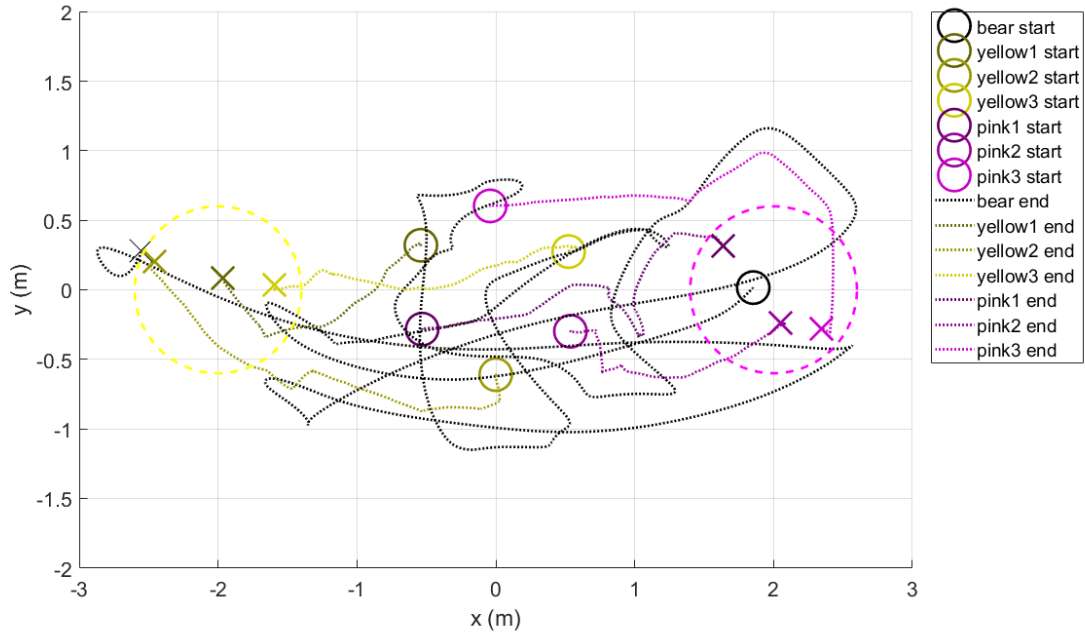


Figure 4-7. The herder and target paths with the objective of partitioning targets by color.

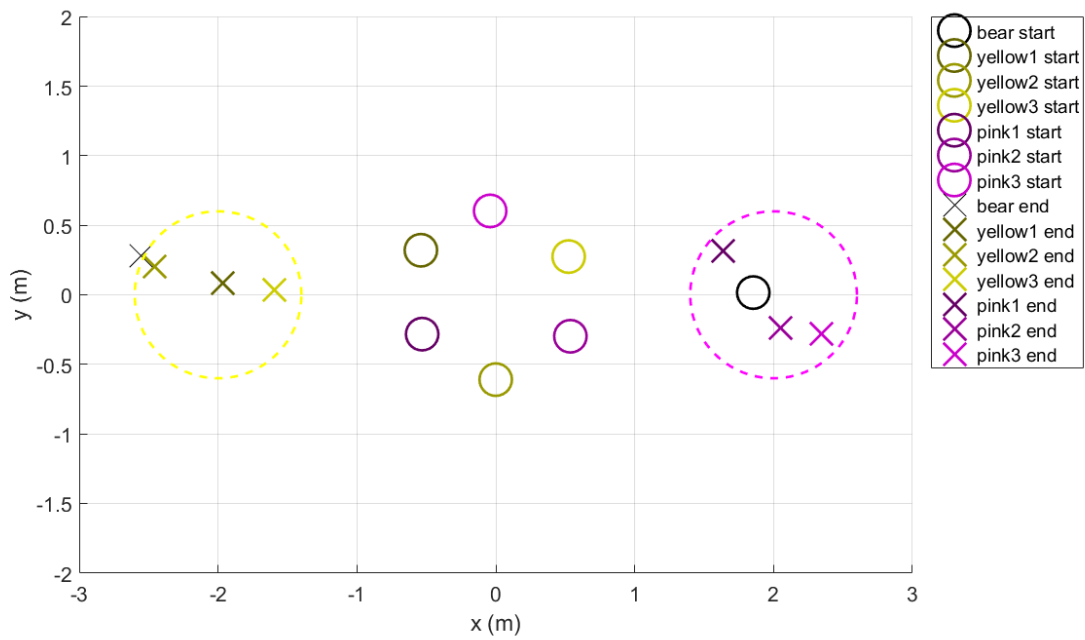


Figure 4-8. The starting and ending herder and target positions for the experiment with the objective of partitioning targets by color.

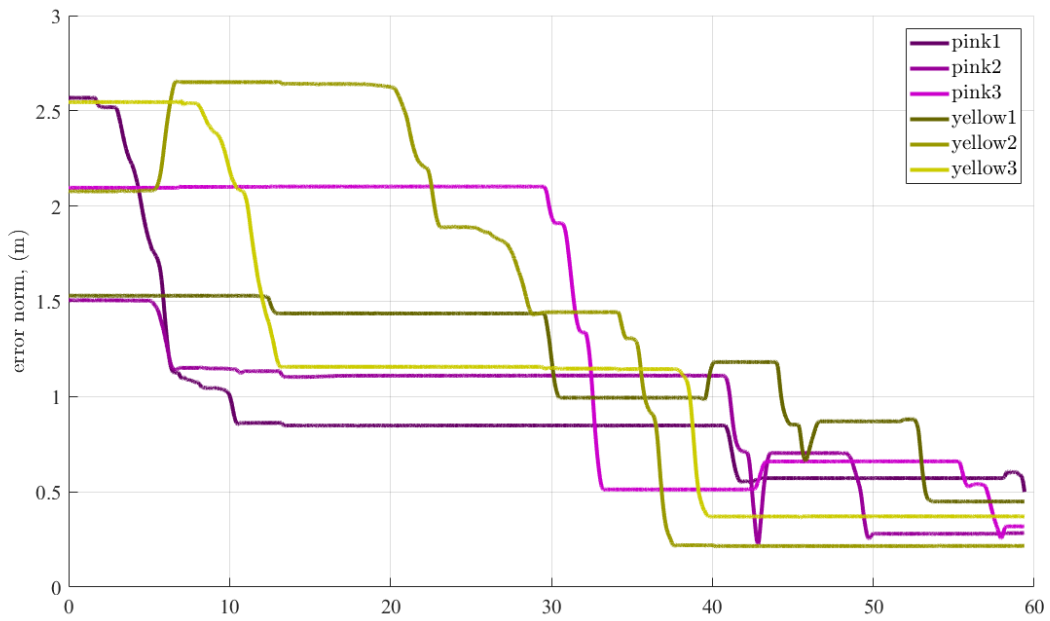


Figure 4-9. The norm of the target positions for the second experiment.

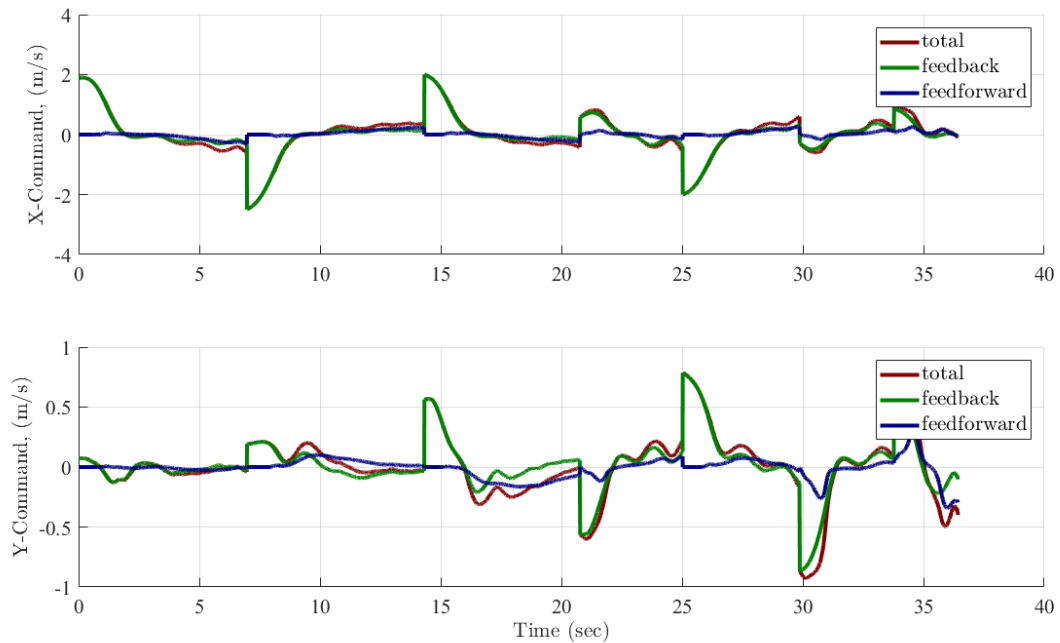


Figure 4-10. The herder controller for the second experiment.

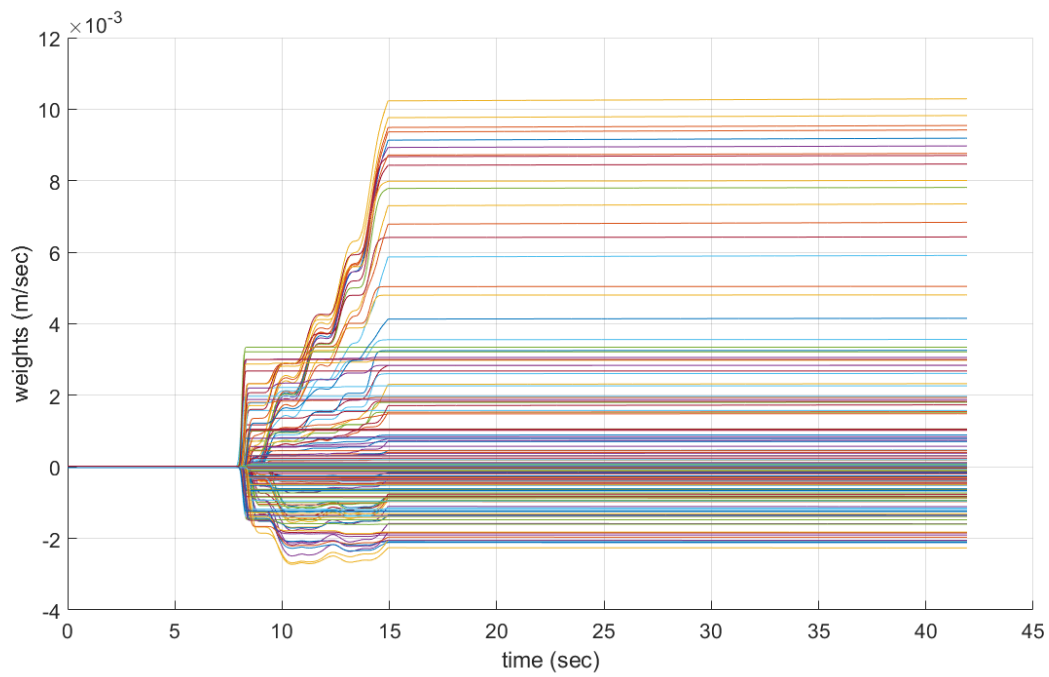


Figure 4-11. Adaptive weight estimates for an example target during the second experiment.

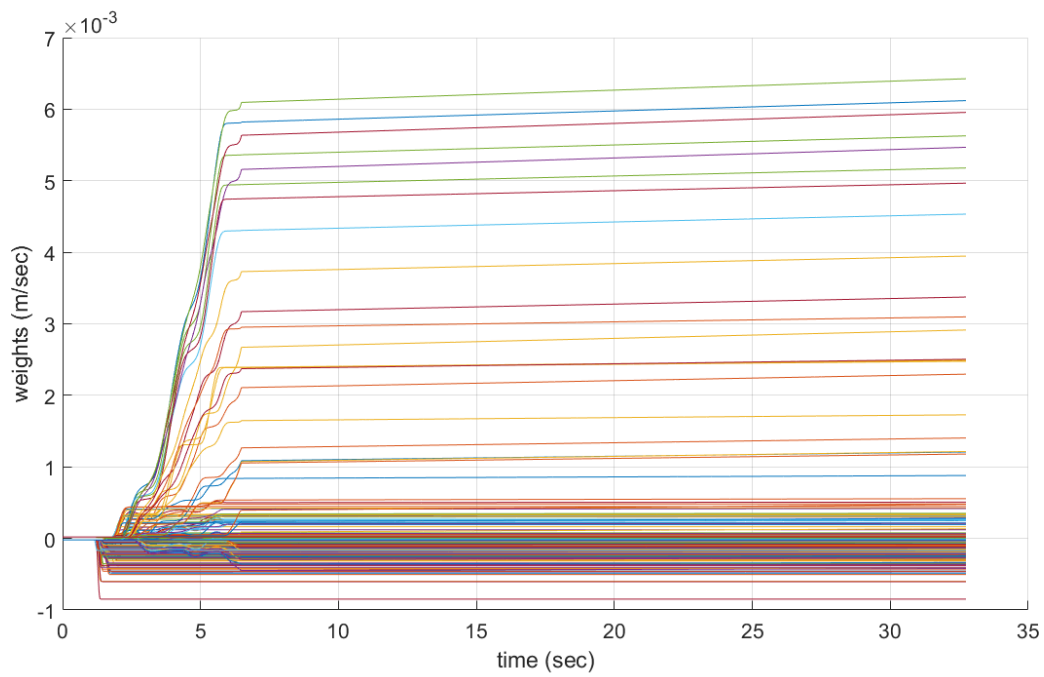


Figure 4-12. Adaptive weight estimates for an example target during the second experiment.

CHAPTER 5
COOPERATIVE TWO-PHASE (GROUP AND RELOCATE) HERDING OF MULTIPLE
AGENTS WITH UNCERTAIN DYNAMICS

This chapter examines a two-phase *indirect* herding problem, where a team of herding agents is controlled to first group and then relocate a team of uncontrollable target agents. To accomplish phase one (grouping), the results in [11, 12], which both solve the *indirect* herding problem with a single herder and multiple uncertain targets, are extended to use multiple herders to group the team of uncertain targets into an ensemble of target agents. Then, inspired by [1, 13], the herders form a frontal arc to relocate the ensemble to a goal location.

5.1 Problem Formulation

A two-phase herding problem is considered in this chapter. A team of $n_h \in \mathbb{Z}_{>0}$ cooperative herding agents are tasked with relocating a larger team of $n_t \in \mathbb{Z}_{>0}$ homogeneous target agents, as a group, to a neighborhood about a specified goal location (where $2 \leq n_h < n_t$). Let the set of herding agents and target agents be denoted by $\mathcal{H} \triangleq \{1, 2, \dots, n_h\}$ and $\mathcal{T} \triangleq \{n_h + 1, \dots, n_h + n_t\}$, respectively. To draw a distinction between the two teams, herders will be represented by $y_j \in \mathbb{R}^2$, $j \in \mathcal{H}$, while targets will be represented by $x_i \in \mathbb{R}^2$, $i \in \mathcal{T}$.

Definition 5.1. During the grouping phase, a target x_i is said to be actively *chased* when there is a herder y_j such that $(i, j) \in \mathcal{C}$, where $i \in \mathcal{T}$ and $j \in \mathcal{H}$, and $\mathcal{C} \subseteq \mathcal{T} \times \mathcal{H}$ is the current set of *herder/target* pairs. If $(i, j) \in \mathcal{C}$, y_j is referred to as the *herder*, while x_i is referred to as the *target*. This means that y_j will *chase* x_i to a desired location.

Let the distance between the i^{th} target and the j^{th} herder be defined as $r_{i,j} \triangleq \|x_i - y_j\|$, $\forall i \in \mathcal{T}$, $j \in \mathcal{H}$. Additionally, let the distance between the mean target location and the j^{th} herder be $r_j \triangleq \|\bar{x} - y_j\|$, $\forall j \in \mathcal{H}$, where $\bar{x} \in \mathbb{R}^2$ is defined as $\bar{x} \triangleq \frac{1}{n_t} \sum_{i \in \mathcal{T}} x_i$.

Assumption 5.1. Based on physical constraints depending on implementation, the distance between any herder and any target can be lower bounded by a strictly positive constant for all time (i.e., $\underline{r} \leq r_{i,j}$, $\forall i \in \mathcal{T}$, $j \in \mathcal{H}$, where $\underline{r} \in \mathbb{R}_{>0}$).

In the first (grouping) phase, the objective is to regulate all of the target agents into an ensemble and then, in the second (relocating) phase, push the ensemble to a desired goal location.

Definition 5.2. The targets will be considered to be an *ensemble* if and only if, $\forall i \in \mathcal{T}$, $x_i \in B_r(\bar{x})$, where \bar{x} is the mean target location and $B_r(\bar{x}) \triangleq \{q \in \mathbb{R}^2 \mid \|q - \bar{x}\| \leq r\}$, $\forall r \in [r_{\min}, r_{\max}]$, where $r_{\min}, r_{\max} \in \mathbb{R}_{>0}$ and $\bar{r} \leq r_{\min}$.

During the grouping phase, the herders will individually *chase* each target (similar to [11, 12]) to a neighborhood about the initial mean position of all target agents, $B_{r_{\min}}(\bar{x}_0) \triangleq \{q \in \mathbb{R}^2 \mid \|q - \bar{x}_0\| \leq r_{\min}\}$, where $\bar{x}_0 \triangleq \frac{1}{n_t} \sum_{i \in \mathcal{T}} x_i(0) \in \mathbb{R}^2$. Since the herders are outnumbered, they must switch between *chasing* the targets, potentially only part of the way at a time, until all targets are successfully regulated to $B_{r_{\min}}(\bar{x}_0)$. A given target may be *chased* partially to $B_{r_{\min}}(\bar{x}_0)$ by one herder (who must then switch to another target), and then *chased* part of the rest of the way by another herder, and so on, until the target is regulated to $B_{r_{\min}}(\bar{x}_0)$. Once the grouping phase is complete, the herders begin the relocating phase, during which the entire ensemble of targets is regulated to the final goal location. The regulation objective is accomplished by the herders forming a frontal arc (positioned on a circle centered at the mean target location) designed to influence the ensemble in a particular direction. The final goal location is defined as the neighborhood $B_{r_g}(x_g) \triangleq \{q \in \mathbb{R}^2 \mid \|q - x_g\| \leq r_g\}$, where $x_g \in \mathbb{R}^2$ and $r_g \in \mathbb{R}_{>0}$ are the center and radius of the desired final goal location. While operating in the relocating phase, the herders will adjust the radius of the circle that defines the frontal arc to compensate for any dispersion by the ensemble.

All agent states are assumed to be measurable at all times for feedback control. As in previous chapters, only the herders are controllable, while the targets can only be influenced by exploiting the uncertain interaction between herders and targets. The target agent dynamics are modeled by taking the negative gradient of the potential

function $\Phi = \sum_{i \in \mathcal{T}} \sum_{j \in \mathcal{H}} \alpha_t \frac{1}{\|x_i - y_j\|}$, yielding

$$\dot{x}_i = -\nabla_{x_i} \Phi = \alpha_t \sum_{j \in \mathcal{H}} \frac{(x_i - y_j)}{\|x_i - y_j\|^3}, \quad (5-1)$$

$\forall i \in \mathcal{T}$, where $\alpha_t \in \mathbb{R}$ is an unknown positive constant that is bounded by $\underline{\alpha}_t \leq \alpha_t \leq \bar{\alpha}_t$, where $\underline{\alpha}_t, \bar{\alpha}_t \in \mathbb{R}$ are known positive constants.

The controllable herder dynamics, which include a repulsion term to ensure collision avoidance between targets and herders, are given by

$$\dot{y}_j = \alpha_h \sum_{i \in \mathcal{T}} \frac{(y_j - x_i)}{\|y_j - x_i\|^3} + u_j, \quad (5-2)$$

$\forall j \in \mathcal{H}$, where $\alpha_h \in \mathbb{R}$ is an unknown positive constant that is bounded by $\underline{\alpha}_h \leq \alpha_h \leq \bar{\alpha}_h$, where $\underline{\alpha}_h, \bar{\alpha}_h \in \mathbb{R}$ are known positive constants, and $u_j \in \mathbb{R}^2$ is the subsequently designed controller for the j^{th} herder. The following development requires that the following assumption is satisfied.

Assumption 5.2. The velocities of the herders, $\dot{y}_j, \forall j \in \mathcal{H}$, are measurable and known to all herders.

5.2 Grouping Phase

During the grouping phase, since $n_t > n_h$, the outnumbered team of herders must utilize a switching strategy to ensure that all targets are regulated to the neighborhood $B_{r_{\min}}(\bar{x}_0)$. The herders will each select a target to *chase* towards $B_{r_{\min}}(\bar{x}_0)$ initially, and then will switch between them as needed to ensure all targets are regulated to $B_{r_{\min}}(\bar{x}_0)$. To facilitate the control design, the herders consider each target to be operating in either a *chased* or *unchased* mode at any given time. To this end, let $t_{i,k}^c \in \mathbb{R}$ and $t_{i,k}^u \in \mathbb{R}$ denote the time of the k^{th} instance when the i^{th} target is switched to the *chased* or *unchased* mode, respectively, where $k \in \mathbb{N}$. The contiguous dwell time in the k^{th} activation of the i^{th} target operating in the *chased* or *unchased* mode is denoted by $\Delta t_{i,k}^c \in \mathbb{R}$ and $\Delta t_{i,k}^u \in \mathbb{R}$, and defined as $\Delta t_{i,k}^c \triangleq t_{i,k}^u - t_{i,k}^c$ and $\Delta t_{i,k}^u \triangleq t_{i,k+1}^c - t_{i,k}^u$, respectively. The total amount of time each of these modes is active between switching

instances a and b are denoted $T_i^c(a, b) \triangleq \sum_{l=a}^b \Delta t_{i,l}^c$ and $T_i^u(a, b) \triangleq \sum_{l=a}^b \Delta t_{i,l}^u$, respectively.

5.2.1 Grouping Objective

To quantify the grouping objective, the herding error for each target, denoted by $\tilde{x}_i \in \mathbb{R}^2$, is defined as

$$\tilde{x}_i(t) \triangleq x_i(t) - \bar{x}_0,$$

$\forall i \in \mathcal{T}$. Note that \bar{x}_0 is held constant during the grouping phase (i.e., the targets are regulated to the neighborhood of the location that was the mean target position at the start of the grouping phase). Additionally, the uncertain parameters in (5-1) and (5-2) are grouped into the uncertain vector

$$\theta \triangleq \begin{bmatrix} \alpha_t & \alpha_h \end{bmatrix}^T. \quad (5-3)$$

To facilitate the subsequent control design and stability analysis, let $\hat{\theta} \in \mathbb{R}^2$ denote an adaptive estimate of θ , and let $\tilde{\theta} \in \mathbb{R}^2$ be the parameter estimation error, defined as

$$\tilde{\theta}(t) \triangleq \theta - \hat{\theta}(t).$$

As in previous chapters, given that the target agent dynamics in (5-1) do not explicitly contain a control input, a backstepping strategy is used to inject the desired herder states as a virtual controllers into the dynamics of *chased* targets. Let $y_{d,1}, y_{d,2}, \dots, y_{d,n_h} \in \mathbb{R}^2$ denote the desired state of herders y_1, y_2, \dots, y_{n_h} , respectively. Then, the backstepping error $e_j \in \mathbb{R}^2$, is defined as

$$e_j(t) \triangleq y_{d,j}(t) - y_j(t), \quad \forall j \in \mathcal{H}. \quad (5-4)$$

5.2.2 Grouping Controller

Since $n_h < n_t$, every herder will be paired up with a target to *chase* in the grouping phase (but not all targets are being *chased* at all times unless $n_h = n_t$). Let $C \in \mathcal{H}$ and

$c \in \mathcal{T}$ be a *herder/target* pair such that $(c, C) \in \mathcal{C}$ (e.g., if the target x_5 is currently being chased by the herder y_2 , then $(5, 2) \in \mathcal{C}$).

The control development for the C^{th} herder to *chase* the c^{th} target to the neighborhood $B_{r_{\min}}(\bar{x}_0)$ entails the following backstepping strategy. Substituting (5-4) into (5-1) yields

$$\dot{\tilde{x}}_c = \frac{\alpha_t}{r_{c,C}^3} \left(x_c + e_C - y_{d,C} + \sum_{\substack{j \in \mathcal{H} \\ j \neq C}} \left(\frac{r_{c,C}^3}{r_{c,j}^3} (x_c - y_j) \right) \right). \quad (5-5)$$

To regulate the target error, the herder's desired state is designed as

$$y_{d,C} \triangleq K_x \tilde{x}_c + \bar{x}_0 + \sum_{\substack{j \in \mathcal{H} \\ j \neq C}} \left(\frac{r_{c,C}^3}{r_{c,j}^3} (x_c - y_j) \right), \quad (5-6)$$

where $K_x = k_{x1} + k_{x2}$ and $k_{x1}, k_{x2} \in \mathbb{R}$ are positive constant control gains. Using (5-6), (5-5) can be rewritten as

$$\dot{\tilde{x}}_c = \frac{\alpha_t}{r_{c,C}^3} ((1 - K_x) \tilde{x}_c + e_C). \quad (5-7)$$

To ensure that the herder follows the desired herder state, the backstepping error dynamics must also be considered. Taking the time derivative of (5-4), and substituting the target and herder dynamics in (5-1) and (5-2), yields

$$\dot{e}_C = \begin{bmatrix} Y_{t,c,C} & Y_{h,c,C} \end{bmatrix} \begin{bmatrix} \alpha_t \\ \alpha_h \end{bmatrix} + G_{c,C} - u_C, \quad (5-8)$$

where $Y_{t,c,C}, Y_{h,c,C}, G_{c,C} \in \mathbb{R}^2$ are known functions containing the target state $x_i, \forall i \in \mathcal{T}$ and the herder state and velocity $y_j, \dot{y}_j, \forall j \in \mathcal{H}$. The expression in (5-8) can be rewritten as

$$\dot{e}_C = Y_{c,C} \theta + G_{c,C} - u_C, \quad (5-9)$$

where $Y_{c,C} \in \mathbb{R}^{2 \times 2}$ is the regression matrix associated with the *herder/target* pair $(c, C) \in \mathcal{C}$, defined as $Y_{c,C} = \begin{bmatrix} Y_{t,c,C} & Y_{h,c,C} \end{bmatrix}$, and $\theta \in \mathbb{R}^2$ is defined in (5-3). The C^{th}

herders control law is designed as

$$u_C = K_y e_C + Y_{c,C} \hat{\theta} + G_{c,C}, \quad (5-10)$$

where $K_y = k_{y1} + k_{y2}$ and $k_{y1}, k_{y2} \in \mathbb{R}$ are positive constant control gains, and $\hat{\theta} \in \mathbb{R}^2$ is the current adaptive estimate of θ . Using (5-10), the closed-loop backstepping dynamics can be rewritten as

$$\dot{e}_C = Y_{c,C} \tilde{\theta} - K_y e_C. \quad (5-11)$$

During the grouping phase, the adaptive estimate $\hat{\theta}$ in (5-10) is generated based on the following adaptive update law using ICL

$$\dot{\hat{\theta}} \triangleq \text{proj} \left\{ \Gamma \sum_{(i,j) \in \mathcal{C}} Y_{i,j}^T e_j + k_{CL} \Gamma \sum_{l=1}^N \sum_{(i,j) \in \mathcal{C}} \left(\mathcal{Y}_{i,j,l}^T \left(\Delta e_{j,l} - \mathcal{G}_{i,j,l} + \mathcal{U}_{j,l} - \mathcal{Y}_{i,j,l} \hat{\theta} \right) \right) \right\}, \quad (5-12)$$

where $\text{proj} \{ \cdot \}$ is a smooth projection operator,¹ $\Gamma \in \mathbb{R}^{2 \times 2}$ and $k_{CL} \in \mathbb{R}$ are constant, positive definite control gains, $N \in \mathbb{Z}$ is a constant that represents the number of saved data points for the data stack, $t_l \in (\Delta t, t]$ are time points at which measurements are available, $\Delta t \in \mathbb{R}$ is a positive constant denoting the size of the window of integration, $\mathcal{Y}_{i,j,l} \triangleq \mathcal{Y}_{i,j}(t_l) \in \mathbb{R}^{2 \times 2}$, $\mathcal{G}_{i,j,l} \triangleq \mathcal{G}_{i,j}(t_l) \in \mathbb{R}^{2 \times 2}$, and $\mathcal{U}_{j,l} \triangleq \mathcal{U}_j(t_l) \in \mathbb{R}^{2 \times 2}$ are the integrals of $Y_{i,j}$, $G_{i,j}$, and u_j , respectively, at $t = t_l$, defined as

$$\mathcal{Y}_{i,j}(t) \triangleq \begin{cases} 0_{2 \times 2} & t \in [0, \Delta t] \\ \int_{t-\Delta t}^t Y_{i,j}(x(\varsigma), y(\varsigma)) d\varsigma & t > \Delta t \end{cases}, \quad (5-13)$$

$$\mathcal{G}_{i,j}(t) \triangleq \begin{cases} 0_{2 \times 1} & t \in [0, \Delta t] \\ \int_{t-\Delta t}^t G_{i,j}(x(\varsigma), y(\varsigma)) d\varsigma & t > \Delta t \end{cases},$$

¹ See Remark 3.6 or Section 4.4 in [33] for details of the projection operator.

$$\mathcal{U}_j(t) \triangleq \begin{cases} 0_{2 \times 1} & t \in [0, \Delta t] \\ \int_{t-\Delta t}^t u_j(\varsigma) d\varsigma & t > \Delta t \end{cases},$$

$0_{2 \times 2}$ denotes a 2×2 matrix of zeros, $0_{2 \times 1}$ denotes a 2×1 vector of zeros, $x \triangleq \begin{bmatrix} x_1^T & x_2^T & \dots & x_{n_t}^T \end{bmatrix}^T$, and $y \triangleq \begin{bmatrix} y_1^T & y_2^T & \dots & y_{n_h}^T \end{bmatrix}^T$. The data points that are saved are selected to maximize the minimum eigenvalue of $\sum_{l=1}^N \sum_{(i,j) \in \mathcal{C}} (\mathcal{Y}_{i,j,l}^T \mathcal{Y}_{i,j,l})^2$.

Taking the integral of (5–9), $\forall t \in (\Delta t, \infty)$, yields

$$\begin{aligned} \int_{t-\Delta t}^t \dot{e}_C(\varsigma) d\varsigma &= \int_{t-\Delta t}^t Y_{c,C}(x(\varsigma), y(\varsigma)) \theta d\varsigma + \int_{t-\Delta t}^t G_{c,C}(x(\varsigma), y(\varsigma)) d\varsigma \\ &\quad - \int_{t-\Delta t}^t u_C(\varsigma) d\varsigma. \end{aligned} \quad (5-14)$$

Using the Fundamental Theorem of Calculus and (5–13), (5–14) can be rewritten as

$$e_C(t) - e_C(t - \Delta t) = \mathcal{Y}_{c,C}(t) \theta + \mathcal{G}_{c,C}(t) - \mathcal{U}_C(t), \quad \forall t \in [\Delta t, \infty). \quad (5-15)$$

Using (5–15), the adaptive update law in (5–12) can be rewritten in the following equivalent, but non-implementable, form

$$\dot{\hat{\theta}} \triangleq \text{proj} \left\{ \Gamma \sum_{(i,j) \in \mathcal{C}} Y_{i,j}^T e_j + k_{CL} \Gamma \sum_{l=1}^N \sum_{(i,j) \in \mathcal{C}} (\mathcal{Y}_{i,j,l}^T \mathcal{Y}_{i,j,l}) \tilde{\theta} \right\}. \quad (5-16)$$

5.2.3 Grouping Stability Analysis

The stability analysis for the grouping phase is analyzed in three stages, each considering the overall stability of the states associated with the i^{th} target. First, Lemma 5.1 in Section 5.2.3.1 will prove that the i^{th} target is at least asymptotically stable during periods in which it operates in *chased* mode. Second, in Section 5.2.3.2, Lemma 5.2 shows that the states are bounded for all bounded t when the i^{th} target operates in

² See [34] for methods of selecting data.

unchased mode. Finally, the switched systems analysis in Section 5.2.3.3 provides worst-case ultimate bounds for the system states associated with the i^{th} target.

During the grouping phase, two distinct times must be also considered, an initial learning phase before sufficient data has been collected to satisfy the FE condition, and a second phase after sufficient excitation has occurred. Specifically, the use of an ICL-based scheme assumes that the following FE condition is satisfied [39, 40]

$$\exists \lambda, \tau > 0 : \forall t \geq \tau, \lambda_{\min} \left\{ \sum_{l=1}^N \sum_{(i,j) \in \mathcal{C}} (\mathcal{Y}_{i,j,l}^T \mathcal{Y}_{i,j,l}) \right\} \geq \lambda, \quad (5-17)$$

where $\lambda_{\min} \{ \cdot \}$ refers to the minimum eigenvalue of $\{ \cdot \}$.

To facilitate the following analysis, let $V_i : \mathbb{R}^n \times \mathbb{R}^n \times \mathbb{R}^2 \rightarrow \mathbb{R}$ be a positive definite, continuously differentiable candidate Lyapunov function, defined as

$$V_i(z_i(t)) \triangleq \frac{1}{2} \tilde{x}_i^T \tilde{x}_i + \sum_{j \in \mathcal{H}} \frac{1}{2} e_j^T e_j + \frac{1}{2} \tilde{\theta}^T \Gamma^{-1} \tilde{\theta}, \quad (5-18)$$

which can be bounded by

$$\beta_1 \|z_i(t)\|^2 \leq V_i(z_i(t)) \leq \beta_2 \|z_i(t)\|^2, \quad (5-19)$$

where $z_i \triangleq \left[\tilde{x}_i^T \ e_1^T \ \dots \ e_{n_h}^T \ \tilde{\theta}^T \right]^T$ and $\beta_1, \beta_2 \in \mathbb{R}$ are known positive bounding constants. Moreover, since the use of the projection algorithm in (5-16) ensures that $\tilde{\theta}_i, \hat{\theta}_i \in \mathcal{L}_\infty$, then the Lyapunov function candidate can also be upper bounded as

$$V_i(z_i(t)) \leq \beta_3 \left\| \left[\tilde{x}_i^T \ e_1^T \ \dots \ e_{n_h}^T \right] \right\|^2 + \beta_4, \quad (5-20)$$

where $\beta_3, \beta_4 \in \mathbb{R}$ are known positive bounding constants.

5.2.3.1 Target i is operating in the *chased* mode

Lemma 5.1. *The controllers given in (5-6), (5-10), and the adaptive update law in (5-12) ensure that all system signals associated with the i^{th} target are bounded under*

closed-loop operation and that $\forall t \in [t_{i,k}^c, t_{i,k}^u), \forall k \in \mathbb{N}$,

$$\|z_i(t)\|^2 \leq \frac{\beta_2}{\beta_1} \|z_i(t_{i,k}^c)\|^2 e^{-\lambda_1(t-t_{i,k}^c)} + \frac{\beta_4}{\beta_1} \quad (5-21)$$

provided that the gains are selected according to the sufficient conditions

$$k_{x2} \geq \frac{3\bar{\alpha}_t}{2\underline{\alpha}_t} \quad \text{and} \quad k_{y2} \geq \frac{\bar{\alpha}_t}{2r^3}. \quad (5-22)$$

Moreover, provided the inequality in (5-17) is satisfied (i.e., the trajectories are sufficiently exciting), then $\forall t \in [t_{i,k}^c, t_{i,k}^u) \cap [\tau_i, \infty), \forall k \in \mathbb{N}$,

$$\|z_i(t)\|^2 \leq \frac{\beta_2}{\beta_1} \|z_i(t_{i,k}^c)\|^2 e^{-\lambda_2(t-t_{i,k}^c)}. \quad (5-23)$$

Proof. Since the i^{th} target is operating in the *chased* mode in the analysis in this section, there must exist a $j \in \mathcal{H}$ such that $(i, j) \in \mathcal{C}$. Maintaining the notation used in Section 5.2.2, (5-18) can be rewritten using the *herder/target* pair $(c, C) \in \mathcal{C}$, where $c \in \mathcal{T}$ and $C \in \mathcal{H}$, as

$$V_c(z_c(t)) \triangleq \frac{1}{2} \tilde{x}_c^T \tilde{x}_c + \frac{1}{2} e_C^T e_C + \sum_{\substack{j \in \mathcal{H} \\ j \neq C}} \frac{1}{2} e_j^T e_j + \frac{1}{2} \tilde{\theta}^T \Gamma^{-1} \tilde{\theta}. \quad (5-24)$$

Using (5-7), (5-11), and (5-16), and provided that the gain conditions in (5-22) are satisfied, the time derivative of (5-18) during $t \in [t_{i,k}^c, t_{i,k}^u), \forall k \in \mathbb{N}$ can be upper bounded as

$$\dot{V}_c(z_c(t)) \leq -k_{x1} \frac{\underline{\alpha}_t}{r_{c,C}^3} \|\tilde{x}_c\|^2 - k_{y1} \sum_{j \in \mathcal{H}} \|e_j\|^2.$$

Since V_c is positive definite and \dot{V}_c is negative semi-definite, $V_c \in \mathcal{L}_\infty$; therefore, $\tilde{x}_c, e_j, \tilde{\theta} \in \mathcal{L}_\infty, \forall j \in \mathcal{H}$. Since $\tilde{x}_c, \tilde{\theta} \in \mathcal{L}_\infty$, and the constant unknown parameters θ and initial mean position \bar{x}_0 are constant, $x_c, \hat{\theta} \in \mathcal{L}_\infty$. Since $\sum_{j \in \mathcal{H}} e_j \in \mathcal{L}_\infty$ and $y_{d,j}$ contains the other herder states $y_l, l \in \mathcal{H}, l \neq j$, it can be shown that $y_{d,j} \in \mathcal{L}_\infty, \forall j \in \mathcal{H}$, and thus $y_j \in \mathcal{L}_\infty, \forall j \in \mathcal{H}$. Since $x_c, y_j \in \mathcal{L}_\infty, \forall j \in \mathcal{H}$, then $r_{c,j}, r_j \in \mathcal{L}_\infty, \forall j \in \mathcal{H}$. Since $r_{c,j} \in \mathcal{L}_\infty$,

then $\exists \bar{r} > 0 : r_{c,j}(t) \leq \bar{r}, \forall t \geq 0, \forall j \in \mathcal{H}$. Then, since $x_c, y_j, r_{c,j} \in \mathcal{L}_\infty$, it can be shown that $\tilde{x}_c, \dot{y}_{d,j} \in \mathcal{L}_\infty \implies \dot{y}_j, \forall j \in \mathcal{H}$, and thus $Y_{c,j}, G_{c,j} \in \mathcal{L}_\infty \implies u_j \in \mathcal{L}_\infty, \forall j \in \mathcal{H}$.

The expression in 5.2.3.1 can be upper bounded as

$$\dot{V}_c(z_c(t)) \leq -k_{x1} \frac{\alpha_t}{\bar{r}^3} \|\tilde{x}_c\|^2 - k_{y1} \sum_{j \in \mathcal{H}} \|e_j\|^2. \quad (5-25)$$

Based on (5-20), the inequality in (5-25) can be upper bounded as

$$\dot{V}_c(z_c(t)) \leq -\lambda_1 (V_c(z_c(t)) - \beta_4) \quad (5-26)$$

where $\lambda_1 \triangleq \frac{1}{\beta_3} \min \{k_{x1} \frac{\alpha_t}{\bar{r}^3}, k_{y1}\}$. Applying the Comparison Lemma [29, Lemma 3.4] to (5-26) yields

$$V_i(z_i(t)) \leq V_i(z_i(t_{i,k}^c)) e^{-\lambda_1(t-t_{i,k}^c)} + \beta_4,$$

$\forall t \in [t_{i,k}^c, t_{i,k}^u), \forall k \in \mathbb{N}$, which can be used with (5-19) to yield (5-21).

Once sufficient data has been collected (i.e., $t \in [t_{i,k}^c, t_{i,k}^u) \cap [\tau_i, \infty)$), (5-19) can be used to upper bound the time derivative of (5-24) as

$$\dot{V}_c \leq -k_{x1} \frac{\alpha_t}{\bar{r}^3} \|\tilde{x}_c\|^2 - \sum_{j \in \mathcal{H}} k_{y1} \|e_j\|^2 - k_{CL\Delta} \|\tilde{\theta}\|^2,$$

which can be further upper bounded as

$$\dot{V}_c(z_c(t)) \leq -\lambda_2 V_c(z_c(t)), \quad (5-27)$$

$\forall t \in [t_{i,k}^c, t_{i,k}^u) \cap [\tau_i, \infty), \forall k \in \mathbb{N}$, where $\lambda_2 \triangleq \frac{1}{\beta_2} \min \{k_{x1} \frac{\alpha_t}{\bar{r}^3}, k_{y2}, k_{CL\Delta}\}$. Applying the Comparison Lemma [29, Lemma 3.4] to (5-27) yields

$$V_i(z_i(t)) \leq V_i(z_i(t_{i,k}^c)) e^{-\lambda_2(t-t_{i,k}^c)}$$

$\forall t \in [t_{i,k}^c, t_{i,k}^u) \cap [\tau_i, \infty), \forall k \in \mathbb{N}$, which can be used with (5-19) to yield (5-23). \square

5.2.3.2 Target i is operating in the *unchased* mode

Lemma 5.2. *During $t \in [t_{i,k}^u, t_{i,k+1}^c)$, $\forall k \in \mathbb{N}$, the system states associated with the i^{th} target remain bounded.*

Proof. Using (5–1), (5–11), and (5–12), the time derivative of (5–18) during $t \in [t_{i,k}^u, t_{i,k+1}^c)$, $\forall k \in \mathbb{N}$ can be upper bounded as

$$\dot{V}_i(z_i(t)) \leq \kappa_1 \|z_i(t)\|^2 + \kappa_2,$$

where $\kappa_1, \kappa_2 \in \mathbb{R}$ are positive constants. Using (5–19), (5–26) can be upper bounded as

$$\dot{V}_i(z_i(t)) \leq \frac{\kappa_1}{\beta_1} V_i(z_i(t)) + \kappa_2. \quad (5-28)$$

After applying the Comparison Lemma [29, Lemma 3.4] to (5–28), the following upper bound can be obtained:

$$V_i(z_i(t)) \leq \left(V_i(z_i(t_{i,k}^u)) + \frac{\kappa_2 \beta_1}{\kappa_1} \right) e^{\frac{\kappa_1}{\beta_1}(t-t_{i,k}^u)} - \frac{\kappa_2 \beta_1}{\kappa_1}.$$

□

5.2.3.3 Combined analysis

The following switched systems analysis follows exactly from Section 3.3.3 in Chapter 3, and is therefore omitted from this chapter. The analysis results in the states being ultimately bounded by

$$\limsup_t \|z_i(t)\|^2 \leq \frac{\nu_2}{\beta_1(1-\nu_1)} e^{\frac{\kappa_1}{\beta_1} T_{i,\max}^u},$$

for all time $t \in [0, \tau_i)$, and then ultimately bounded by

$$\limsup_t \|z_i(t)\|^2 \leq \frac{\nu_4}{\beta_1(1-\nu_3)} e^{\frac{\kappa_1}{\beta_1} T_{i,\max}^u},$$

for all time $t \in [\tau_i, \infty)$, where $\nu_1, \nu_2, \nu_3, \nu_4 \in \mathbb{R}$ are known positive constants, provided that the dwell time conditions

$$T_i^u(km, (k+1)m-1) < \frac{\lambda_1 \beta_1}{\kappa_1} T_i^c(km, (k+1)m-1)$$

and

$$T_i^u(km, (k+1)m-1) < \frac{\lambda_2 \beta_1}{\kappa_1} T_i^c(km, (k+1)m-1),$$

respectively, are satisfied. It is important to note that $\nu_4 \leq \nu_2$ and $\nu_3 \leq \nu_1$, meaning that the ultimate bound is smaller once the FE condition is satisfied.

5.3 Relocating Phase

Once all targets have been regulated to the neighborhood $B_{r_{\min}}(\bar{x}_0)$, the relocation phase is initiated. As targets are regulated to $B_{r_{\min}}(\bar{x}_0)$, eventually there will be more unpaired herders than targets that still need to be grouped. In this scenario, any unpaired herders³ will hold their position until the relocating phase begins. During this phase, the herders will work as a team to form a frontal arc that pushes the ensemble, as a group, to the neighborhood $B_{r_g}(x_g)$, while maintaining all targets within the ensemble.

5.3.1 Relocating Objective

For the relocation objective, it is advantageous to model the collection of target agents as a single controllable ensemble. Consider the ideal unicycle model from [41] used in [1] (see Figure 5-1), with forward velocity $v \in \mathbb{R}$ in the direction of the heading $\phi \in \mathbb{R}$ with respect to a fixed global reference frame G . Fixed to the nonholonomic ideal unicycle is the reference frame Q (with origin \bar{x}), with v defined along the q_x direction and $q_y \perp q_x$. Further, consider a point $p \in \mathbb{R}$, which lies on q_x a distance $L \in \mathbb{R}_{>0}$ from

³ The herders will select targets to *chase* until there are no *unchased* targets that lie outside of $B_{r_{\min}}(\bar{x}_0)$.

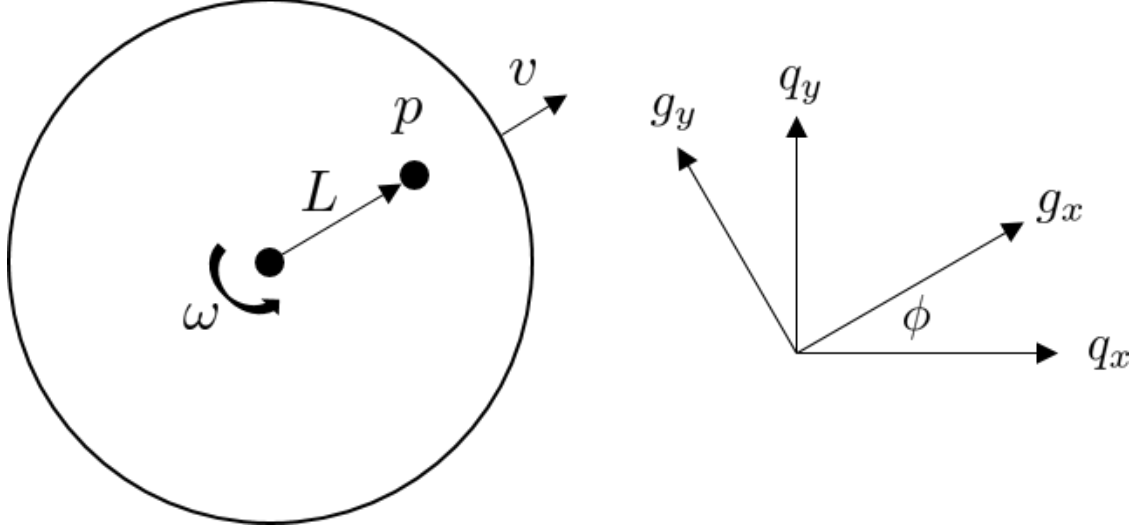


Figure 5-1. The ideal unicycle model in [1] is used to model the ensemble of target agents.

the center of the vehicle, defined as

$$p \triangleq \bar{x} + Lq_x,$$

where $q_x = \begin{bmatrix} \cos(\phi) & \sin(\phi) \end{bmatrix}^T$ and $q_y = \begin{bmatrix} -\sin(\phi) & \cos(\phi) \end{bmatrix}^T$. The relocation strategy entails driving the point p to the center of the goal location, x_g , which will ensure that the center of the vehicle (and therefore the mean target location) is regulated to the neighborhood $B_L(x_g) \triangleq \{q \in \mathbb{R}^2 \mid \|q - x_g\| \leq L\}$. Moreover, to ensure that all targets are regulated to the neighborhood $B_{r_g}(x_g)$, the maximum allowable radius of the *herd* is defined as $r_{\max} \triangleq r_g - L$ (see Figure 5-2).

Since the objective is to drive the point p to the goal point x_g , let $e_p \in \mathbb{R}$ be the point offset error, defined as

$$e_p \triangleq p - x_g. \quad (5-29)$$

From [41], the dynamics of the point offset $\dot{p} \in \mathbb{R}$ can be related to v and $\omega \triangleq \dot{\phi}$ as

$$\begin{bmatrix} v \\ \omega \end{bmatrix} = \begin{bmatrix} \cos(\phi) & \sin(\phi) \\ -\frac{\sin(\phi)}{L} & \frac{\cos(\phi)}{L} \end{bmatrix} \dot{p}. \quad (5-30)$$

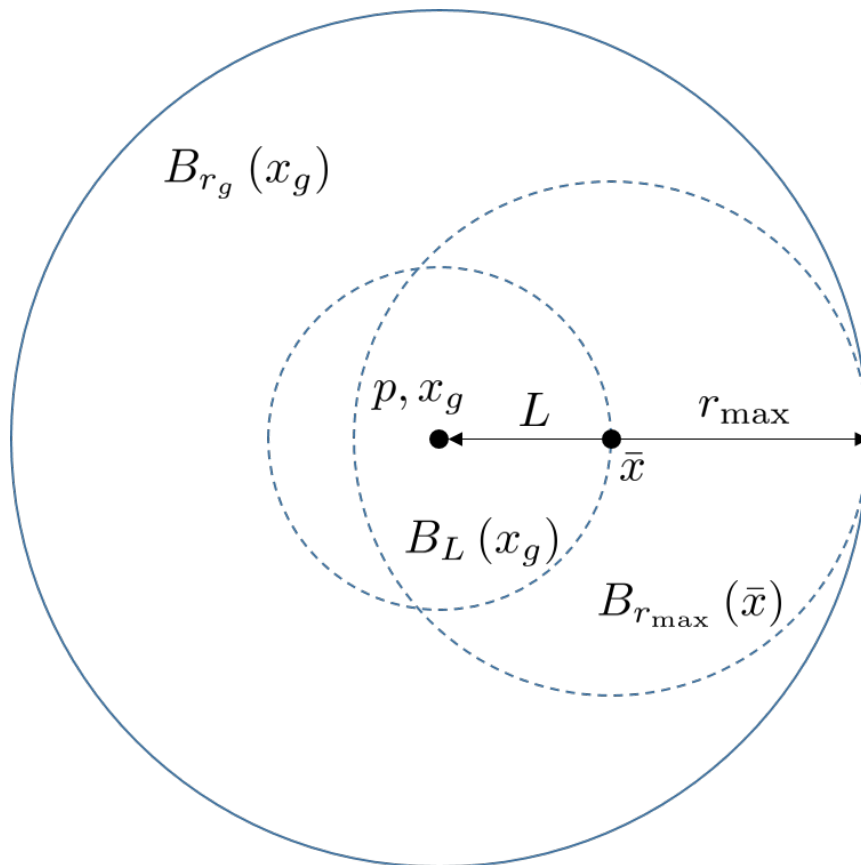


Figure 5-2. To ensure that all target agents are regulated to the neighborhood $B_{r_g}(x_g)$, the maximum allowable radius of the *herd* is $r_{\max} = r_g - L$.

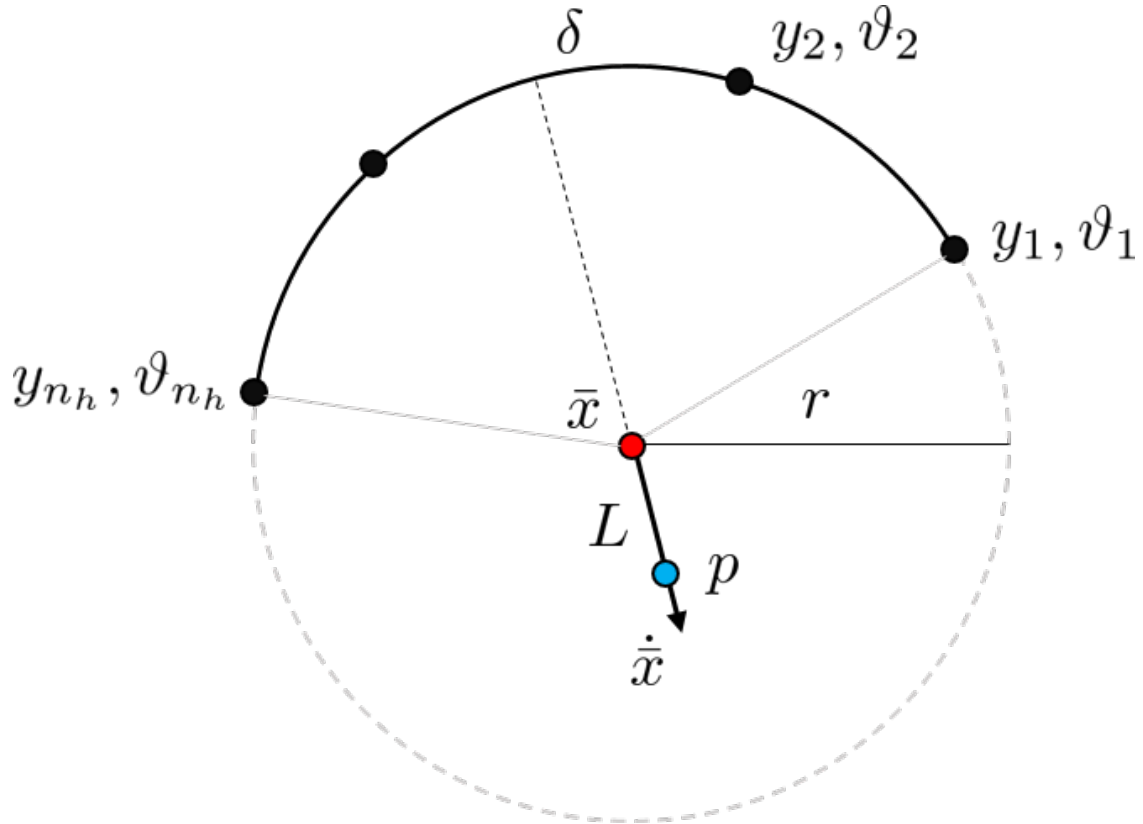


Figure 5-3. The configuration with n_h herders and a single target is shown. The target, \bar{x} , represents a single sheep as an example, but will later represent the mean target location.

5.3.1.1 Multiple herders and a single target

The following control development follows a similar approach as in [1]. First, the problem will be formulated for n_h herders and just a single target and is then extended to the general ensemble centered at the mean target location. As illustrated in Figure 5-3, the objective is to evenly distribute herders along a frontal arc lying on a circle centered at \bar{x} . The angle spanned by the entirety of the arc is defined as $\delta \triangleq \vartheta_{n_h} - \vartheta_1$, where $\vartheta_j \in \mathbb{R}$ is the angular orientation of the j^{th} herder relative to the horizontal, $\forall j \in \mathcal{H}$. In this example, \bar{x} will represent a single sheep, however, in the subsequent development, \bar{x} will be used to represent the mean target location when a *herd* is considered. The j^{th}

herder's position on the arc can be written in terms of its angular orientation as

$$y_j = \bar{x} + r_j \begin{bmatrix} \cos(\vartheta_j) \\ \sin(\vartheta_j) \end{bmatrix}. \quad (5-31)$$

Furthermore, when the herders are in relocating mode and have arrived at their positions on the frontal arc, their distances from \bar{x} all become equivalent (i.e., $r = r_1 = r_2 = \dots = r_{n_h}$), and thus (5-31) can be rewritten as

$$y_j = \bar{x} + r \begin{bmatrix} \cos(\vartheta_j) \\ \sin(\vartheta_j) \end{bmatrix}. \quad (5-32)$$

Likewise, during the relocation phase, the target dynamics in (5-1) can be rewritten in terms of herder angular orientation as

$$\dot{\bar{x}} = \frac{-\alpha_t}{r^2} \begin{bmatrix} \sum_{j \in \mathcal{H}} \cos(\vartheta_j) \\ \sum_{j \in \mathcal{H}} \sin(\vartheta_j) \end{bmatrix}. \quad (5-33)$$

The j^{th} herder's angular orientation ϑ_j can be related to the overall orientation of the unicycle vehicle ϕ as

$$\vartheta_j = \phi + \pi + \delta_j, \quad (5-34)$$

where $\delta_j \triangleq \delta \frac{(2j - n_h - 1)}{(2n_h - 1)}$. Then, using (5-34), (5-33) can be rewritten as

$$\dot{\bar{x}} = -F_v(\delta) \begin{bmatrix} \cos(\phi) \\ \sin(\phi) \end{bmatrix}, \quad (5-35)$$

where $F_v : \mathbb{R} \rightarrow \mathbb{R}$ is an unknown, bounded, locally Lipschitz, and invertible⁴ function that represents the magnitude of the ensemble velocity. The dynamics in (5-35) contain

⁴ The mapping F_v is one-to-one and onto (and thus is invertible) as long as the domain of the herder angular separation is restricted to $\delta \in (0, 2\pi)$.

only the state variables ϕ and δ , making it possible to control the ensemble using just two variables, regardless of the number of herders.

5.3.1.2 Extension to an ensemble of targets

When extending this formulation to include an ensemble of targets centered at \bar{x} , the radius r of the frontal arc of herders may grow due to any dispersion by the ensemble during relocation. Thus, a radius controller will be implemented to ensure that the radius does not grow beyond r_{\max} . With \bar{x} being treated as the mean target location (rather than just as a single target in the previous example), the ensemble dynamics may be written as

$$\dot{\bar{x}} = \frac{\alpha_t}{n_t} \sum_{i \in \mathcal{T}} \sum_{j \in \mathcal{H}} \frac{(x_i - y_j)}{\|x_i - y_j\|^3}.$$

Furthermore, an equivalent form of the j^{th} herder dynamics in (5-2) during the relocation mode is determined by taking the time derivative of (5-32) to obtain

$$\dot{y}_j = \dot{\bar{x}} + r\dot{\vartheta}_j \begin{bmatrix} -\sin(\vartheta_j) \\ \cos(\vartheta_j) \end{bmatrix} + \dot{r} \begin{bmatrix} \cos(\vartheta_j) \\ \sin(\vartheta_j) \end{bmatrix},$$

which can be rewritten using (5-34) as

$$\dot{y}_j = \dot{\bar{x}} + r \begin{pmatrix} \dot{\phi} + \dot{\delta}_j \end{pmatrix} \begin{bmatrix} \sin(\phi + \delta_j) \\ -\cos(\phi + \delta_j) \end{bmatrix} + \dot{r} \begin{bmatrix} -\cos(\phi + \delta_j) \\ -\sin(\phi + \delta_j) \end{bmatrix},$$

where

$$\dot{r} = u_r + \frac{2}{n_t} \sum_{i \in \mathcal{T}} (x_i - \bar{x})^T (\dot{x}_i - \dot{\bar{x}}) = u_r + Y_r \theta, \quad (5-36)$$

$Y_r \in \mathbb{R}^{2 \times 2}$ is a known regression matrix, and $u_r \in \mathbb{R}$ is the radius controller to be subsequently designed. The second term in (5-36) accounts for the fact that the size (i.e., standard deviation from the mean) of the ensemble may increase during relocation. Furthermore, let $e_r \in \mathbb{R}$ be the radius error, defined as

$$e_r \triangleq r - r_d, \quad (5-37)$$

where $r_d \in \mathbb{R}$ is the constant desired radius of the *herd* that the herders want to maintain.

5.3.2 Relocation Controller

The strategy is to leverage the constraints that were imposed in Sections 5.3.1.1 and 5.3.1.2 to drive the point p on the ideal unicycle to the center of the desired goal location, x_g . The error dynamics of the point offset will be designed using proportional control as

$$\dot{p} = -k_p e_p, \quad (5-38)$$

where $k_p \in \mathbb{R}$ is a positive constant gain, and thus using (5-38), the time derivative of (5-29) can be written as

$$\dot{e}_p = -k_p e_p. \quad (5-39)$$

Rewriting \bar{x} in the Q reference frame, and using (5-30), (5-39) can be rewritten as

$$\dot{p} = vq_x + L\omega q_y = -k_p (q_x^T e_p) q_x - k_p (q_y^T e_p) q_y.$$

The radius error dynamics can be found by taking the time derivative of (5-37), yielding

$$\dot{e}_r = Y_r \theta + u_r. \quad (5-40)$$

Based on (5-40), the radius control law is designed as

$$u_r = -k_r e_r - Y_r \hat{\theta}, \quad (5-41)$$

where $k_r \in \mathbb{R}$ is a positive constant gain. Using (5-41), (5-40) can be rewritten as

$$\dot{e}_r = Y_r \tilde{\theta} - k_r e_r. \quad (5-42)$$

Leveraging the aforementioned constraints, the herders must be driven to their ideal herder positions y_j^* , $\forall j \in \mathcal{H}$ (based on an ideal velocity and heading of the unicycle).

This configuration entails the herders all lying on the circle of radius r around \bar{x} with angular spacing δ_j . Let the ideal heading ϕ^* be equal to the angle that points the unicycle velocity vector towards the center of the final goal location x_g . Moreover, the dynamics in (5–38) are to be used to compute the ideal velocity v^* that will ensure the ensemble is regulated to $B_{r_g}(x_g)$. Substituting (5–38) into (5–30), the ideal velocity can be determined as

$$v^* = \begin{bmatrix} \cos(\phi) & \sin(\phi) \end{bmatrix} (-k_p e_p).$$

The velocity v of the ensemble is equivalent to the magnitude of the dynamics of the ensemble center, i.e., using (5–35), v can be written as a function of δ as

$$v = \|\dot{\bar{x}}\| = F_v(\delta). \quad (5-43)$$

The mapping in (5–43) is one-to-one and onto as long as $\delta \in (0, 2\pi)$, meaning that the unknown function F_v is invertible on this domain. Thus, the mapping $F_v^{-1} : \mathbb{R} \rightarrow \mathbb{R}$ exists, is bounded and locally Lipschitz, and is defined as

$$\delta^* = F_v^{-1}(v^*).$$

Then, the ideal location for the j^{th} herder can be written as

$$y_j^* = \bar{x} + r \begin{bmatrix} -\cos(\phi^* + \delta_j^*) \\ -\sin(\phi^* + \delta_j^*) \end{bmatrix}.$$

Using y_j^* as the desired herder state, the backstepping error in (5–4) in Section (5.2.1) can be rewritten as

$$e_j = y_j^* - y_j. \quad (5-44)$$

The time derivative of (5–44) is

$$\dot{e}_j = \dot{\bar{x}} + r \begin{bmatrix} \dot{\phi}^* + \dot{\delta}_j^* \\ \dot{\phi}^* + \dot{\delta}_j^* \end{bmatrix} \begin{bmatrix} \sin(\phi^* + \delta_j^*) \\ -\cos(\phi^* + \delta_j^*) \end{bmatrix}$$

$$+ \dot{r} \begin{bmatrix} -\cos(\phi^* + \delta_j^*) \\ -\sin(\phi^* + \delta_j^*) \end{bmatrix} - \alpha_h \sum_{i \in \mathcal{T}} \frac{(y_j - x_i)}{\|y_j - x_i\|^3} - u_j, \quad (5-45)$$

where

$$\dot{\phi}^* = \omega^* = \begin{bmatrix} -\frac{\sin(\phi)}{L} & \frac{\cos(\phi)}{L} \end{bmatrix} (-k_p e_p), \quad (5-46)$$

and

$$\dot{v}^* = \dot{\phi} \begin{bmatrix} -\sin(\phi) & \cos(\phi) \end{bmatrix} (-k_p e_p) + \begin{bmatrix} \cos(\phi) & \sin(\phi) \end{bmatrix} (-k_p^2 e_p). \quad (5-47)$$

Grouping the terms in (5-45), (5-46), and (5-47) into known and unknown functions, (5-45) can be rewritten as

$$\dot{e}_j = Y_j \theta + G_j + F_j - u_j, \quad (5-48)$$

where $Y_j, G_j \in \mathbb{R}^2$ are known functions containing the target and herder states, $x_i \forall i \in \mathcal{T}$, and $y_j, \forall j \in \mathcal{H}$, and $F_j \in \mathbb{R}^2$ is an unknown function, with an unknown structure, which will be approximated using a NN.

Let χ be a compact simply connected set such that $\chi \subset \mathbb{R}^{4n_h+2n_t+1}$, and let $\Upsilon(\chi)$ be defined as the space where $F_j : \chi \rightarrow \mathbb{R}^2$ is continuous, $\forall j \in \mathcal{H}$. The universal approximation property states that there exist weights and thresholds such that $F_j(\eta) \in \Upsilon(\chi)$ can be approximated by a NN as [37]

$$F_j(\eta(t)) = W_j^T \sigma_j(V_j^T \eta) + \varepsilon_j(V_j^T \eta), \quad (5-49)$$

where $\eta = \begin{bmatrix} 1 & x^T & y^T & \dot{y}^T \end{bmatrix}^T \in \mathbb{R}^{4n_h+2n_t+1}$, $\dot{y} = \begin{bmatrix} \dot{y}_1 & \dot{y}_2 & \dots & \dot{y}_{n_h} \end{bmatrix}$, $\sigma_j : \mathbb{R}^{4n_h+2n_t+1} \rightarrow \mathbb{R}^{L+1}$ is a known, bounded, locally Lipschitz, vector of basis functions defined as $\sigma_j(\cdot) \triangleq \begin{bmatrix} 1 & \sigma_{j,1}(\cdot) & \dots & \sigma_{j,L}(\cdot) \end{bmatrix}^T$, $W_j \in \mathbb{R}^{(L+1) \times 2}$ and $V_j \in \mathbb{R}^{(4n_h+2n_t+1) \times L}$ are unknown bounded constant ideal weight matrices, $L \in \mathbb{N}$ is the number of neurons used in the neural network, and $\varepsilon_j : \mathbb{R}^{4n_h+2n_t+1} \rightarrow \mathbb{R}^2$ is the function approximation residual.

Remark 5.1. The function approximation residual error can be upper bounded by a positive constant that can be made arbitrarily small based on the Stone-Weierstrass

theorem [38], i.e., $\bar{\varepsilon}_j \triangleq \sup_{\eta \in \chi, t \in [0, \infty)} \|\varepsilon_j (V_j^T \eta (t))\|$. The Stone–Weierstrass requires that the states remain in a compact set (i.e., $\eta (t) \in \chi$). The subsequent stability proof shows that if $\eta (0)$ is bounded, then $\eta (t) \in \chi$.

Furthermore, let $\tilde{W}_j \in \mathbb{R}^{(L+1) \times 2}$ and $\tilde{V}_j \in \mathbb{R}^{(4n_h + 2n_t + 1) \times L}$ denote the parameter estimation errors for the weights associated with the j^{th} herder, defined as

$$\tilde{W}_j (t) \triangleq W_j - \hat{W}_j (t) \quad \text{and} \quad \tilde{V}_j (t) \triangleq V_j - \hat{V}_j (t),$$

respectively, where $\hat{W}_j \in \mathbb{R}^{(L+1) \times 2}$ and $\hat{V}_j \in \mathbb{R}^{(4n_h + 2n_t + 1) \times L}$ are the subsequently designed adaptive estimates of the ideal weights $\forall j \in \mathcal{H}$. The following property is used in the subsequent stability analysis.

Property 4. (Taylor series approximation). The basis function $\sigma_j (V_j^T \eta)$ may be expanded about the point $V_j^T \eta = \hat{V}_j^T \eta$ using a Taylor series approximation as [37]

$$\begin{aligned} \sigma_j (V_j^T \eta) |_{V_j^T \eta = \hat{V}_j^T \eta} &= \sigma_j (\hat{V}_j^T \eta) + \frac{\partial \sigma_j}{\partial (V_j^T \eta)} (V_j^T \eta - \hat{V}_j^T \eta) + \mathcal{O}_j (\tilde{V}_j^T \eta)^2 \\ &= \sigma_j (\hat{V}_j^T \eta) + \frac{\partial \sigma_j}{\partial (V_j^T \eta)} |_{\hat{V}_j^T \eta} \tilde{V}_j^T \eta + \mathcal{O}_j^2 \\ &= \hat{\sigma}_j + \nabla \hat{\sigma}_j \tilde{V}_j^T \eta + \mathcal{O}_j^2, \end{aligned}$$

where the notation $\sigma_j \triangleq \sigma_j (V_j^T \eta)$, $\hat{\sigma}_j \triangleq \sigma_j (\hat{V}_j^T \eta)$, $\nabla \hat{\sigma}_j \triangleq \frac{\partial \sigma_j (V_j^T \eta)}{\partial (V_j^T \eta)} |_{\hat{V}_j^T \eta}$, and $\varepsilon_j \triangleq \varepsilon_j (V_j^T \eta)$ is used, and $\mathcal{O}_j^2 \in \mathbb{R}^2$ represents higher order terms.

Then, the open-loop backstepping dynamics in (5–48) can be rewritten using (5–49) as

$$\dot{e}_j = Y_j \theta + G_j + W_j^T \sigma_j (V_j^T \eta) + \varepsilon_j (V_j^T \eta) - u_j. \quad (5-50)$$

The j^{th} herder’s relocation-phase control law is designed as

$$u_j = k_{y1} e_j + Y_j \hat{\theta} + G_j + \hat{W}_j^T \sigma_j (\hat{V}_j^T \eta) + (k_{s1} + k_{s2} \|\eta\|) \text{sgn} (e_j), \quad (5-51)$$

where $k_s \in \mathbb{R}$ is a positive constant gain, and $\text{sgn}(\cdot)$ is the signum function. Finally, (5–50) can be simplified using (5–51) as

$$\dot{e}_j = -k_y e_j + Y_j \tilde{\theta} + W_j^T \sigma_j(V_j^T \eta) - \hat{W}_j^T \sigma_j(\hat{V}_j^T \eta) + \varepsilon_j(V_j^T \eta) - (k_{s1} + k_{s2} \|\eta\|) \text{sgn}(e_j). \quad (5-52)$$

After using Property 4 (and the notation defined therein) and some algebraic manipulation, (5–52) can be rewritten as

$$\dot{e}_j = -k_y e_j + Y_j \tilde{\theta} + \tilde{W}_j^T \hat{\sigma}_j + \hat{W}_j^T \nabla \hat{\sigma}_j \tilde{V}_j^T \eta + \rho_j - (k_{s1} + k_{s2} \|\eta\|) \text{sgn}(e_j), \quad (5-53)$$

where $\rho_j \in \mathbb{R}^2$ is defined as $\rho_j \triangleq \tilde{W}_j^T \nabla \hat{\sigma}_j \tilde{V}_j^T \eta + W_j^T \mathcal{O}_j^2 + \varepsilon_j$. Based on Remark (5.1), the NN reconstruction error $\varepsilon_j(\eta)$ can be upper bounded by a positive constant as long as $\eta(t)$ remains in a compact set (the subsequent stability proof illustrates that $\eta(t)$ does in fact remain in a compact set), in which case

$$\|\rho_j(t)\| \leq c_{NN,1} + c_{NN,2} \|\eta\|, \quad \forall j \in \mathcal{H},$$

where $c_{NN,1}, c_{NN,2} \in \mathbb{R}$ are positive bounding constants. Based on (5–53), the adaptive update laws $\dot{\hat{\theta}}(t)$, $\dot{\hat{W}}_j(t)$, and $\dot{\hat{V}}_j(t)$ are designed as

$$\dot{\hat{\theta}} \triangleq \text{proj} \left\{ \Gamma \left(Y_r^T e_r + \sum_{j \in \mathcal{H}} Y_j^T e_j \right) \right\}, \quad (5-54)$$

$$\dot{\hat{W}}_j \triangleq \text{proj} \left\{ \Gamma_W \hat{\sigma}_j e_j^T \right\}, \quad (5-55)$$

and

$$\dot{\hat{V}}_j \triangleq \text{proj} \left\{ \Gamma_V \eta e_j^T \hat{W}_j^T \nabla \hat{\sigma}_j \right\}, \quad (5-56)$$

where $\Gamma_W \in \mathbb{R}^{(L+1) \times (L+1)}$ and $\Gamma_V \in \mathbb{R}^{(4n_h+2n_t+1) \times (4n_h+2n_t+1)}$ are constant, positive definite, symmetric control gain matrices and the projection operator $\text{proj}\{\cdot\}$ was defined in Section (5.2.2).

5.3.3 Relocation Stability Analysis

The following stability analysis will prove that the ensemble converges to the neighborhood $B_{r_g}(x_g)$ based on the development in Section (5.3.2). Ensemble regulation is accomplished by proving that the point p converges to the neighborhood $B_L(x_g)$ and leveraging the end result from Section (5.2) to ensure that all targets are regulated to $B_{r_g}(x_g)$ (see Figure (5-2)).

To facilitate this analysis, let $V_p : \mathbb{R}^2 \times \mathbb{R} \times \mathbb{R}^{2n_h} \times \mathbb{R}^2 \times \mathbb{R}^{2(L+1)} \times \mathbb{R}^{2(4n_h+2n_t+1)} \rightarrow \mathbb{R}$ be a positive definite, continuously differentiable candidate Lyapunov function, defined as

$$V_p \triangleq \frac{1}{2}e_p^T e_p + \frac{1}{2}e_r^2 + \sum_{j \in \mathcal{H}} \frac{1}{2}e_j^T e_j + \frac{1}{2}\tilde{\theta}^T \Gamma^{-1} \tilde{\theta} + \sum_{j \in \mathcal{H}} \frac{1}{2} \text{tr} \left(\tilde{W}_j^T \Gamma_W^{-1} \tilde{W}_j \right) + \sum_{j \in \mathcal{H}} \frac{1}{2} \text{tr} \left(\tilde{V}_j^T \Gamma_V^{-1} \tilde{V}_j \right), \quad (5-57)$$

where $\text{tr}(\cdot)$ denotes the matrix trace operator.

Theorem 5.1. *The controllers given in (5-38), (5-41), (5-51), and the adaptive update laws in (5-54), (5-55), and (5-56) ensure that all system signals are bounded under closed-loop operation and that the targets $x_i, \forall i \in \mathcal{T}$ are regulated to the neighborhood $B_{r_g}(x_g)$, which, provided that the gains are selected according to the sufficient conditions*

$$k_{s1} \geq c_{NN,1}, \quad k_{s2} \geq c_{NN,2}, \quad (5-58)$$

is equivalent to ensuring that

$$\lim_{t \rightarrow \infty} \|e_p(t)\| = 0 \quad (5-59)$$

and

$$\lim_{t \rightarrow \infty} |e_r(t)| = 0. \quad (5-60)$$

Proof. Using (5-39), (5-42), (5-53), (5-54), (5-55), and (5-56), the time derivative of (5-57) can be upper bounded as

$$\begin{aligned} \dot{V}_p \leq & -k_p \|e_p\|^2 - k_r e_r^2 \\ & + \sum_{j \in \mathcal{H}} \left(-k_y \|e_j\|^2 + (c_{NN,1} - k_{s1}) \|e_j\| + (c_{NN,2} - k_{s2}) \|e_j\| \|\eta\| \right). \end{aligned} \quad (5-61)$$

Then, after selecting the gain k_s according to (5–58), (5–61) can be further upper bounded by

$$\dot{V}_p \leq -k_p \|e_p\|^2 - k_r e_r^2 - k_y \sum_{j \in \mathcal{H}} \|e_j\|^2.$$

Since V_p is positive definite and \dot{V}_p is negative semi-definite, $V_p \in \mathcal{L}_\infty$; therefore, $e_p, e_r, e_j, \tilde{\theta}, \tilde{W}_j, \tilde{V}_j \in \mathcal{L}_\infty, \forall j \in \mathcal{H}$. Since $e_p, e_r, \tilde{\theta}, \tilde{W}_j, \tilde{V}_j \in \mathcal{L}_\infty, \forall j \in \mathcal{H}$, it can be shown that $p, r, \bar{x}, \hat{\theta}, \hat{W}_j, \hat{V}_j \in \mathcal{L}_\infty, \forall j \in \mathcal{H}$. Since $p, r, \bar{x} \in \mathcal{L}_\infty$, it is obvious that $y_j^*, x_i \in \mathcal{L}_\infty, \forall i \in \mathcal{T}, j \in \mathcal{H}$, and therefore $y_j, Y_r \in \mathcal{L}_\infty, \forall j \in \mathcal{H}$. It can then be shown that $Y_j, G_j \in \mathcal{L}_\infty, \forall j \in \mathcal{H}$. With all of the required signals being bounded, it is apparent that $u_r, u_j \in \mathcal{L}_\infty, \forall j \in \mathcal{H}$, and therefore $\dot{e}_j \in \mathcal{L}_\infty \implies \dot{y}_j \in \mathcal{L}_\infty, \forall j \in \mathcal{H}$. Thus, the stacked vector $\eta(t)$ is contained for all time in χ , defined as $\chi = \{\eta(t) \mid \|\eta(t)\| \leq \kappa_\chi \|\eta(0)\|\}$, where κ_χ is a positive constant. Thus, the Weierstrass approximation theorem holds. Finally, since it can be shown that $\dot{e}_p, \dot{e}_r \in \mathcal{L}_\infty$, e_p, e_r are uniformly continuous, and since $e_p, e_r \in \mathcal{L}_2$, (5–59) and (5–60) are achieved by [29, Lemma 8.2]. \square

5.4 Simulations

Simulation results were performed for the two-phase herding problem presented in this chapter. Two herders were tasked with grouping and relocating six homogeneous target agents, with $\alpha_t = 1.5$ and $\alpha_h = 0.5$. Figures 5-4 through 5-9 show the agents at different times throughout the simulation. As shown in Figures 5-9 and 5-11, the point p , represented by a black dot, has been regulated to the goal point x_g (green cross). Moreover, the final radius satisfies $r \leq r_{\max}$, where $r_{\max} = r_g - L$. The adaptive parameter estimation error is given in Figure 5-10.

5.5 Concluding Remarks

A two-phase herding strategy is introduced where a small team of herding agents switched between grouping and relocating a herd of uncertain target agents. NN approximation tools are used to estimate unknown dynamics in the system and switched

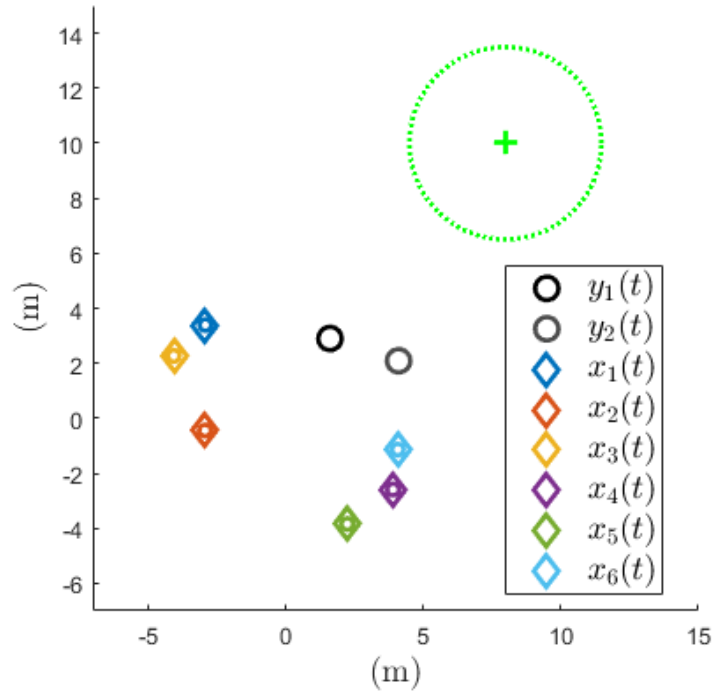


Figure 5-4. The grouping phase is initialized at $t = 0$ s.

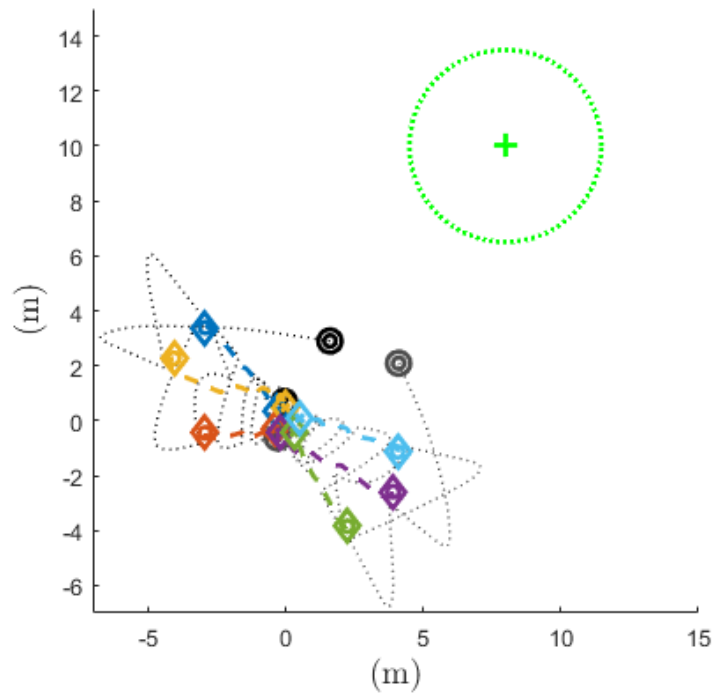


Figure 5-5. The grouping phase is completed at $t = 35$ s.

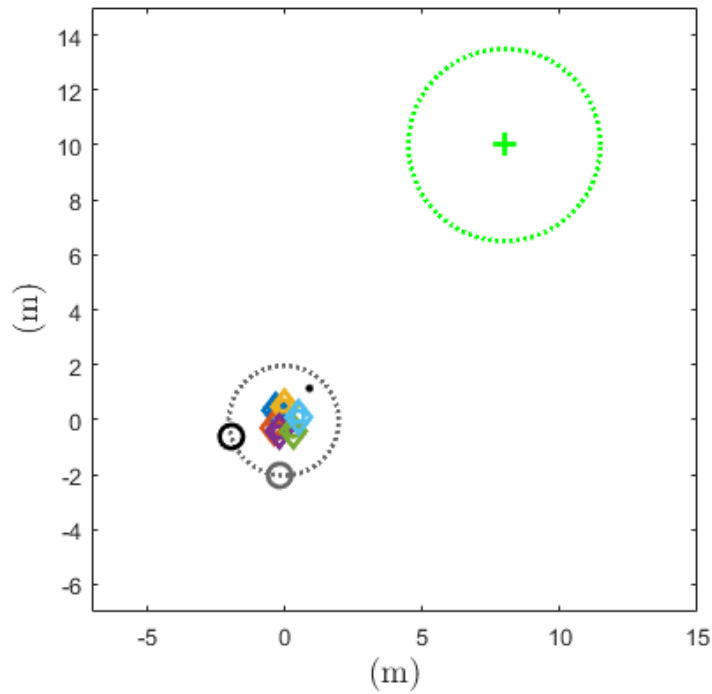


Figure 5-6. The relocating phase is initialized at $t = 36$ s. The point p (black dot) is to be driven to the goal location (green cross).

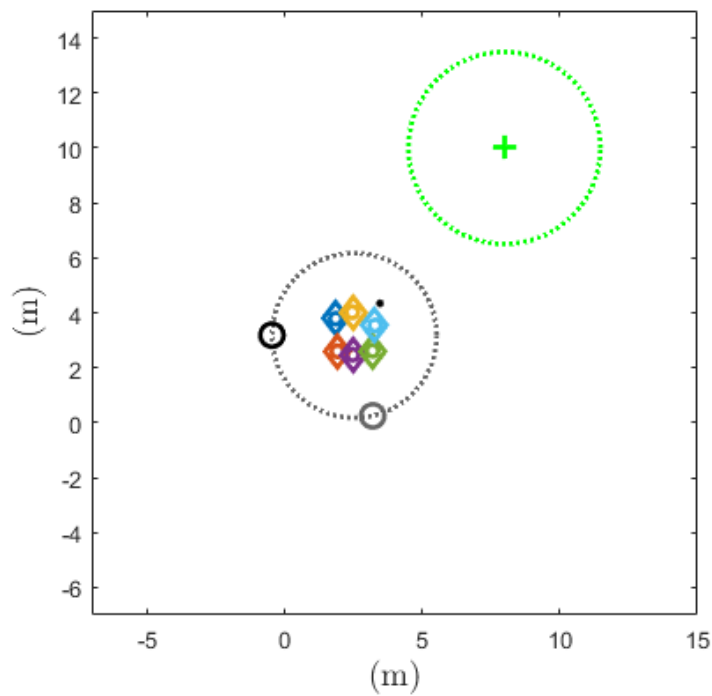


Figure 5-7. The relocating phase continues at $t = 56$ s. Note that the radius of the frontal arc has increased to compensate for ensemble dispersion.

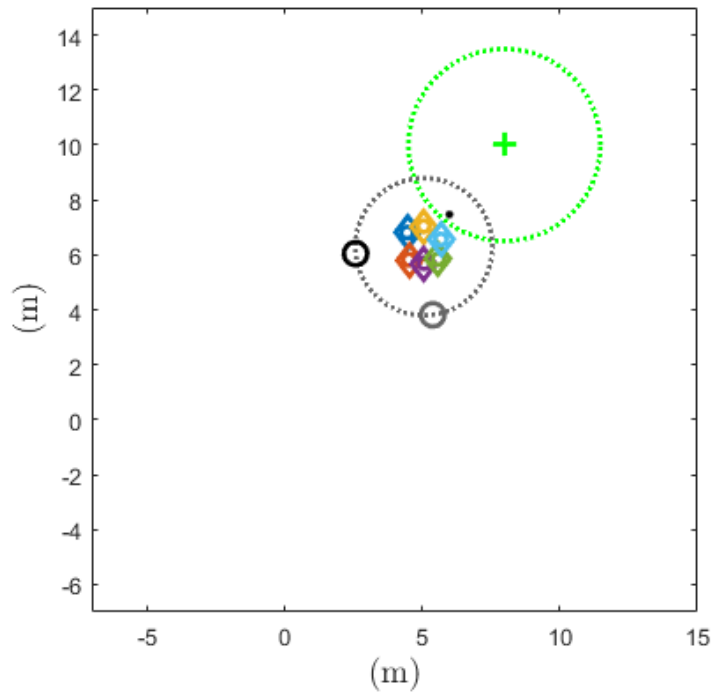


Figure 5-8. The relocating phase continues at $t = 75$ s.

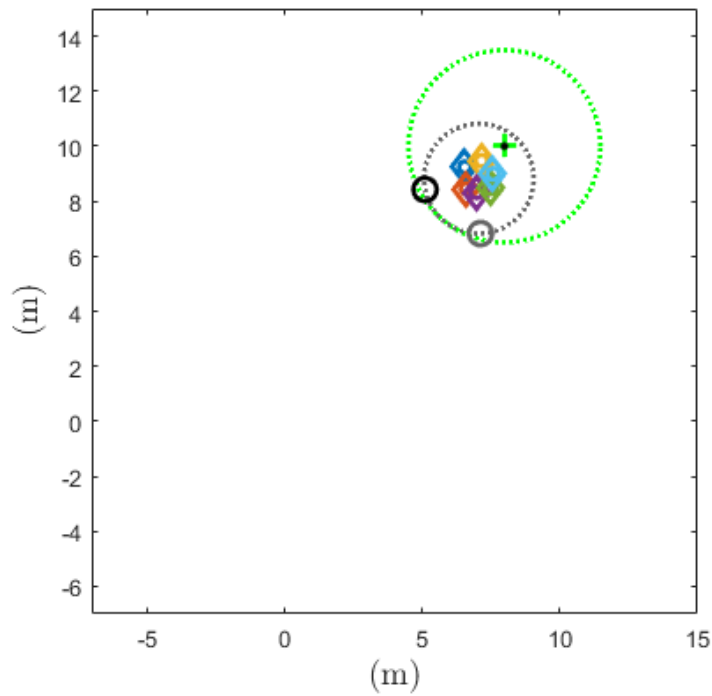


Figure 5-9. The relocating phase is completed at $t = 98$ s. The point p (black dot) has been successfully driven to the goal location x_g . The final radius satisfies $r \leq r_{\max}$, where $r_{\max} = r_g - L$, and thus all targets are regulated to $B_{r_g}(x_g)$.

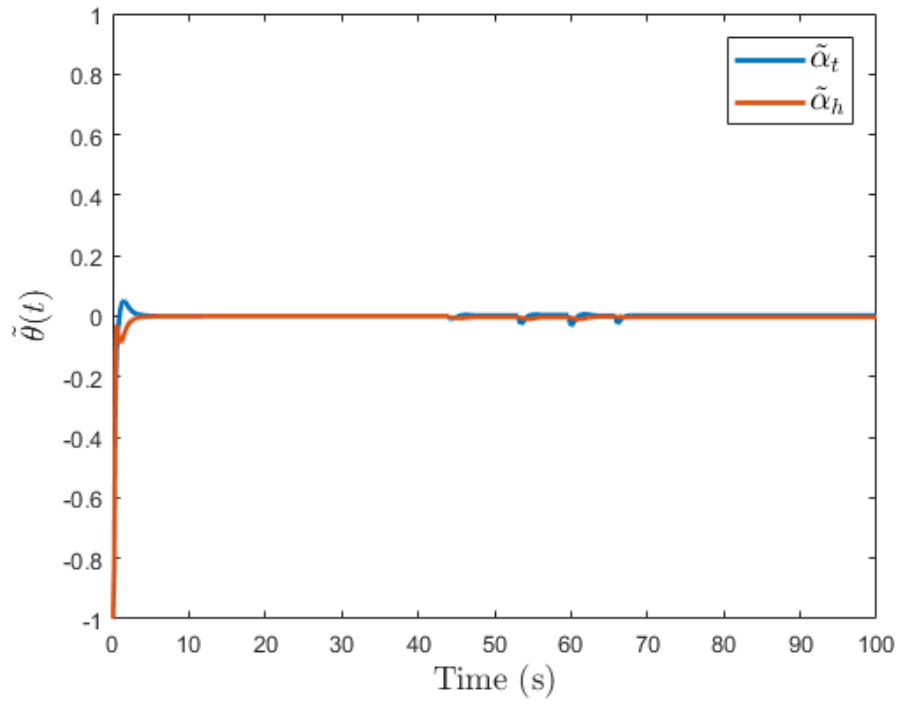


Figure 5-10. The parameter estimation error is shown.

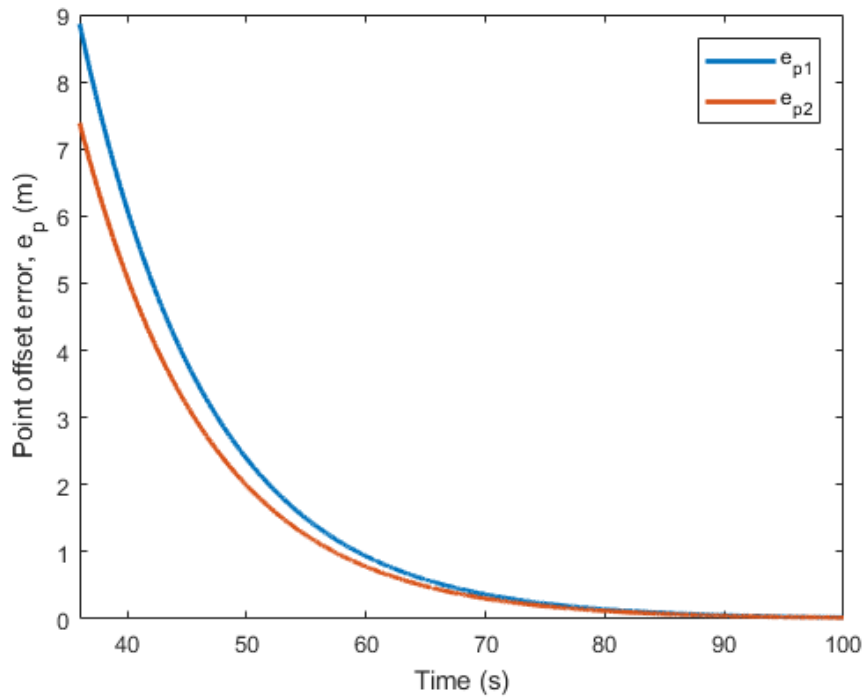


Figure 5-11. The point offset error is shown.

systems analysis is employed to guarantee performance of the developed switching controller.

CHAPTER 6 CONCLUSIONS

As more sensing and control technologies continue to improve reliability, autonomous systems continue to expand into applications including: transportation, delivery, agriculture, entertainment, military, etc. As they expand into such domains, the cost of autonomous systems and associated technologies decrease, opening opportunities for more networks of agents. Networked systems can sometimes contain agents that aren't directly controllable, even if they are crucial to the overall network control objective. In these scenarios, it is advantageous to exploit the possibly uncertain interactions between controllable agents and these uncontrollable agents. The herding problem examined in this dissertation involves such agents, and various methods are used to guarantee that the herding task is accomplished. Adaptive and robust control methods, as well as Lyapunov-based switched systems analysis, are used to learn and/or compensate for any uncertainties in the network.

In Chapter 2, A robust controller and switching conditions were synthesized using Lyapunov-based stability analysis for a single herding agent and multiple target agents. Dwell time conditions must be met to ensure global exponential regulation of n_t uncertain target agents to their unique goal location, despite their tendency to flee and lack of explicit control input. The target dynamics (which satisfy the LP assumption in this chapter) are represented by a potential function-based approach, where the herders affect on them is a function of the distance between them. The contribution of this chapter is the first use of switched systems methods to address scenarios where the herder is outnumbered.

The results in Chapter 2 are extended in Chapter 3 to include adaptive estimation of the LP uncertainty associated with target agents. The development in Chapter 3 utilizes an adaptive switching controller to ensure global uniform ultimate boundedness of n_t nonhomogeneous target agents to unique goal locations. The Lyapunov-based

stability and switching analysis yields dwell time conditions which must be met to ensure all target errors converge to an ultimate bound. This chapter also assumes that the LP assumption is satisfied. An ICL scheme is utilized to improve the parameter estimation error and facilitate the switched systems analysis.

Chapter 4 extends the previous results for multiple nonhomogeneous agents by generalizing the dynamics to unstructured uncertainties. Unknown dynamics are estimated using neural network function approximation techniques. Similar to Chapter 2, the system states are proven to converge to an ultimate bound. An ICL scheme was again used to facilitate the analysis and dwell time conditions were developed.

In Chapter 5, a two-phase herding problem is examined. This chapter considers a team of herding agents tasked with grouping and relocating a larger team of uncontrollable target agents to a desired goal location. The herders use a switching strategy, which must satisfy the designed dwell time conditions, to first group the team of non-cooperative target agents into a herd (neighborhood around their mean location), and then drive the herd to a desired location. Adaptive control and function approximation methods are used to compensate for uncertainties in the system during both phases, and an ICL scheme is used to ensure ultimately bounded stability during the grouping phase.

Extensions to this work may include less aware herders with limited sensing to measure target states for feedback and investigating limits on the herder's control authority. Additionally, herder agent communication constraints could be considered for the multiple herder case. Higher order dynamics could also be taken into account to add objectives at the velocity level. The results in Chapter 5 can be extended to consider non-homogeneous targets with additional (herding, flocking, fleeing, etc.) dynamics. Additional efforts can also be applied to investigate generalized relationships for how many herders are needed to achieve the herding objective given bounds on the speed of the herders and targets and some measure of geographical dispersion.

REFERENCES

- [1] A. Pierson and M. Schwager, "Bio-inspired non-cooperative multi-robot herding," in *Proc. IEEE Int. Conf. on Robot. and Autom.* IEEE, 2015, pp. 1843–1849.
- [2] J. Klotz, T.-H. Cheng, and W. E. Dixon, "Robust containment control in a leader-follower network of uncertain euler-lagrange systems," *Int. J. Robust Nonlinear Control*, vol. 26, pp. 3791–3805, 2016.
- [3] Z. Kan, S. Mehta, E. Pasilliao, J. W. Curtis, and W. E. Dixon, "Balanced containment control and cooperative timing of a multi-agent system," in *Proc. Am. Control Conf.*, 2014, pp. 281–286.
- [4] Z. Kan, J. R. Klotz, E. Doucette, J. Shea, and W. E. Dixon, "Decentralized rendezvous of nonholonomic robots with sensing and connectivity constraints," *ASME J. Dyn. Syst. Meas. Control*, vol. 139, no. 2, pp. 024 501–1–024 501–7, 2017.
- [5] J. R. Klotz, Z. Kan, J. M. Shea, E. L. Pasilliao, and W. E. Dixon, "Asymptotic synchronization of a leader-follower network of uncertain Euler-Lagrange systems," *IEEE Trans. Control Netw. Syst.*, vol. 2, no. 2, pp. 174–182, Jun. 2015.
- [6] D. Xie, D. Yuan, J. Lu, and Y. Zhang, "Consensus control of second-order leader-follower multi-agent systems with event-triggered strategy," *Trans. Inst. Meas. Control*, vol. 35, no. 4, pp. 426–436, Jun. 2013.
- [7] T.-H. Cheng, Z. Kan, J. A. Rosenfeld, and W. E. Dixon, "Decentralized formation control with connectivity maintenance and collision avoidance under limited and intermittent sensing," in *Proc. Am. Control Conf.*, 2014, pp. 3201–3206.
- [8] M. Egerstedt and X. Hu, "Formation constrained multi-agent control," *IEEE Trans. Robot. Autom.*, vol. 17, no. 6, pp. 947–951, Dec. 2001.
- [9] H. G. Tanner, A. Jadbabaie, and G. J. Pappas, "Flocking in fixed and switching networks," *IEEE Trans. Autom. Control*, vol. 52, no. 5, pp. 863–868, May 2007.
- [10] Q. Chen and J. Y. S. Luh, "Coordination and control of a group of small mobile robots," in *Proc. IEEE Int. Conf. on Robot. Autom.*, May 1994, pp. 2315–2320.
- [11] R. Licitra, Z. Hutcheson, E. Doucette, and W. E. Dixon, "Single agent herding of n-agents: A switched systems approach," in *IFAC World Congr.*, 2017.
- [12] R. Licitra, Z. I. Bell, E. Doucette, and W. E. Dixon, "Single agent indirect herding of multiple targets: A switched adaptive control approach," *IEEE Control Syst. Lett.*, vol. 2, no. 1, pp. 127–132, January 2018.
- [13] M. Bacon and N. Olgac, "Swarm herding using a region holding sliding mode controller," *J. Vib. Control*, vol. 18, no. 7, pp. 1056–1066, 2012.

- [14] T. H. Chung, G. A. Hollinger, and V. Isler, "Search and pursuit-evasion in mobile robotics," *Autonomous robots*, vol. 31, no. 4, p. 299, 2011.
- [15] R. Vidal, O. Shakernia, H. Kim, D. Shim, and S. Sastry, "Probabilistic pursuit-evasion games: theory, implementation, and experimental evaluation," *IEEE Trans. Robot. and Autom.*, vol. 18, no. 5, pp. 662–669, Oct. 2002.
- [16] A. D. Khalafi and M. R. Toroghi, "Capture zone in the herding pursuit evasion games," *Appl. Math. Sci.*, vol. 5, no. 39, pp. 1935–1945, 2011.
- [17] S. A. Shedied, "Optimal control for a two player dynamic pursuit evasion game; the herding problem," Ph.D. dissertation, Virginia Polytechnique Institute, 2002.
- [18] P. Kachroo, S. A. Shedied, J. S. Bay, and H. Vanlandingham, "Dynamic programming solution for a class of pursuit evasion problems: the herding problem," *IEEE Trans. Syst. Man Cybern.*, vol. 31, no. 1, pp. 35–41, Feb. 2001.
- [19] A. S. Gadre, "Learning strategies in multi-agent systems-applications to the herding problem," *M.S. thesis, Dept. Elect. Comput. Eng., Virginia Tech, Blacksburg, VA, USA*, 2001.
- [20] Z. Lu, "Cooperative optimal path planning for herding problems," Ph.D. dissertation, Texas A&M University, 2006.
- [21] J.-M. Lien, O. B. Bayazit, R. T. Sowell, S. Rodriguez, and N. M. Amato, "Shepherding behaviors," in *Proc. IEEE Int. Conf. on Robot. and Autom.*, vol. 4, Apr. 2004, pp. 4159–4164.
- [22] J.-M. Lien, S. Rodriguez, J.-P. Malric, and N. M. Amato, "Shepherding behaviors with multiple shepherds," in *Proc. IEEE Int. Conf. on Robot. and Autom.*, 2005, pp. 3402–3407.
- [23] R. Vaughan, N. Sumpter, J. Henderson, A. Frost, and S. Cameron, "Experiments in automatic flock control," *Robot. Autom. Syst.*, vol. 31, no. 1, pp. 109–117, 2000.
- [24] T. Miki and T. Nakamura, "An effective simple shepherding algorithm suitable for implementation to a multi-mmoble robot system," in *Proc. of the First Int. Conf. on Innov. Computing, Inf., and Control*, vol. 3, Washington, DC, USA, 2006, pp. 161–165.
- [25] D. Strömbom, R. P. Mann, A. M. Wilson, S. Hailes, A. J. Morton, D. J. T. Sumpter, and A. J. King, "Solving the shepherding problem: heuristics for herding autonomous, interacting agents," *J. of the R. Society Interface*, vol. 11, no. 100, 2014.
- [26] R. Sharma, M. Kothari, C. N. Taylor, and I. Postlethwaite, "Cooperative target-capturing with inaccurate target information," in *Proc. Am. Control Conf.*, Jun. 2010, pp. 5520–5525.

- [27] B. N. Pshenichnyi, "Simple pursuit by several objects," *Cybernetics*, vol. 12, no. 3, pp. 484–485, 1975.
- [28] A. Howard, M. J. Matarić, and G. S. Sukhatme, "Mobile sensor network deployment using potential fields: A distributed, scalable solution to the area coverage problem," in *Distributed Autonomous Robotic Systems 5*. Springer, 2002, pp. 299–308.
- [29] H. K. Khalil, *Nonlinear Systems*, 3rd ed. Upper Saddle River, NJ: Prentice Hall, 2002.
- [30] M. A. Müller and D. Liberzon, "Input/output-to-state stability of switched nonlinear systems," in *Proc. Am. Control Conf.*, Baltimore, MD, 2010, pp. 1708–1712.
- [31] M. A. Müller and D. Liberzon, "Input/output-to-state stability and state-norm estimators for switched nonlinear systems," *Automatica*, vol. 48, no. 9, pp. 2029–2039, 2012.
- [32] A. Parikh, T.-H. Cheng, and W. E. Dixon, "A switched systems approach to vision-based localization of a target with intermittent measurements," in *Proc. Am. Control Conf.*, Jul. 2015, pp. 4443–4448.
- [33] W. E. Dixon, A. Behal, D. M. Dawson, and S. Nagarkatti, *Nonlinear Control of Engineering Systems: A Lyapunov-Based Approach*. Birkhauser: Boston, 2003.
- [34] G. Chowdhary and E. Johnson, "A singular value maximizing data recording algorithm for concurrent learning," in *Proc. Am. Control Conf.*, 2011, pp. 3547–3552.
- [35] W. Rudin, *Principles of Mathematical Analysis*. McGraw-Hill, 1976.
- [36] R. Licitra and Z. Bell, "Adaptive switched herding control experiment," <https://youtu.be/o6e1XnC3xAY>, Sep. 2017.
- [37] F. L. Lewis, "Nonlinear network structures for feedback control," *Asian J. Control*, vol. 1, no. 4, pp. 205–228, 1999.
- [38] N. E. Cotter, "The stone-weierstrass theorem and its application to neural networks," *IEEE Trans. Neural Netw.*, vol. 1, no. 4, pp. 290–295, 1990.
- [39] A. Parikh, R. Kamalapurkar, and W. E. Dixon. (2015) Integral concurrent learning: Adaptive control with parameter convergence without PE or state derivatives. arXiv:1512.03464.
- [40] Z. Bell, A. Parikh, J. Nezvadovitz, and W. E. Dixon, "Adaptive control of a surface marine craft with parameter identification using integral concurrent learning," in *Proc. IEEE Conf. Decis. Contr.*, 2016.

- [41] N. Michael and V. Kumar, "Planning and control of ensembles of robots with non-holonomic constraints," *The International Journal of Robotics Research*, vol. 28, no. 8, pp. 962–975, 2009.

BIOGRAPHICAL SKETCH

Ryan Licitra received his Bachelor of Science degree in mechanical engineering from the University of Florida in 2013. During his senior year, he worked for a semester as an undergrad in the Nonlinear Controls and Robotics (NCR) lab, and then continued his studies at UF as a direct entry PhD student under the supervision of Dr. Warren E. Dixon, director of the NCR group. During each summer from 2014-2016, Ryan worked as a visiting researcher at the University of Florida Research and Engineering Education Facility in collaboration with Eglin Air Force Base. He received his Master of Science degree in 2015, and his Doctor of Philosophy degree in 2017, with a focus on control of nonlinear uncertain networks and switched systems.